



Regulation of kinetochore localization of the Spindle checkpoint kinase Bub1

Thèse

Adeel Asghar

Doctorat en biologie cellulaire et moléculaire
Philosophiae doctor (Ph.D.)

Québec, Canada

© Adeel Asghar, 2016

Regulation of kinetochore localization of the Spindle checkpoint kinase Bub1

Thèse

Adeel Asghar

Sous la direction de:

Directrice de recherche: Sabine Elowe

Résumé

Le point de contrôle d'assemblage du fuseau mitotique (SAC) est un système de surveillance conservé chez les eucaryotes permettant un attachement précis entre les kinétochores et les microtubules. Le SAC empêche la progression mitotique jusqu'à ce que soit généré un attachement et une tension correcte entre les kinétochores et les microtubules. La dérégulation du SAC a des conséquences graves avec de l'aneuploïdie retrouvée dans la plupart des tumeurs solides. BUB1 est une kinase sérine/thréonine requise pour le fonctionnement du SAC. Elle possède à la fois des rôles dépendants et indépendants de sa fonction kinase. Ce projet définit plusieurs fonctions associées à BUB1 lors de la mitose. L'utilisation d'outils *in vivo* et *in vitro* ont permis d'identifier plusieurs sites d'autophosphorylation sur Bub1. Nous avons testé et confirmé le site T589 de BUB1 comme un site d'autophosphorylation. Un mutant de ce site (BUB1-T589A) a été exprimé de manière stable et un anticorps phosphospécifique a été généré pour étudier ce site.

Le rôle structural des domaines de BUB1 a été rapporté précédemment. Nous montrons que quand le domaine d'extension du domaine kinase (aa 724-780) située en N-terminal du domaine kinase est nécessaire pour l'autophosphorylation de BUB1-T589 et l'activité de la kinase BUB1, le TPR à l'extrémité N-terminale est localisée normalement kinétochores et n'est pas requis pour l'activité kinase. BUB1-T589A a modifié le taux de renouvellement au kinétochores. Cela conduit à la propagation des signaux de SGO1 et de H2ApT120 au niveau des bras des chromosomes. Enfin, l'autophosphorylation en T589 régule le congression des chromosomes mais pas la fonction de BUB1 pour le SAC.

De plus nous montrons que l'inhibition de PLK1, une autre kinase sérine/thréonine, augmente la localisation de BUB1 aux kinétochores après la suppression BUB3 dans les cellules humaines. Ainsi, PLK1 peut réguler la localisation de BUB1 aux kinétochores. Nous montrons également que cette régulation se produit à travers KNL1, une protéine d'échafaudage du SAC. PLK1 pourrait régler BUB1 kinétochore localisation pour influencer la

progression mitotique. Des futures études se concentreront sur l'élucidation de mécanismes derrière ces interactions.

Abstract

The Spindle assembly checkpoint (SAC) is a monitoring system conserved in eukaryotes for accurate attachments between kinetochores and microtubules. The SAC precludes mitotic progression until correct attachments and tension between kinetochores and microtubules is generated. Deregulation of the SAC has the severe consequence of aneuploidy found in most solid tumors. BUB1 is a serine/threonine kinase required for the SAC function. It has both kinase-dependent and kinase-independent roles. This project defines several BUB1 associated functions during mitosis. Using *in vivo* and *in vitro* tools several autophosphorylation sites on BUB1 were identified. We tested and confirmed BUB1 T589 as an autophosphorylation site. A mutant of this site (BUB1-T589A) was stably expressed in cells and a phosphospecific antibody was generated to study this site.

The role of structural domains of BUB1 has been studied earlier. We show that while the kinase extension domain (aa 724-780) located N-terminal to the kinase domain is required for BUB1-T589 autophosphorylation and BUB1 kinase activity, the TPR at the N-terminus localizes normally to kinetochores and is not required for kinase activity. BUB1-T589A has altered turnover at kinetochores. This leads to the spread of SGO1 and H2ApT120 signal to chromosome arms. Finally, autophosphorylation at T589 regulates chromosome congression but not the SAC function of BUB1.

We further show that inhibition of PLK1, another serine/threonine kinase, increases BUB1 kinetochore localization after BUB3 depletion in human cells. Thus, PLK1 can regulate BUB1 kinetochore localization. We also show that this regulation occurs through KNL1, a scaffold protein of the SAC. It is possible that PLK1 could regulate BUB1 kinetochore localization to influence mitotic progression. Future studies will focus on elucidation of mechanism behind these interactions.

Table of Contents

Résumé.....	iii
Abstract	v
Table of Contents.....	vi
List of Tables	ix
List of Figure.....	x
List of Abbreviations	xi
Foreword	xiii
1. INTRODUCTION.....	1
1.1. Cell cycle and Checkpoints	1
1.1.1. <i>G1 or gap1 phase</i>	1
1.1.2. <i>G1/S checkpoint</i>	2
1.1.3. <i>S phase (Synthesis phase)</i>	3
1.1.4. <i>G2 phase (Gap2 phase)</i>	3
1.1.5. <i>G2/M checkpoint</i>	4
1.1.6. <i>M phase (Mitosis)</i>	4
1.2. Kinetochore- proteinaceous structures on chromosomes during mitosis	7
1.3. Spindle assembly checkpoint (SAC)	11
1.3.1. <i>SAC monitors specific attachments between kinetochores and microtubules</i>	11
1.3.2. <i>SAC senses tension and kinetochore attachments</i>	11
1.3.3. <i>The strength of the SAC varies during mitosis</i>	13
1.3.4. <i>SAC Components</i>	13
1.3.5. <i>Mitotic checkpoint complex (MCC)</i>	14
1.3.6. <i>Molecular basis of APC/C inhibition and anaphase delay</i>	16
1.3.7. <i>APC/C activation and mitotic progression</i>	19
1.3.8. <i>SAC Silencing</i>	19
1.3.8.1. <i>SAC silencing through Phosphoregulation</i>	19
1.3.8.2. <i>Stripping of SAC components</i>	20
1.3.8.3. <i>MCC disassembly</i>	22
1.3.9. <i>Importance of SAC</i>	23
1.3.10. <i>Shugoshin-1 (SGO1)</i>	26
1.3.10.1. <i>Structure of SGO1</i>	26
1.3.10.2. <i>Functions of SGO1 during mitosis</i>	27
1.3.10.2.1. <i>SGO1 acts as modulator of cohesin removal</i>	27
1.3.10.2.2. <i>SGO1 in chromosome biorientation</i>	29
1.3.11. <i>Protein phosphatase 2A (PP2A)</i>	31
1.3.11.1. <i>Structure of PP2A</i>	32
1.3.11.2. <i>Role of PP2A during mitosis</i>	33
1.3.12. <i>PLK1 (Polo-like kinase 1)</i>	34
1.3.12.1. <i>Functions of PLK1 in cell cycle</i>	35
1.3.12.2. <i>Function of PLK1 during mitosis</i>	35
1.3.13. <i>MPS1 (Monopolar spindle 1)</i>	36
1.3.13.1. <i>MPS1 functions</i>	37
1.3.13.1.1. <i>SAC function</i>	37
1.3.13.1.2. <i>Function at Centrosome</i>	37
1.4. BUB1 (budding uninhibited by benzimidazole 1)	39

1.4.1. Structure of BUB1	39
1.4.2. BUB1 kinetochore recruitment.....	39
1.4.3. Regulation of BUB1 activation.....	40
1.4.4. BUB1 Functions	42
1.4.4.1. BUB1 role in mitosis	42
1.4.4.2. BUB1 requirement for SAC	42
1.4.4.3. BUB1 kinase activity and SAC.....	42
1.4.4.4. BUB1 and recruitment of kinetochore components	44
1.4.4.5. BUB1 in chromosome congression, biorientation and segregation....	47
1.4.4.6. BUB1 in Aneuploidy and Cancer development	48
1.5. Hypothesis and Objectives	50
2. CHAPTER2	53
2.1. ABSTRACT	54
2.2. RÉSUMÉ.....	55
2.3. INTRODUCTION.....	56
2.4. RESULTS.....	57
2.4.1. Identification of Bub1 autophosphorylation sites	57
2.4.2. Regulation of Bub1 activation and autophosphorylation	61
2.4.3. Bub1 T589 autophosphorylation regulates mitotic progression	64
2.4.4. Bub1 autophosphorylation restricts H2A-pT120 to centromeres	67
2.4.5. Bub1-KD and -T589A display increased cytoplasmic residency.....	70
2.4.6. Kinetochore-tethered Bub1-T589A refocuses H2A-pT120 and Sgo.....	73
2.5. DISCUSSION	76
2.6. Materials and Methods	80
2.6.1. Cell culture and transfection.....	80
2.6.2. Chromosome Spreads	80
2.6.3. Cloning and mutagenesis	81
2.6.4. Immunofluorescence and antibodies	81
2.6.5. Fractionation, immunoprecipitation and Western Blotting	82
2.6.6. Microscopy, Live cell imaging, and FRAP	82
2.6.7. SILAC labelling and Mass spectrometry.....	83
2.6.8. Nano-LC-MS/MS Analysis.....	84
2.6.9. Data processing and analyses.....	85
2.6.10. Phosphopeptide analysis	86
2.6.11. Quantification and statistical analysis	86
2.7. ACKNOWLEDGEMENTS:	87
2.8. Author Contributions:.....	88
2.9. REFERENCES:	89
2.10. Supplementary Information	96
3. CHAPTER 3	101
3.1. Introduction	102
3.2. Hypothesis and objectives.....	103
3.3. Results	103
3.3.1. PLK1 inhibition causes rescue of SGO1 localization in BUB1 T589A.....	103
3.3.2. PLK1 inhibition enhances BUB1 localization in Bub3 depleted HeLa cells	104
3.3.3. PLK1 regulates BUB1 localization through KNL1	107
3.4. Discussion and Perspectives	110
3.5. Materials and Methods	113

3.5.1. <i>Cell culture, transfection and drug treatment</i>	113
3.5.2. <i>Immunofluorescence and Microscopy</i>	113
3.6. Refernces	115
4. CHAPTER 4	118
4.1. Discussion and Perspectives	118
4.2. Current understanding of Bub1 activity in SAC	119
4.3. References	122
4.4. References- Introduction	123

List of Tables

Table1	47
Table S1.....	100

List of Figure

Figure 1.1	Four phases of cell cycle.....	2
Figure 1.2	Stage of mitosis	5
Figure 1.3	kinetochore is a trilaminar multiprotein complex.....	8
Figure 1.4	Assembly of Kinetochore proteins	9
Figure 1.5	Attachments monitored by SAC.....	12
Figure 1.6	SAC signal prevents mitotic progression	14
Figure 1.7	MCC formation	16
Figure 1.8	Inhibition of APC/C	18
Figure 1.9	SAC silencing by Phosphoregulation.....	20
Figure 1.10	SAC silencing by stripping	21
Figure 1.11	Disassembly of MCC.....	23
Figure 1.12	Structure of human Sgo1	27
Figure 1.13	SGO1 and cohesin removal during mitosis	29
Figure 1.14	SGO1 role in biorientation	30
Figure 1.15	PP2A holoenzyme	33
Figure 1.16	PLK1 structure and activation.....	34
Figure 1.17	MPS1 recruits SAC proteins at KNL1.....	38
Figure 1.18	Structural domains of human BUB1	40
Figure 2.1	Identification of Bub1 autophosphorylation sites.....	59
Figure 2.2	Full Bub1 activation is mitotic specific and requires the kinase extension domain	62
Figure 2.3	Loss of Bub1 phosphorylation at T589 causes chromosome congression defects.....	66
Figure 2.4	Uniform H2A-T120 phosphorylation, ectopic Sgo recruitment and impaired sister chromatid resolution in cells expressing Bub1-T589A	68
Figure 2.5	Bub1-KD and Bub1-T589A display increased residency in the cytosol.....	71
Figure 2.6	Bub1-KD and Bub1-T589A display aberrant kinetochore shuttling dynamics	74
Figure 2.7	Model of Bub1 activation and autoregulation	75
Supplementary Figure 1.	Characterization of the pT589 and pS679 Bub1 antibodies	96
Supplementary Figure 2.	Characterization of the isogenic MYC-GFP Bub1 WT, KD and T589A HeLa cell lines.....	97
Supplementary Figure 3	Aurora recruitment and activation are normal in Bub1-T589Aexpressing cells.....	98
Supplementary Figure 4.	Original non-cropped Western Blots presented in this manuscript	99
Figure 3.1.	PLK1 and AURORA B inhibition recovers SGO1 loss from centromeres while H2ApT120 remains unchanged in BUB1 T589A cells	105
Figure 3.2.	PLK1 inhibition recruits cytosolic BUB1, SGO1 and H2ApT120 in BUB3 depleted cells	106
Figure 3.3.	PLK1 inhibition impairs KNL1 binding and MELTs phosphorylation at kinetochores.....	108
Figure 3.4.	BUB1 localization is regulated by PLK1 at KNL1	109
Figure 3.5.	Perspective experiments of BUB1 regulation by PLK1	112

List of Abbreviations

APC/C	Anaphase promoting complex/cyclosome
aa	Amino acid
ATM	<i>Ataxia telangiectasia mutated</i>
ATR	<i>Ataxia telangiectasia and Rad3-related protein</i>
Bub1	Budding uninhibited by benzimidazole 1
BuBR1	Bub1-related protein 1
CCAN	Constitutive Centromere-Associated Network
Cdc	Cell division cycle
Cdk	Cyclin-dependent kinase
CENP	Centromere protein
CPC	Chromosomal passenger complex
D-Box	Destruction Box
FRAP	Fluorescence recovery after photo-bleaching
GLEBS	Gle2-binding sequence
Hec1	Highly enhanced in cancer
KD	Kinase Dead
KEN-box	Lys-Glu-Asn-box
KNL1	kinetochore null protein 1
Mad	Mitotic arrest deficient
MELT	Met-Glu-Leu-Thr
MCAK	Mitotic associated Kinesin
MCC	Mitotic checkpoint complex
<i>Mis12</i>	Minichromosome instability 12
Mps1	Monopolar spindle 1
Ndc80	nuclear division cycle protein 80
PBD	Polo-box domain
Plk1	Polo-like kinase 1
PP1	Protein phosphatase 1
PP2A	Protein Phosphatase 2A
SAC	Spindle assembly checkpoint
SILAC	Stable isotope labeling in cell culture
siRNA	Small interfering RNA
TPR	Tetratricopeptide Repeat
WT	Wild type

“Take a moment to think about the context in which your next decision will occur: You did not pick your parents or the time and place of your birth. You didn't choose your gender or most of your life experiences. You had no control whatsoever over your genome or the development of your brain. And now your brain is making choices on the basis of preferences and beliefs that have been hammered into it over a lifetime - by your genes, your physical development since the moment you were conceived, and the interactions you have had with other people, events, and ideas. Where is the freedom in this? Yes, you are free to do what you want even now. But where did your desires come from?”

-Sam Harris, Free Will 2012

Foreword

I would like to express my sincere gratitude to my supervisor Dr. Sabine Elowe who welcomed me in her lab and guided me throughout my PhD research work at CHUL. I am grateful for the time and knowledge she shared with me during my research. I am also deeply indebted to Audrey Lajeunesse, a former master's student, for her support and guidance in the lab when I started this program. Also, her initial observations on Bub1 shaped my research project. I want to say many thanks to Philippe Thebault for this help in the lab. Dr. Danielle Caron provided her support and help on numerous occasions for which I am very thankful. I especially thank Guillaume Combes for his friendship, support and ideas during these four years. I will not forget others who have helped me in one way or another. I want to say my sincere thanks to Luciano Braga Gama, Michelle Mathieu and Abraham Alharbi for their support and friendship. Finally, I want to thank to those who participated in my research project in some way. I may not know them however, without their support this work could not have been accomplished.

The thesis presents analyses and results obtained during my Ph.D on the Bub1 kinase. The results describe the identification of autophosphorylation sites on Bub1 which was done prior to start of my Ph.D. The characterization and observation of Bub1 T589 site was done with the help of my colleagues, especially Audrey Lajeunesse. For better reading, I have divided this thesis into 4 chapters. The first chapter, the introduction, provides general discussion on past and recent literature. This chapter describes Cell cycle and its checkpoints. Then, I have given a brief summary of kinetochores since SAC activity takes place on them. Next, I have explained SAC and its importance which is followed by relevant proteins for this project: Sgo1, PP2A, Plk1 and Mps1. I have discussed past and recent literature on Bub1 in detail. Finally, I have discussed the Hypotheses and aims of this doctoral thesis.

Chapter 2 presents already published work on the Bub1 autophosphorylation site T589. The article titled "Bub1 autophosphorylation feeds back to regulate kinetochore docking and promote localized substrate phosphorylation" (Nature Communications 6, Article number: 8364 doi: 10.1038/ncomms9364) was published on 24 September 2015. I have contributed for this research article in Figure 2.1 (b,c,d), Figure 2.4 (a-d), Figure 2.5 (c-f), Figure 2.6 (b-e), Supplementary Figure 1 d, Supplementary Figure 2, Supplementary Figure 4 (except 2e). Chapter 3 provides unpublished initial results on regulation of Bub1 localization by Plk1. I have provided results in the form of a mini article. Fourth and final chapter presents discussion and future directions for research work Bub1.

1. Introduction

1.1. Cell cycle and Checkpoints

Most among billions of cells in human body remain in a reversible quiescent state (1, 2). The rest, cycle to duplicate their genomic content and divide into two daughter cells (3, 4). The cell cycle can be broadly divided into two phases: the actively dividing mitosis or M phase and non-dividing interphase (Figure 1.1). The cell cycle can also be divided into four distinct phases of G1, S, G2 and M (mitosis) phase (3, 5). The traverse through each phase is governed by regulatory protein complexes of cyclin dependent kinases (CDKs) and cyclins (6). A number of CDKs have been discovered e.g. CDK1, CDK2, CDK4 and CDK6 which are activated by specific cyclins e.g. cyclin B, cycline D, and Ccclin A during each phase of cell cycle. Cyclin expression is regulated throughout cell cycle to allow for controlled activation of CDKs (7-9). To protect cells from external influence that may induce errors, cells have developed "checkpoints" to regulate cell cycle timing for correction of errors (10, 11). Checkpoints are defined as "mechanisms by which the cell actively halts progression through the cell cycle until it can ensure that an earlier process, such as DNA replication or mitosis, is complete" (12).

There are three major checkpoints in eukaryotes: the G1/S checkpoint, the G2/M checkpoint and the spindle assembly checkpoint (SAC). The transition from G1 to S is monitored by G1/S checkpoint while the passage from G2 to M is controlled by G2/M checkpoint. The final major checkpoint, the SAC, lies within M phase.

1.1.1. G1 or gap1 phase

Cells enter G1 after cell division (3). During G1 phase cells synthesize proteins necessary for the next cell cycle phase called the S phase. The cells may also enter a reversible quiescent state called G0 or resting phase (5). G1 progression is regulated by CDK4/6-cyclin D and CDK2/cyclin E (9). The progression through early G1 is controlled by the regulation of retinoblastoma (Rb), a tumor suppressor protein involved in the repression of transcription factors e.g. E2F (13). Kinases CDK4 or 6, after activation by cyclin D, phosphorylate retinoblastoma (Rb) to dissociate it from histone deacetylase

(HDAC) proteins causing the repression of retinoblastoma and activation of E2F transcription factor to allow for gene transcription required for S Phase initiation (14).

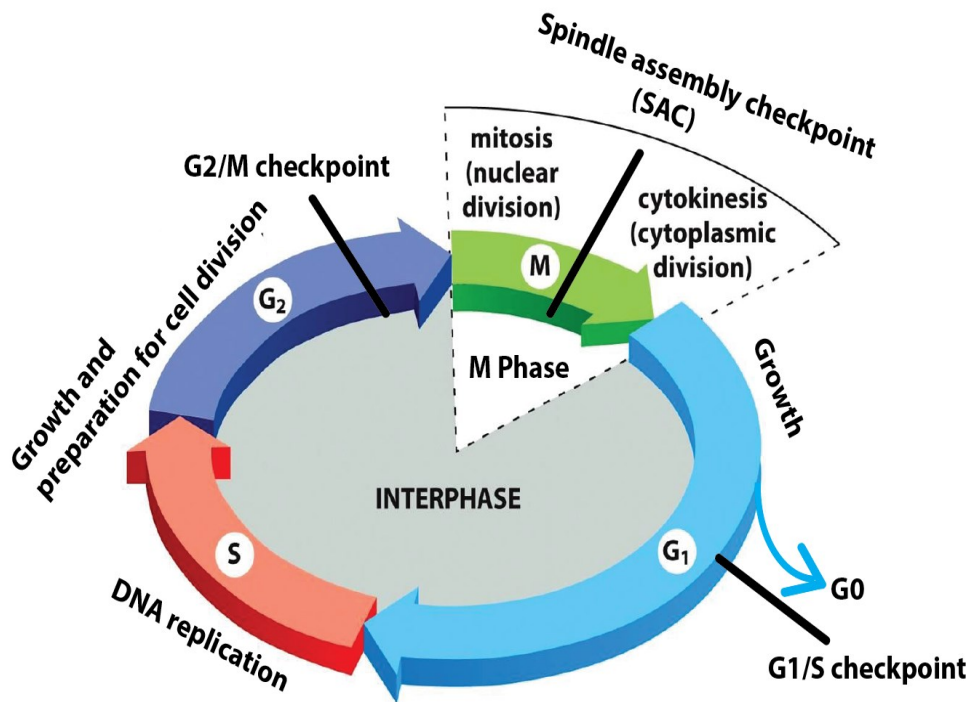


Figure 1.1 Four phases of cell cycle: G₁, S, G₂ and M shown with their respective activities and checkpoints. During G₁ cells start to mature and grow in size. It is during G₁ that cells decide whether to continue cell cycle or go into a quiescent state called G₀. G₀ is reversible and cells can enter cell cycle upon return of external growth factors. After G₁, cells enter S phase during which DNA replication occurs. After S phase cells have made a copy of their DNA which will allow equal distribution of genomic content into daughter cells during cell division. Next, the cells enter G₂ phase where they grow in size and prepare for cell division. Before entry into M phase, G₂/M checkpoint checks for DNA damage. The cells enter M phase during which their genomic content is equally divided into two daughter cells, thus completing cell cycle. SAC, the third checkpoint, delays mitotic progression until chromosomes are correctly captured by microtubules during mitosis. Modified from (15)

1.1.2. G₁/S checkpoint

The transition from G₁ to S is monitored by G₁/S checkpoint also known as Restriction -(R) point in mammalian cells and START in yeast (16). Removal of growth factors before this point brings cells into G₀ or quiescent state but

beyond that point withdrawal of growth factors does not affect the cell cycle as the cell becomes committed to cell cycle completion (17, 18). Rb proteins play a crucial role and prevent entry into S phase by transcription factor inhibition, however, after the decision to enter S phase, CDK4 or 6/Cyclin D and CDK2/cyclin E complex phosphorylate Rb to inactivate it and promote activation transcription factor E2F for S phase entry (19-21). During G1, DNA damage resulting in double stranded breaks activates the ATM (Ataxia telangiectasia mutated) kinase that phosphorylates CHK2 and p53 and represses the activation of CDK4/6-cyclin D and CDK2/cyclin E. In case of UV exposure DNA damage, the ATR (Ataxia telangiectasia and Rad3 related) complex phosphorylates its substrates that include CHK1 which in turns phosphorylates CDC25a phosphatase and causes its degradation by ubiquitination, hence CDC25a cannot activate phosphorylated CDK2 required for cell cycle progression (12, 22).

1.1.3. S phase (Synthesis phase)

During S phase, DNA replication synthesizes another copy of its DNA that will be received by one of the two daughter cells after mitosis. E2F transcription factor activity is required for synthesis of products to enter S phase (23), while activation of CDK2 by cyclin A or E is required for the initiation of DNA synthesis and progression from late G1 to S phase (24). The termination of DNA replication is mediated by a negative feedback loop in which E2F transcription factor helps synthesize cyclin A that activates CDK2 (6, 25, 26). Near the end of S phase, CDK2/cyclin A phosphorylates E2F1 factor for its dissociation from DNA and termination of DNA replication (6, 27).

1.1.4. G2 phase (Gap2 phase)

After the successful DNA replication in S phase, cells enter G2 phase to prepare for cell division (19). CDK1/cyclin A is required for cell cycle progression during G2 and is implicated in the activation of CDK1/cyclin B required for mitotic progression (28, 29). During G2, CDK2/cyclin A and CDK1/cyclin B phosphorylate a transcription factor FoxM1 to relieve its inhibition for gene expression required during mitosis (9).

1.1.5. G2/M checkpoint

The G2/M checkpoint or DNA damage checkpoint monitors DNA damage at the end of S phase before cells can divide their genetic material in M phase, thus allowing time for DNA repair (30). The target of G2/M checkpoint is CDK1 whose activation is required for mitotic entry (30, 31). Kinases WEE1 and MYT phosphorylate CDK1 leading to its inactivation, while the phosphatase CDC25 reverses this phosphorylation for activation by cyclin B (32). Upon DNA damage, both ATM and ATR pathways are activated depending on the nature of DNA damage (33). Phosphorylation of CDC25 phosphatase by ATM and ATR kinases binds it to 14-3-3 for its sequestration in cytoplasm and degradation. Meanwhile, WEE1 kinase phosphorylates CDK1 to keep it inactivated and cell cycle arrest is achieved (34, 35).

1.1.6. M phase (Mitosis)

M phase or mitosis is an important step for equal distribution of genetic material i.e. chromosomes, into two daughter cells (Figure 1.2) (36). The progression of M phase is monitored by CDK1/cyclin B also known as the mitotic promotion factor/maturation promoting factor (MPF) (8). CDK1/cyclin B kinase function promotes chromosome condensation, spindle generation and nuclear envelope breakdown (37).

There are five distinct steps of mitosis: prophase, prometaphase, metaphase, anaphase and telophase followed by cytokinesis for cytoplasmic content division into two daughter cells (Figure 1.2)(4). Prophase is the first distinct phase of mitosis identified by condensation of chromatin, a complex of DNA and its proteins (38). Further compaction of chromatin results in the formation of chromosomes which are held together by a protein complex known as cohesin (39). Cohesin is wrapped around chromatids during S phase and acts as a "glue" to keep sister chromatids together (Figure 1.2). It is removed from chromosome arms during prophase and later from centromeres during anaphase (40-42). At later stages of mitosis, chromosomes are captured by microtubules, the hollow cylindrical structures, arising from two centrosomes which are the microtubule organizing centers consisting of a pair of centrioles (Figure 1.2a) (43, 44). During prophase,

centrosomes start moving to the opposite poles and microtubules start to radiate from them.

The nuclear envelope is broken down during prometaphase to allow microtubules to access chromosomes to align them in the center by search and capture, a process during which microtubule growth and shrinkage allows them to search and bind special proteinaceous structures on centromeres called kinetochores (Figure 1.2b) (45, 46). Search and capture is a complex process that also requires motor proteins kinesin activity for kinetochore-microtubule interactions (45, 47, 48). The next stage, metaphase follows (Figure 1.2c) during which microtubules bind kinetochores from opposite poles in a bi-oriented manner and chromosomes align in the center of the cell (49, 50). Tension is generated due to pulling force of microtubules from opposite ends and resistance of cohesion between sister chromatids, thus stabilizing chromosomes in the middle.

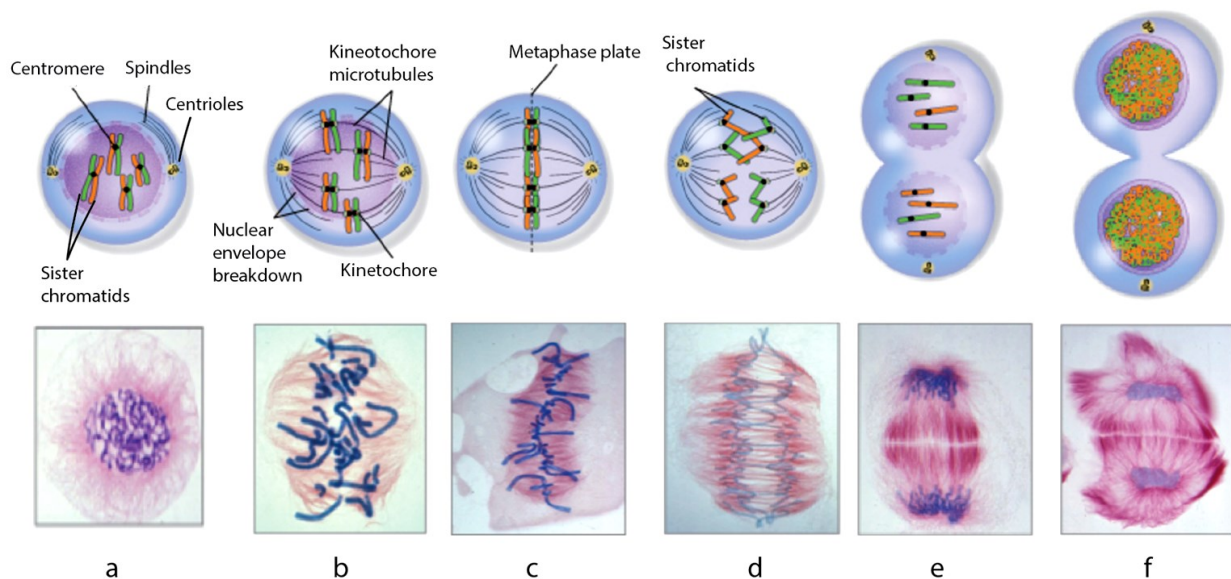


Figure 1.2 Stage of mitosis: a) Prophase is the first stage of mitosis. During this phase the chromatin becomes compact and takes the shape of a visible chromosome. The chromosomes appear to have x-shape connected by centromeres consisting of sister chromatids, the two identical copies forming a chromosome. The two centrosomes from opposite pole have their microtubule nucleation increased forming a dynamic spindle. b) Prometaphase: The nuclear envelop breaks down and microtubule can access chromosomes. Microtubules start to attach chromosomes at kinetochores. c) During Metaphase chromosomes after attaching with microtubules form metaphase plate, a plane perpendicular to the spindle, in the middle. d) Once

correct kinetochore-microtubule attachments are established the sister chromatids are separated during anaphase. e) The separated sister chromatids reach opposite poles and nuclear membrane starts to form around them during telophase. f) The cytoplasmic content of the cell are divided into two daughter cells during cytokinesis, thus completes division of genetic and cellular contents. Modified from <http://www.nature.com/scitable/topicpage/mitosis-and-cell-division-205#>

Anaphase ensues after correct chromosome alignment in the center. The sister chromatids are separated by cleavage of cohesin around them (Figure 1.2d) (51). There are two stages of anaphase: A and B (52). During Anaphase A, kinetochore microtubules (kMT) are shortened due to depolymerisation resulting in a force that drives poleward movement of separated sister chromatids. During anaphase B, centrosomes move further toward the periphery which pulls separated chromatids apart even more (53, 54). The separated chromatids reach opposite poles which marks the last step, the telophase (Figure 1.2e). The nuclear envelope starts to form around them and the newly separated chromosomes start to decondense (55). The final step, cytokinesis separate and equally divide cytoplasmic content into two nascent daughter cells thus, completing the cell division (Figure 1.2f).

1.2. Kinetochores- proteinaceous structures on chromosomes during mitosis

Kinetochores are proteinaceous structures formed on chromosomes during mitosis to mediate binding between chromosomes and microtubules, thus are crucial for proper chromosome segregation (55, 56). They are assembled on special regions on chromosomes called centromeres (57, 58). Specifically, kinetochores assemble on inner centromeres composed of DNA and proteins that are collectively called constitutive centromere-associated network (CCAN), and are required for kinetochore assembly (59, 60). Microtubules bind kinetochores during mitosis and the number of microtubules binding to each kinetochore vary among organisms. While in budding yeast (*Saccharomyces cerevisiae*) only one microtubule binds a kinetochore (61, 62), it is estimated that approximately 15-30 microtubules attach each kinetochore in humans (63). The number of microtubules also determines the strength of SAC on each kinetochore in organisms where more than one microtubule binds to a kinetochore (64).

Vertebrate kinetochores appear to have a "trilaminar" structure (Figure 1.3a, b) i.e. having three distinct layers: the inner, the middle and the outer layer (65, 66). The inner kinetochore (inner plate) is located next to the inner centromere. The middle layer follows to the exterior and outer kinetochore (outer plate) is first to encounter kinetochore microtubules (kMT). Fibrous structures emerging away from outer kinetochores are called the fibrous corona (67).

There are about 100 kinetochore proteins identified in humans (55, 68). The outer kinetochore layer (Figure 1.3) contains SAC proteins that include MAD1 (mitotic arrest deficient 1), MAD2 (mitotic arrest deficient 2), RZZ (Rod-Zwilch-ZW10) complex, CENP-E (Centromere Protein-E) MPS1(monopolar spindle 1), BUB1(budding uninhibited by benzimidazoles 1), BUBR1(BUB1-related 1) and BUB3 (budding uninhibited by benzimidazoles 3) as well as KMN network proteins: KNL1 (kinetochore null protein 1) complex, MIS12 (mis-segregation 12) complex or MIS12C and NDC80 (nuclear division cycle protein 80) complex or NDC80C (Figure 1.3) important for microtubule binding and spindle assembly checkpoint (69).

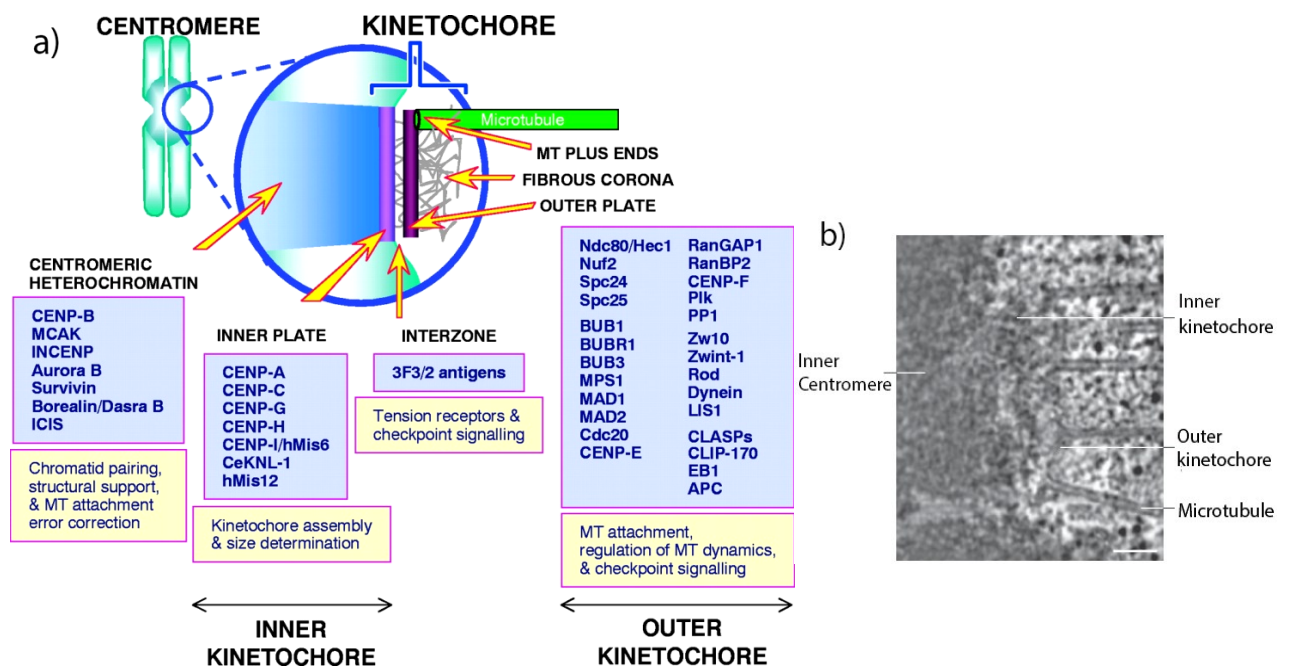


Figure 1.3 Kinetochore is a trilaminar multiprotein complex: a) Kinetochores are trilaminar structures i.e. having three layers, an inner, middle and outer region. They host a variety of proteins required for its assembly and microtubule binding. The CENP proteins at the inner kinetochores are required for kinetochore structure and assembly while the outer kinetochore contains SAC proteins for correct attachment kinetochore-microtubule attachments. Image from (69). b) Electron micrograph showing trilaminar human kinetochore bound to microtubules. Scale bar, 100 nm. Modified from (55).

KMN network proteins are composed of several subunits. KNL1 forms a complex with ZWINT (Zeste white 10 interactor). The MIS12 complex is composed of 4 subunits: MIS12, NSL1, DSN1 and NNF1 while the NDC80C also contains 4 subunits: SPC24, SPC25, NUF2 and NDC80 (70). The inner plate hosts various CENP proteins e.g. CENP-A, CENP-C, CENP-H/-I, required for kinetochore structural integrity (69, 71, 72).

Once at kinetochores, KMN proteins bind stably at kinetochores which are important for various functions during mitosis (72). The Spc24 and Spc25 heterodimer is required for end-on kinetochore attachment whereas NDC80

and NUF2 contact microtubules (Figure 1.4) (73, 74). The NDC80C interacts with MAD1 to promote its recruitment and also supports recruitment of MAD2, MPS1 and RZZ, and therefore, acts as a scaffold for checkpoint protein recruitment (75-78).

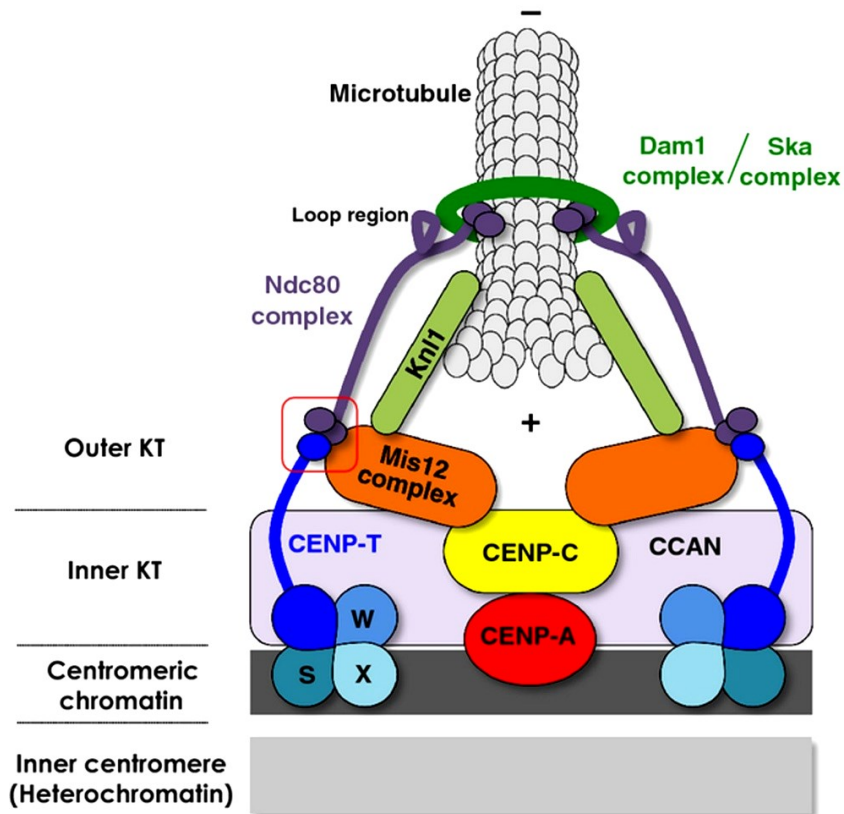


Figure 1.4 Assembly of kinetochore proteins: Kinetochores assembled on the inner centromere contain CCAN proteins. In vitro analyses have shown that CENP-T forms a complex with CENP-W, -S, and -X required for DNA supercoiling. NDC80C is recruited through interaction with CENP-T and also binds microtubules. NDC80C also binds DAM1 complex (SKA in humans) through its loop region. Together with NDC80C, SKA complex is required for stable kinetochore-microtubule binding. CENP-A connects inner kinetochore components and CCAN network via CENP-C. CENP-C recruits MIS12C at kinetochores. Once at kinetochores, MIS12C acts a scaffold for KNL1 and NDC80C. KNL1 also acts as scaffold for core SAC proteins and forms interactions with microtubule via its N-terminus. Image from (58).

MIS12C binds directly with centromeric DNA and CCAN to promote its recruitment and acts as a scaffold for KNL1C and NDC80C to mediate kinetochore assembly (Figure 1.4) (68, 74). KNL1 is recruited to kinetochores by MIS12C where it heterodimerizes with ZWINT and is required for

recruitment of CENP-F and protein phosphatase PP1 (68, 79-81). In vitro analyses have shown that KNL1 can bind microtubules that could lead to SAC silencing (74, 82). In addition to microtubule binding, KNL1 is a well-known anchor for components of SAC that include BUB3, BUB1 and BUBR1, thus promote SAC activation (79, 83). More specifically, KNL1 is a target of MPS1 kinase whose phosphorylation is required to recruit these proteins which is explained in more detail in MPS1 section (84-87).

1.3. Spindle assembly checkpoint (SAC)

The SAC also known as mitotic or spindle checkpoint is a surveillance mechanism that delays mitotic progression until correct attachments between kinetochores and microtubules are established (88-90). For this reason, the SAC signal is emitted from unattached kinetochores to ensure accurate attachments and equal distribution of chromosomes into daughter cells and thus it preserves genomic integrity (88-91).

1.3.1. SAC monitors specific attachments between kinetochores and microtubules

The attachments between microtubules and kinetochores are very specific to allow for equal division of chromosomes i.e. each kinetochore must bind microtubules only from one pole (amphitelic attachment) to achieve bi-orientation (92-94) (Figure 1.5). However, incorrect attachments may occur which include syntelic attachments, when both kinetochores of a chromosome are attached to microtubules from the same pole; merotelic attachments occur when kinetochores attach microtubules from both poles. Merotelic attachments eventually segregate chromosome normally but when they persist till anaphase they can cause aneuploidy (95-97). Monotelic attachments predominantly prevail during prometaphase before bi-orientation (92, 93). Hence, the goal of SAC is to achieve amphitelic attachments or bi-orientation between chromosomes and microtubules.

1.3.2. SAC senses tension and kinetochore attachments

The establishment of bi-orientation causes tension across kinetochores due to microtubule driven pulling forces from opposite poles which stabilizes these attachments (98). Therefore, nature of SAC regarding tension and attachment has been a matter of debate (99). Pioneering work on kinetochore-microtubule attachments discovered that kinetochores emitted a "wait anaphase signal" in the presence of mono-oriented chromosomes that can be relieved by laser induced destruction of unattached kinetochore suggesting that SAC senses attachment at kinetochores (100). Meanwhile, studies in preying mantid spermatocytes revealed that tension exerted by micromanipulator needle on misoriented chromosome reduced mitotic delay (101). Later, micro-needle manipulation studies demonstrated that a mono-

oriented chromosome created from bi-oriented chromosome lost tension however, the number of microtubules on the sister kinetochores were also reduced (102). A recent study in budding yeast using isolated kinetochores and their interaction with microtubules concluded that tension increases the stability of kinetochore-microtubule attachments (98). Hence, tension encourages stable kinetochore-microtubule attachments and the SAC responds to both tension and kinetochore-microtubule attachments (99).

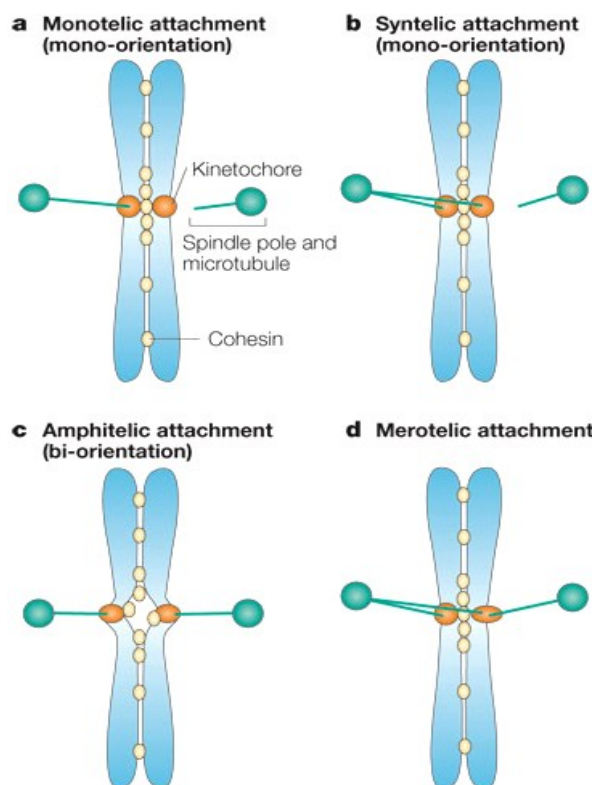


Figure 1.5 Attachments monitored by SAC: **a)** Monotelic attachments occur in prometaphase before amphitelic attachment is achieved. **b)** Syntelic attachments are attachments when both kinetochores bind microtubules from the same pole. **c)** The amphitelic attachments are correct attachments between chromosomes and microtubules needed for genomic integrity during which two sister kinetochores on a chromosome are captured by microtubules from opposite poles, thus each kinetochore experiences tension from one centrosome. **d)** Merotelic attachments occur when one kinetochore is bound by microtubules from both centrosomes. Image from (97) .

1.3.3. The strength of the SAC varies during mitosis

Recent studies have shown that SAC is more dynamic than it was believed to be and functions more like a rheostat than a toggle switch i.e. having variation in its strength rather than working in an on/off fashion (103, 104). Previously, it was demonstrated that a single kinetochore was enough to arrest cells in mitosis for “wait anaphase” signal (100). However, in agreement with the rheostat model recent mouse studies have shown that after depletion of CENP-E, a protein required for stable kinetochore-microtubule binding, SAC strength diminishes and cells exit mitosis in the presence of one or few unattached kinetochores suggesting that the strength of SAC is graded (103). Studies by laser microsurgery for chromosome detachment in human cells revealed that individual chromosomes did not impose SAC efficiently compared to controls in which complete spindle disruption occurred (105). Furthermore, a recent study concluded that APC/C (anaphase promoting complex/cyclosome) strength can modulate SAC in humans i.e. the strength of APC/C can dictate the SAC strength (106). APC/C is activated by CDC20 (cell division cycle 20) to promote mitotic exit, whereas MCC (mitotic checkpoint complex) inhibits APC/C and mitotic exit. CDH1(CDC20 homolog 1) is another APC/C adaptor protein that is required for the activation of APC/C; however it is not needed for mitotic exit for it is required in G1 phase (107) and thus will not be discussed in this manuscript. Analyses of APC/C and MCC revealed that MCC can bind two CDC20 molecules to inhibit APC/C activation pointing to a rapid response upon reactivation of spindle assembly checkpoint (108). Data in *C.elegans* embryogenesis have demonstrated that SAC strength depends on cell size rather than development stage (109). In summary, above studies clearly show that SAC does not work in a switch like manner on the contrary SAC strength is graded.

1.3.4. SAC Components

SAC components were discovered in the 1990s in budding yeast genetic screens in which cells could not arrest in mitosis when challenged with spindle poisons to induce spindle damage (110-112) . It was suggested that failure to arrest in these conditions i.e. spindle damage, which normally

induce mitotic arrest was a result of a dysfunctional checkpoint and the mutant genes isolated were components of that checkpoint (110). The core mitotic checkpoint proteins include BUB1, BUBR1 and BUB3 (110, 111, 113); MAD1 and MAD2 (111, 114, 115), MPS1 (112), PLK1 (*polo like kinase 1*) (116, 117), AURORA B, RZZ complex (118, 119) and CENP-E (120). BUB1 and MAD1 are stably bound kinetochore proteins while others e.g. BUBR1, MPS1 are exchanged frequently (89, 121). The main target of SAC is APC/C, a multiprotein E3 ubiquitin ligase (89, 108, 122, 123). SAC members converge on unattached kinetochore to orchestrate MCC formation required for inhibition of APC/C activation (122, 124) (Figure 1.6).

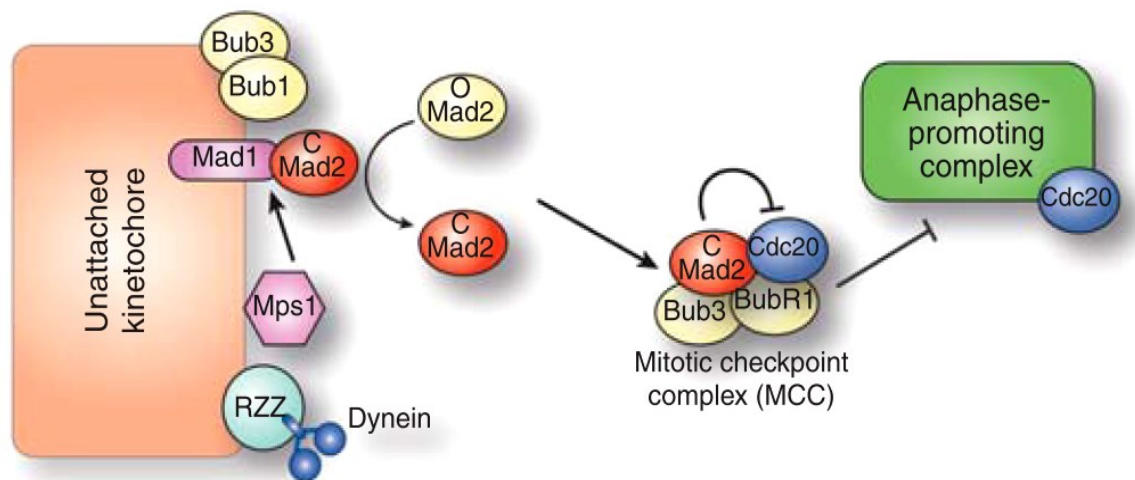


Figure 1.6 SAC signal prevents mitotic progression: SAC proteins accumulate at unattached kinetochores. Assembly of core SAC proteins MPS1, MAD1, MAD2, BUB1, BUB3, and BUBR1 promotes the formation of an inhibitory complex, MCC (Mitotic checkpoint complex) to prevent activation of APC required for mitotic progression. APC/C requires CDC20 cofactor for its activation. As a result mitosis is halted by SAC proteins until unattached kinetochores achieve correct attachments. Modified from (57)

1.3.5. Mitotic checkpoint complex (MCC)

MCC is composed of checkpoint proteins MAD2, BUBR1, BUB3 and CDC20 (122, 125, 126). Both MAD2 and BUBR1 can directly bind CDC20 (122, 124). The “template model” of MAD2 activation (Figure 1.7a) is the contemporary model that explains MCC formation and inhibition of APC/C activation (127).

MAD2 has the ability to adopt two distinct topological conformations: Open MAD2 (O-MAD2) and Closed MAD2 (C-MAD2) (128, 129). O-MAD2 is cytosolic, inactive and cannot bind to MAD1 or CDC20, thus cannot inhibit APC/C activation (130, 131). The other conformation, C-MAD2, is active and bound MAD2 conformation that makes adjustments in its carboxy-terminal β -sheet to wrap around and lock MAD1 or CDC20 in a "safety belt" manner. Therefore, this region of MAD2 is termed as safety belt (Figure 1.7a) (132-134). A kinetochore bound MAD1-C-MAD2 complex catalyzes the conformational change of inactive O-MAD2 to an intermediate MAD2 (I-MAD2), a transition state, before it can become active C-MAD2, capable of binding CDC20 (129-131, 135). In vitro studies showed that CDC20-C-MAD2 complex is identical to MAD1-C-MAD2 complex and can promote conversion of O-MAD2 to C-MAD2 in the cytosol like MAD1-C-MAD2 does on unattached kinetochores (127, 136). However, C-MAD2 surface in the cytosol is involved in interactions with BUBR1 or p31comet, a SAC silencing protein (137, 138) and may not provide for conformational conversion of MAD2 (129, 139). Finally, BUBR1-BUB3 also joins CDC20 and C-MAD2 (Figure 1.7b) and completes the formation of MCC (124, 129, 138).

The SAC kinases, MPS1 and BUB1 also contribute to the formation of MCC. It has been shown that MPS1 inhibition abrogates MCC formation and BUB1, MAD1, MAD2 and BUBR1 localization is reduced (140). Furthermore, MPS1 kinase function recruits O-MAD2 to kinetochore bound MAD1-C-MAD2 and inhibition of MPS1 leads to the eviction of MAD2 from partially intact MCC (CDC20-BUBR1) causing SAC defects (140-143). In budding yeast, MPS1 phosphorylates BUB1 to promote BUB1-MAD1 complex at kinetochores (144). BUB1 kinase is also implicated in the recruitment of MAD1 and MAD2 at kinetochores to facilitate MCC formation (145-148). BUB1 phosphorylates MAD1 in vitro (149), however, a number of studies have reported that while BUB1 is required for MAD1 recruitment its kinase activity is redundant for this function (145, 148, 150, 151). Both MPS1 and BUB1 are required for the recruitment of BUBR1 at unattached kinetochores and thus contribute in MCC formation (140, 146).

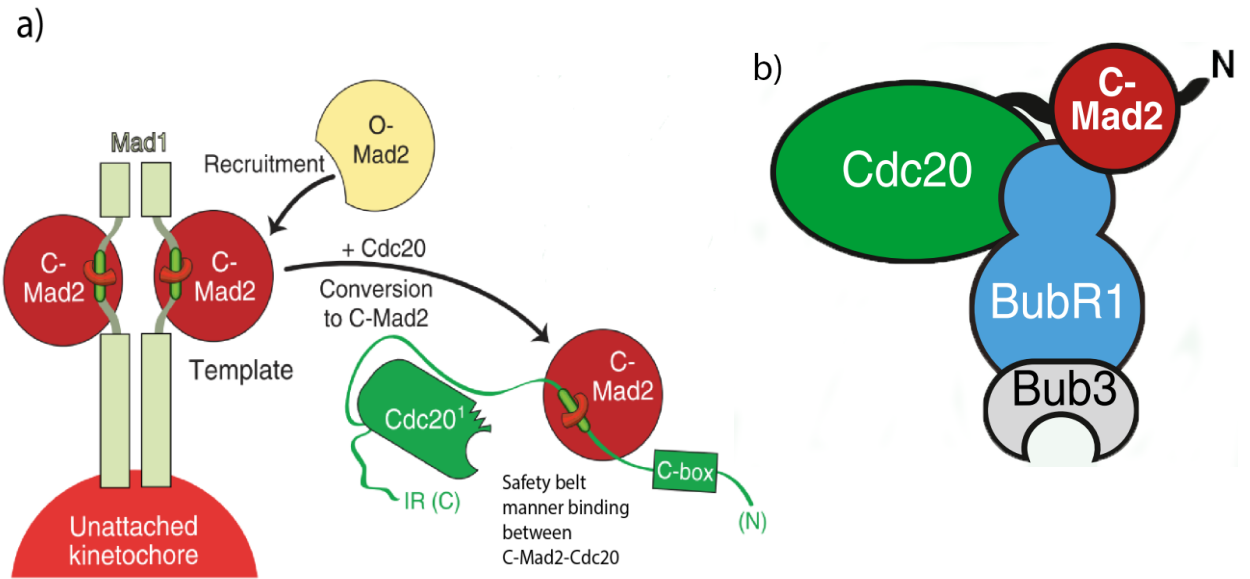


Figure 1.7 MCC formation: a) MAD2 exists in two conformations: O-MAD2 (Open MAD2) and C-MAD2 (Closed MAD2). MAD2 in C-MAD2 conformation can bind MAD1 and CDC20. MAD1-C-MAD2 complex at unattached kinetochores recruits O-MAD1 and converts into C-MAD2 that can bind CDC20. The interaction of O-MAD2 with CDC20 is facilitated by MAD1-MAD2 complex. **b)** CDC20-C-MAD2 becomes part of a functional MCC by incorporation of BUBR1/BUB3 complex that binds between CDC20 and C-MAD2 and forms simultaneously interactions with CDC20 and C-MAD2. Modified from (88).

1.3.6. Molecular basis of APC/C inhibition and anaphase delay

Rapidly exchanging CDC20 at kinetochore has major structural domains that include seven WD40 domains arranged into a β -propeller structure for protein-protein interactions; a C-Box; a KEN (lysine-glutamate-asparagine) box; a CRY box (Cysteine, Arginine, Tyrosine); a MAD2 interacting motif (MIM); and a C terminal IR (isoleucine-arginine) tail (152, 153). The N-terminus, C-Box and C-terminus IR-tail are required to bind CDC20 with APC/C (134, 154). KEN and CRY boxes are involved in regulation of CDC20 stability (155, 156).

Protein degradation is regulated through recognition of degradation signal or degron defined "as a minimal element within a protein that is sufficient for recognition and degradation by a proteolytic apparatus" (157). CDC20 has dual activity towards APC/C i.e. it acts as a suppressor when bound to MCC and as an activator of APC/C near the start of anaphase (122, 152, 154, 158). When acting as an activator of APC/C, CDC20 recruits substrates and activates APC/C through recognition of two degrons called destruction (D-box) box and KEN box of substrates which allows for their destruction by ubiquitylation (126, 152, 156, 159, 160).

CDC20 acts an inhibitor of APC/C when present in complex with C-MAD2 and BUBR1. It blocks substrate recognition sites thus preventing APC/C activation (124, 161). The C-terminal "safety belt" of C-MAD2 wraps around CDC20 MIM, a region that overlaps with APC/C binding region (124, 162-164). A recent study showed that MAD2 can bind to a short conserved motif known as KILR (Lysine-Isoleucine-leucine-arginine) present in MIM required for APC/C activation and thus competes with APC/C for CDC20 binding (134). Mutagenesis studies have shown that MIM can separate activator and repressor function of CDC20 (88). MIM mutant unable to bind MAD2 overrides the SAC and has efficient APC/C activity (162, 165). C-MAD2 also promotes BUBR1-CDC20 binding and acts synergistically with BUBR1 for APC/C inhibition (125, 166). However, BUBR1:CDC20 complex can be formed without MAD2 suggesting MAD2-CDC20 acts as diffusible amplifier of BUBR1-CDC20 to sustain MCC activity (167-170).

BUBR1 interacts with both CDC20 and C-MAD2 (Figure 1.8)(88). Through its N-terminus region, it binds two conserved residues (Arg133 and Gln134) of C-MAD2 for inhibition of APC/C (138), while its two KEN boxes, KEN1 and KEN2 have been studied for interaction with CDC20 (160, 171-174). BUBR1 KEN1 box is essential for MCC formation and inhibiting APC/C activity by blocking KEN degron binding on CDC20, thus acting as a pseudosubstrate inhibitor of CDC20 (124, 160, 175). However, a recent study in human cells has shown that mutating KEN1 box does not affect CDC20 kinetochore recruitment although it severely reduces MCC formation (176). Instead

another region termed as internal CDC20 binding domain (IC20BD) (aa 490–560) that encompasses a Phe box (contains two phenylalanines) and a D-box binds CDC20 and promotes SAC silencing (176). The second BUBR1 KEN box (KEN2) is required for inhibition of activated APC/C-CDC20 (124, 160). It was confirmed recently that KEN2 along with D-box is required to bind a second CDC20, thus forming MCC^{2Cdc20} for rapid inactivation of activated APC/C (Figure 1.8)(108). Studies have confirmed that the BUBR1 middle region (BUBR1M) containing D-box and an ABBA (Cyclin A, BUBR1, BUB1 and Acm1) motif, also known as Phe box or A box binds CDC20 for maintaining MCC (161, 177). In summary, inactivation of APC/C requires extensive interactions of BUBR1 and C-MAD2 with CDC20.

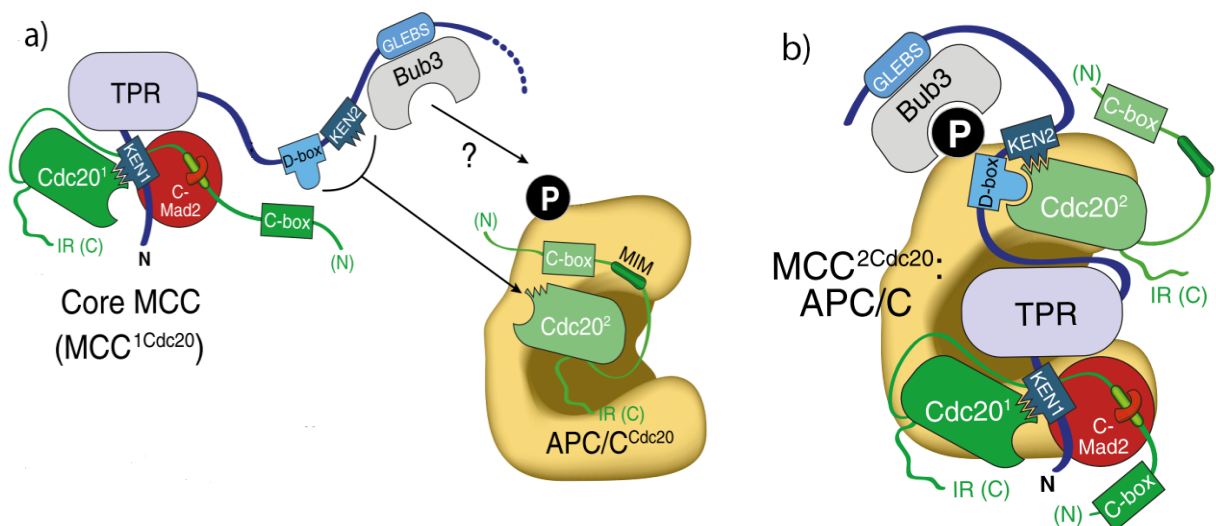


Figure 1.8 Inhibition of APC/C: **a)** BUBR1 KEN box motifs occupy CDC20 KEN1 box recognition motif thus blocking its activity toward APC/C substrate. BUBR1 also binds to MAD2 via its N-terminus TPR region KEN box motif. C-MAD2 binds CDC20 through “safety belt” thus; forming a Core MCC with only 1 CDC20 that can bind to APC/C for its inhibition. **b)** BUBR1 has a second KEN box that binds a second CDC20 and forming an MCC with 2 CDC20 molecules (MCC^{2Cdc20}) for effective inhibition of APC/C. The binding of a second CDC20 may also help when rapid inactivation of APC/C is needed after its initial activation. Modified from (88).

1.3.7. APC/C activation and mitotic progression

Upon accurate kinetochore attachments, SAC is turn-off and APC/C is activated by CDC20 (Figure 1.8) (89, 129, 178). Activated APC/C-CDC20 promotes transition from metaphase to anaphase through two key regulatory events that involve destruction of APC/C substrates: a) APC/C polyubiquitylates cyclin B for its degradation to inactivate CDK1. b) APC/C polyubiquitylation of securin, an inhibitor of separase enzyme, for its destruction (Figure 1.8). Separase enzyme then cleaves cohesin between two sister chromatids to separate them (88, 89, 159).

1.3.8. SAC Silencing

1.3.8.1. SAC silencing through Phosphoregulation

SAC activity is immensely promoted by the activity of kinases, thus its inactivation must require phosphatase activity (Figure 1.9). For this reason, a tight balance between phosphorylation and dephosphorylation has been observed during mitosis (179). SAC proteins orchestrate their own removal from kinetochores by recruiting phosphatases through a negative feedback mechanism (180, 181). Several studies have highlighted the role of PP1 (Protein phosphatase 1) and PP2A (Protein phosphatase 2A) in the regulation of SAC (80, 180-186).

The studies in budding and fission yeast have shown that PP1 activity is required for SAC silencing by reversing the phosphorylation needed for SAC activation (182, 183). PP1 binds at KNL1 N-terminus conserved SILK (Serine, Isoleucine, Leucine and Lysine) and RVSF (Arginine, Valine, Serine, Proline) motifs to negatively regulate the recruitment of BUB1 and other downstream SAC proteins thus, promotes SAC silencing (80, 184, 185, 187).

BUBR1 binds PP2A for regulation of mitotic progression and kinetochore-microtubule attachments (188-190). Kinetochore recruitment of BUBR1-PP2A complex is promoted by MPS1 and PLK1 kinase activity at KNL1 (84, 85, 191-194). Studies in human cells have demonstrated that PP2A removes KNL1 phosphorylation needed for SAC activation, thus can efficiently counter SAC activation (181). Recent studies have proposed that the negative feedback mechanism sufficiently explains rapid SAC On/Off when an opposing

phosphatase is already bound to core SAC protein but it will pose a problem for an efficient SAC signaling (195). For this reason, negative feedback phosphatase PP2A does not directly antagonize SAC at KNL1, instead it opposes AURORA B substrate phosphorylation that promotes PP1 binding to KNL1 which then promotes SAC silencing that eventually removes PP2A-B56 from kinetochores (Figure 1.9) (180, 195, 196). This added layer of control may provide enough temporal separation between SAC activation and silencing (195).

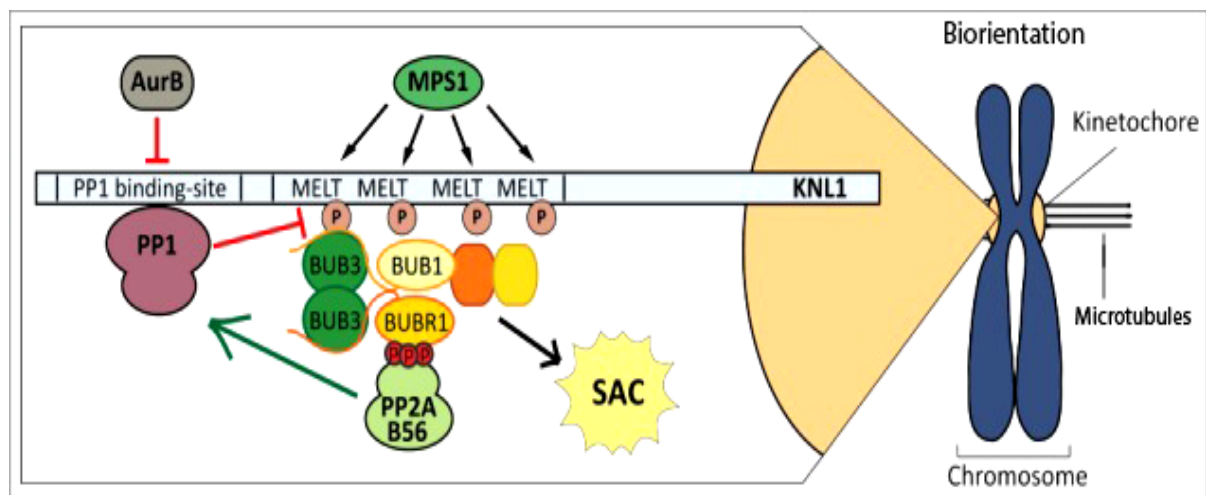


Figure.1.9 SAC silencing by Phosphoregulation: Phosphorylation of KNL1 by MPS1 helps mount SAC by recruiting BUB3 that binds BUB1 and BUBR1 which later recruit downstream SAC proteins including MAD1, MAD2 and CDC20 etc. BUBR1 binds PP2A-B56 phosphatase and recruits it to kinetochores. AURORA B activity counteracts PP1 kinetochore localization at SILK and RVSF motifs. Upon correct attachments, phosphatase activity of PP2A opposes AURORA B activity leading to PP1 binding to KNL1. PP1 then antagonizes MPS1 activity thus, removing BUB3, BUB1, BUBR1 and PP2A-B56 from kinetochores. In this negative feedback mechanism PP2A promotes PP1 recruitment that effectively silences SAC. Overall, SAC proteins recruited by kinase function, bring phosphatases for their own regulation at kinetochore leading to SAC silencing. Modified from (195).

1.3.8.2. Stripping of SAC components

Localization of core SAC proteins MAD1, MAD2, BUB1, BUBR1 and BUB3 is reduced at kinetochores during anaphase providing evidence that SAC proteins are removed from kinetochores for SAC silencing (113, 115, 197-

201). Stripping or physical removal of SAC proteins has been proposed to achieve SAC silencing via the minus-end directed microtubule motor Dynein complex (202, 203).

Dynein binds its cofactor Dynactin, a multisubunit activator complex, required for its motor function (204-207). In addition, Dynein-dynactin complex requires RZZ, a complex essential for functional SAC, and Spindly, a Dynein recruitment factor, for its kinetochore binding (Figure 1.10) (208-211).

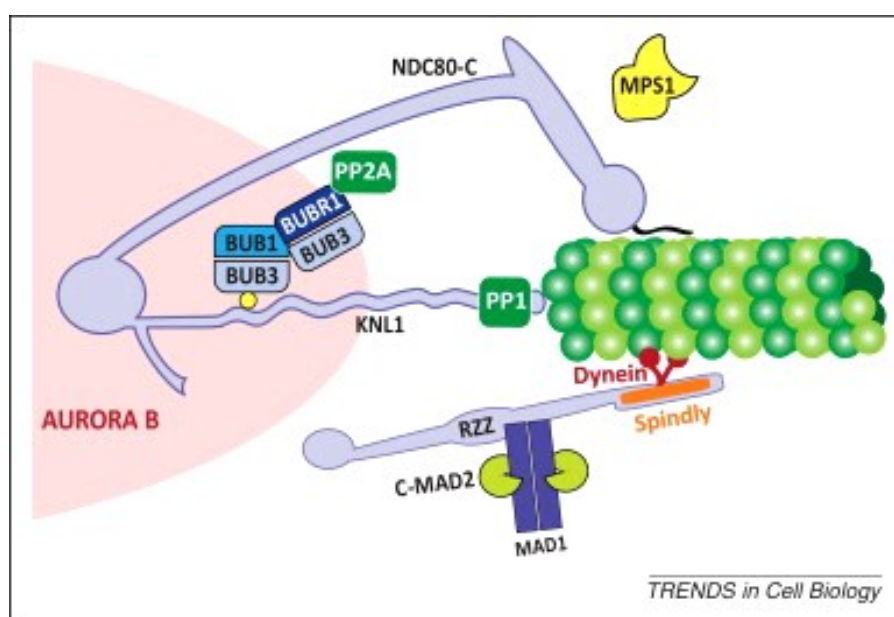


Figure 1.10 SAC silencing by stripping: Dynein, a motor protein complex, is recruited to kinetochores through interactions with RZZ and Spindly and moves towards minus ends (polewards) on microtubules. Dynein complex is important for stripping of MAD1-MAD2 and therefore also for silencing the SAC. Retention of Spindly suppresses SAC silencing for this reason Dynein mediated removal of Spindly and RZZ is required for SAC silencing. Image from (212).

MAD1 and MAD2 are carried towards microtubule minus-ends by Dynein-Dynactin complex after accurate kinetochore-attachments as inhibition of Dynein complex leads to retention of residual MAD2 and persistent checkpoint activity (213-215). Although, these studies explain SAC protein stripping from kinetochores, others have suggested that stripping is more likely an auxiliary pathway for SAC silencing because the depletion of human Spindly causes Dynein recruitment defects yet MAD1, MAD2, BUBR1, Zwilch, and CENP-E are still removed and SAC is silenced suggesting a Dynein-

independent SAC silencing mechanism (210, 214). Interestingly, mutants of Spindly that impaired Dynein recruitment and localized normally to kinetochores still had MAD1, MAD2 and RZZ complex and defective SAC silencing (214). Therefore, SAC silencing occurs only after removal of Spindly, suggesting that Spindly may suppress the SAC protein stripping mechanism, and removal of both Spindly and RZZ by Dynein is crucial for SAC silencing (214, 216).

1.3.8.3. MCC disassembly

MCC disassembly provides another way of SAC silencing. p31^{comet} was discovered in yeast as a MAD2 partner whose overexpression caused premature securin destruction leading to precocious mitotic exit and its RNAi-mediated depletion promoted anaphase onset delay (217, 218). p31^{comet} can bind C-MAD2 on the same surface where BUBR1 or O-MAD2 binds, thus p31^{comet} promotes MCC disassembly and SAC silencing (Figure 1.11) (137, 219). A "capping model" has been proposed in which p31^{comet} caps C-MAD2 in MAD1-C-MAD2 complex and interferes with the recruitment of O-MAD2 (137, 220, 221). However, later studies suggested that capping model is not efficient in explaining SAC silencing as depletion or overexpression of p31^{comet} does not change O-MAD2 levels at kinetochores (222, 223). p31^{comet} also binds C-MAD2 in complex with CDC20 to cause disruption of MCC complex and activation of APC/C (Figure 1.11) which is considered more plausible for p31^{comet} mediated SAC silencing (222, 224). p31^{comet} binding to MAD2 also encourages conformational changes in CDC20 that leads to CDK phosphorylation of CDC20 and promotes its dissociation from BUBR1 (225). Recent analyses of MCC disassembly points to a two-step process: BUBR1 is released from MCC by p31^{comet} that binds to the same surface on C-MAD2 and requires CDK activity. In the next step CDC20-C-MAD2 subcomplex disassembly requires p31^{comet} and ATPase Thyroid Receptor Interacting Protein 13 (TRIP13) (226).

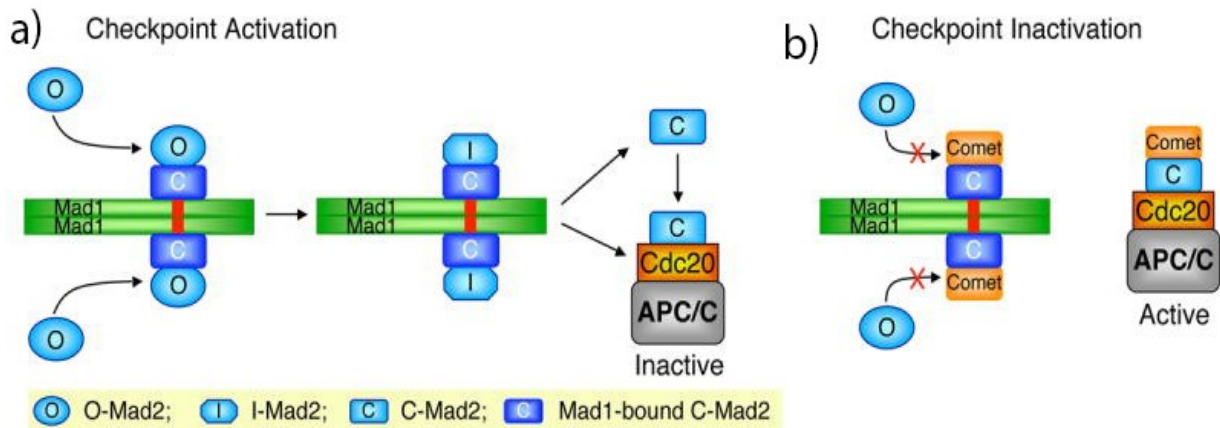


Figure 1.11 Disassembly of MCC: **a)** MAD1-C-MAD2 complex recruits O-MAD2 to convert it into C-MAD2 by binding to CDC20 and effectively promotes APC/C inhibition. **b)** During SAC silencing, p31^{comet} competes with MAD2 and interferes in the process of O-MAD2 recruitment to MAD1-C-MAD2 thus inhibits the conversion of active C-MAD2. p31^{comet} also directly binds to CDC20 and antagonizes MAD2 binding, thus inhibiting MCC formation (modified from (219)).

1.3.9. Importance of SAC

Aneuploidy refers to “an abnormal karyotype that is not a multiple of haploid complement” (227). It is reported that aneuploidy is present in over 90% of tumors and has the potential to cause cancer (228, 229). While the SAC ensures genomic integrity due to its ability to halt the progression of mitosis in case of incorrect microtubule attachments with kinetochores, its deregulation has been implicated in aneuploidy and tumorigenesis reviewed in (230, 231). Partial loss of the SAC manifested in deregulation of SAC protein expression contributes to chromosome instability rather than complete loss of SAC (232, 233). A complete loss of the SAC has been implicated in embryonic mortality at early stages which seems to be conserved in *Drosophila* and mouse models. Studies involving a null MAD2 resulted in embryonic death and initial studies on *Drosophila* showed embryonic mortality in BUB1 null embryos (234, 235). Thus, the CIN effects are only detected in partially defective checkpoint perhaps due to requirement the SAC for cell survival during early development. One of the earliest studies on SAC reported that mutations in BUB1 contributed to chromosomal instability (CIN) (236). The mutations of BUB1 paralog BUBR1

have been associated with growth defects and cancers (237). Moreover, altered MAD2 expression in breast cancer has been reported (238). The SAC genes overexpression is also reported as a cause of aneuploidy. Upregulation of *Bub1*, *Bub3/BubR1* has been reported in breast and gastric cancers respectively (239). *Mad2* overexpression has also been shown to promote aneuploidy (240). Studies have reported a role of parallel signaling pathways that can contribute to altered SAC gene expression. Studies in human cells have shown that mutations in proto-oncogene p53 could alter the expression of *Mad1* SAC genes (241, 242). The overexpression of SAC components induces persistent mitotic arrest, change in mitotic timing and merotelic attachments (reviewed in (232)). Kinase function of bona fide mitotic kinases has also been implicated in progression of cancer. For example, MPS1 kinase is shown to be overexpressed in many human cancers and may promote proliferation and survival of tumor cells (243-245). Overexpression of AURORA kinases can promote polyploidy and chromosome instability while overexpression of PLK1 has been associated with human cancer and weak prognosis (reviewed in(246)). MPS1 inhibition in combination with drugs affecting microtubules known as microtubule targeting agents (MTAs) has been suggested as anti-cancer strategy due to increased in chromosome segregation defects that cannot sustain survival of cancer cells. Indeed, MPS1 inhibition in combination with low doses of Taxol drug has been effective in tumor cell sensitization (247). BUB1 kinase function has been shown to promote cell growth through transforming growth factor- β (TGF β) receptor and BUB1 inhibition severely affected TGF β pathway in human cancer cells (248). Therefore, inhibition of these core SAC kinases by chemical inhibitors provides an attractive strategy against tumor proliferation and growth and is a subject of intense current research.

SAC components that include BUB1, MPS1 and MAD2 are also involved in the control of accurate division during meiosis, a process of germ cell division (249-252). Similar to mitosis, knockdown of MAD2 and BUB1 leads to precocious meiosis I, chromosome misalignment and aneuploidy in mouse (253) and BUB1 depletion causes centromeric cohesion defects in both mouse and yeast (252, 254). Also mutations in *Bub1* gene cause age-related aneuploidy in mouse (255). Studies on human oocytes have shown that

younger females had better chromosome alignment than older females and showed reduced expression of *Bub1* and *Mad2* genes that could causes age-related aneuploidy leading to birth defects such as Down's syndrome (256, 257). Despite the role SAC role in meiosis, it is suggested that the SAC of meiosis is less robust than the SAC of mitosis because the cells with a misaligned X chromosome spends the same time in meiosis I as in controls in female mice whereas a single unattached kinetochore is sufficient to halt mitotic progression (258). In summary, studies mentioned above underline the importance of SAC as a defense against cellular anomalies.

1.3.10. Shugoshin-1 (SGO1)

The equal distribution of chromosomes into daughter cells dictates that sister chromatids remain together till anaphase during which they are separated and move towards opposite poles (259, 260). The *Mei-S332* gene in *Drosophila* was defined as protector of chromosome cohesion during meiosis and mutants of *mei-S332* had premature loss of centromeric cohesion (261). *Mei-S322* homologs were later discovered in budding and fission yeast as protectors of cohesion and named "Shugoshins" (meaning guardian spirit in Japanese) (262-264). Among eukaryotes, fission yeast and humans have two SGO proteins: SGO1 or SGOL1 (Shugoshin-Like 1) and SGO2 or SGOL2 (Shugoshin-Like 2), whereas budding yeast and *Drosophila* have only one SGO protein (265, 266). During fission yeast meiosis, SGO1 is only required for meiosis I whereas, SGO2 paralog is associated with centromere region in both cell divisions of meiosis and mitosis (260, 266, 267). In humans, although both SGO1 and SGO2 are present, SGO1 is primarily required for cohesion protection during mitosis as depletion of it causes chromosome missegregation defects (268-271). BUB1 kinase activity is required for proper localization of SGO1 because preventing BUB1 kinase activity mislocalizes SGO1 from centromeres. Moreover, SGO1 forms a complex with PP2A (protein phosphatase 2A) and localizes to centromeres in BUB1 kinase dependent manner for protection of cohesion (more detail in BUB1 section) (269, 270, 272-274).

1.3.10.1. Structure of SGO1

Human SGO1 is encoded by *Sgo1* gene is a paralog of SGO2 protein (264). It contains an N-terminal coiled coil (CC) domain and a C-terminal SGO region (Figure 1.12) (264). CC domain and SGO are conserved throughout eukaryotes, whereas other motifs are variable (260). SGO1 CC is required for PP2A binding and depletion or mutation in this region impairs SGO1-PP2A interaction (270). K492 (Lysine 492) of SGO recognizes and binds Histone H2A phosphorylated by BUB1 at T120 (275). Thus, CC and SGO region are required for PP2A and H2A binding respectively. SGO1 also has a KEN box (aa 310-312) and three D-boxes: D-Box1 aa 192-200, D-Box-2(aa 438-446) and D-Box3 (aa 457-465) (276, 277). The D-and KEN-Boxes are implicated

in SGO1 degradation by APC/C during mitotic exit (276). Finally, SGO1 has a CDK1 phosphorylation site at T346 (Threonine 346) required for cohesin binding. Therefore, SGO1 T346 mutant is unable to bind cohesin and has defective chromosome cohesion protection (275).

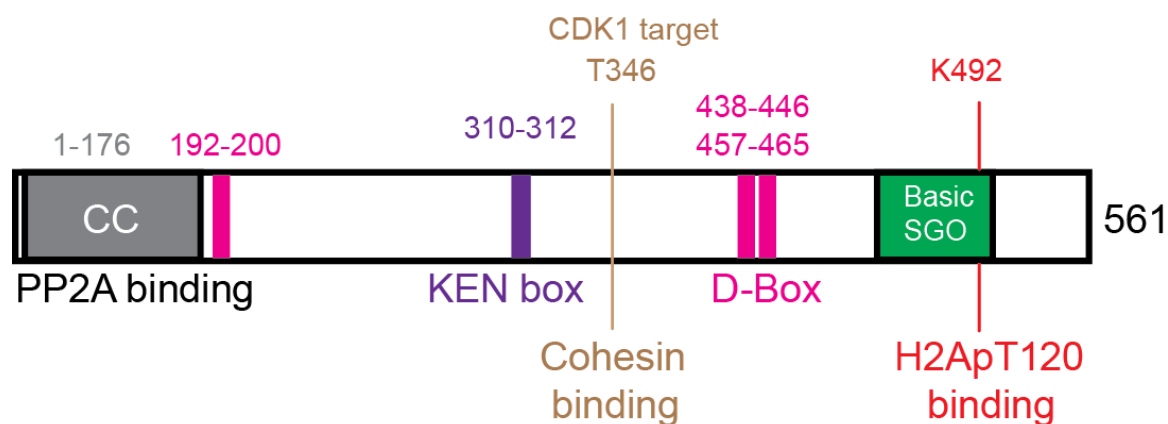


Figure.1.12 Structure of human SGO1: N-terminus Coiled coil (CC) domain is a PP2A binding site. SGO1 is phosphorylated by CDK1 at conserved motif T346 required for SGO1 cohesin interaction. KEN box and D-box serve to regulate SGO1 expression and are likely recognition site for APC/C ubiquitylation. C-terminus Basic region “SGO motif” contains K492 residue needed for H2ApT120 interaction. SGO and CC motifs are conserved in yeast, drosophila, mice, *xenopus* and humans. Adapted from (267, 275, 276).

1.3.10.2. Functions of SGO1 during mitosis

1.3.10.2.1. SGO1 acts as modulator of cohesin removal

Cohesion between sister chromatids is required to achieve accurate attachments between kinetochores and microtubules. Therefore, cohesion plays a crucial role for proper distribution of chromosomes in daughter cells (278, 279). The cohesion between sister chromatids depends on cohesin proteins assembled onto chromosomes during S phase (39, 280). Cohesin comprises SMC1, SMC3 (structural maintenance of chromosome 1 and 3), a Kleisin subunit SCC1 (Sister chromatid cohesion protein 1)/RAD21 and SCC3 subunit (SA in animal cells, REC8 in meiosis) (36, 41, 281). The presence of cohesin is essential to keep a balance between tension generated due to kinetochore-microtubule attachment and cohesion on sister chromatids (282). While the cohesin complex is central to chromosome cohesion, other

cohesin-associated proteins are also required for cohesion including PDS5 (precocious dissociation of sisters protein 5), WAPL (wings apart-like), a protein needed for cohesin removal in prophase and Sororin, a protein required for maintaining cohesin. Vertebrate PDS5 binds to cohesin to maintain and establish sister chromatid cohesion (283, 284). Sororin forms a complex with PDS5 to stabilize cohesin on chromosomes by opposing WAPL and depletion of Sororin causes sister chromatid cohesion loss (285, 286). WAPL also interacts with PDS5 leading to assembly of a cohesin releasing complex called "releasin" for cohesin removal from chromosome arms in prophase (287-289). Recent evidence has shown that WAPL and Sororin share a conserved motif required for PDS5 binding and thus WAPL and Sororin antagonize each other through binding competition to regulate chromosome cohesion (290, 291).

In vertebrates, cohesin assembly at chromosomes is temporally regulated by a two-step sequestration of cohesin from chromosomes in mitosis to allow for preservation of chromatin integrity (Figure 1.13) (42, 292). A large portion of cohesin is removed from chromosome arms but retained at centromeres to prevent premature sister chromatids separation (293, 294). The removal of cohesin in this step is separase and cleavage independent and SCC1 remains unaffected (295). The second removal of cohesin depends upon entry into anaphase and APC/C activation and results in cleavage of SCC1 by separase which removes cohesin from centromeres (295).

Phosphorylation catalyzed by kinases PLK1, CDK1 and AURORA B, is the molecular trigger governing the first step removal of cohesin from chromosome arms (39, 296-298). During this step, SGO1-PP2A helps maintain centromere PDS5-Sororin complex by preventing Sororin phosphorylation and therefore, inhibits PDS5-WAPL formation and cohesin removal (273, 298). The SGO1-PP2A complex also counters PLK1 activity towards SA2 (Scc3 homolog 2) to prevent cohesin removal (268, 292). Finally, SGO1 competes with WAPL for SA2 binding counters WAPL binding, and thus acts as protector of cohesion during mitosis (267, 292, 299).

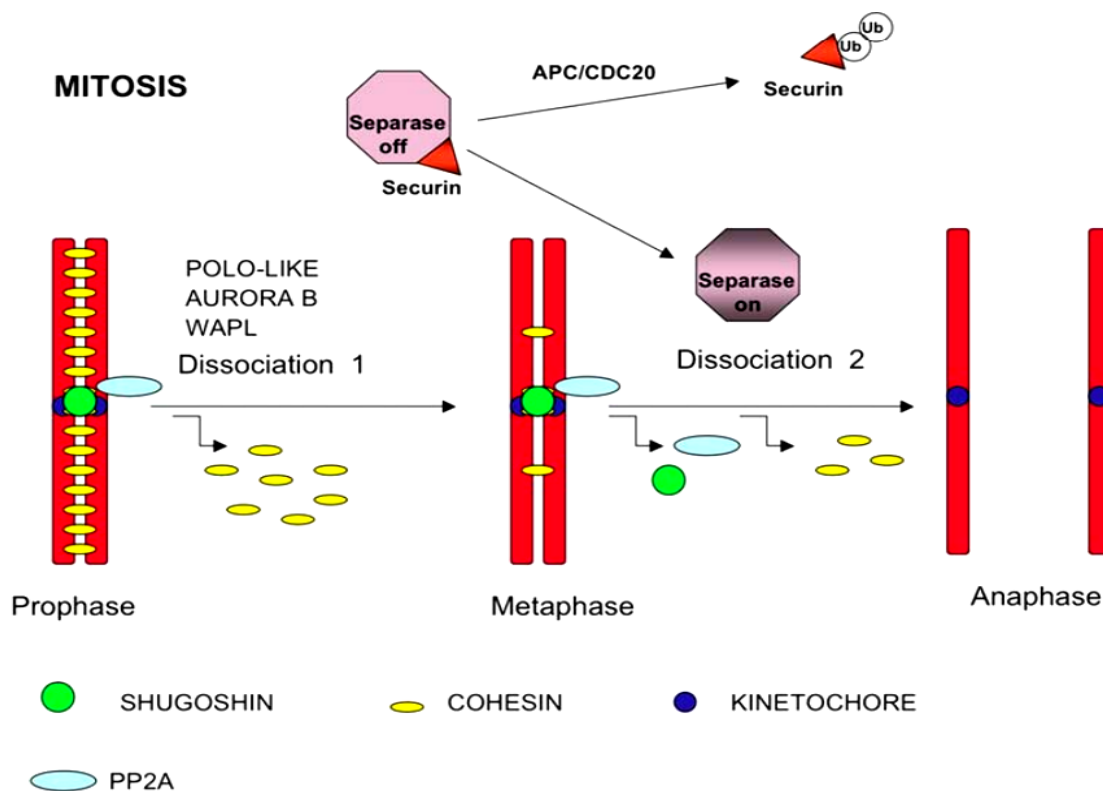


Figure 1.13 SGO1 and cohesin removal during mitosis: During prophase cohesin binds chromosome along the arms and on centromeres. Most of the cohesin is removed from the arms by the end of prophase due to phosphorylation of cohesin subunit SA2 by kinases PLK1 and AURORA B and CDK1. WAPL binds cohesin at PDS5 (not shown) and destabilizes cohesin. At centromeres, the presence of SGO1-PP2A is sufficient to counteract phosphorylation of kinases due to presence of PP2A hence; SGO1-PP2A complex protects cohesin at centromeres. By the end of metaphase, when correct attachments between kinetochores and microtubules are established, SGO1-PP2A complex is delocalized as a result of SAC silencing. APC/C is activated and destroys separase enzyme inhibitor securin by promoting its ubiquitination to release separase which cleaves cohesin. Image from (300).

1.3.10.2.2. SGO1 in chromosome biorientation

Tension generated between sister kinetochores due to resistance of cohesin in response to microtubule pull is an indicator of establishment of chromosome biorientation (93, 267). Lack of kinetochore-microtubule attachments due to cohesin defects promotes the activity of AURORA B kinase to remove defective kinetochore-microtubule attachments and activate SAC to stabilize PDS1(securin), an indicator of APC/C inactivation (301). SGO proteins have been described as sensors of tension at kinetochores and

biorientation (267, 302-306). In budding yeast, repression of a cohesin component MCD1 (RAD21 in fission yeast) generates lack of tension phenotype. In these cells simultaneous depletion of SGO1 (SGO1Δ) could not promote SAC activation indicating that SGO1 is required for sensing tension (307). Combination of biochemical and cellular analyses shows that SGO1 is removed from the pericentromere in a tension dependent manner which marks the achievement of biorientation (308). These studies suggest that SGO1 acts as a sensor of tension between sister chromatids in mitosis, although less prominent role has been observed in meiosis (305).

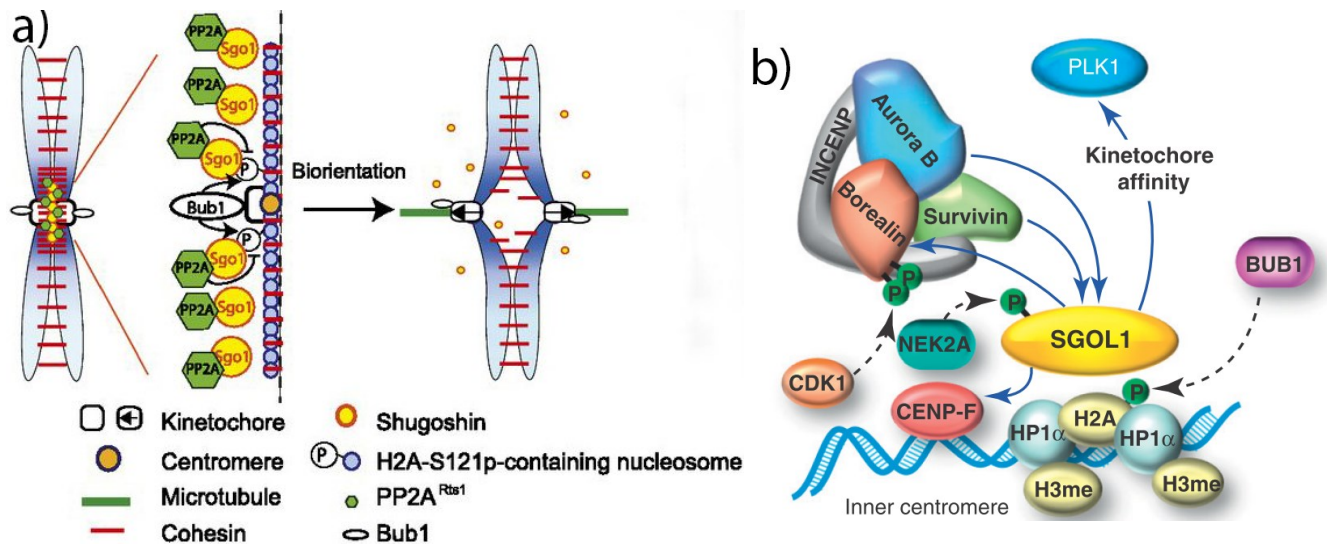


Figure 1.14 SGO1 role in biorientation: **a)** SGO1 with PP2A-RTS1 is recruited to pericentromere region after phosphorylation of H2A at S121 in yeast by BUB1. PP2A RTS1 regulates SGO1 localization by repeatedly removing H2A phosphorylation. Upon achieving biorientation, tension removes BUB1 from kinetochore which delocalizes SGO1 from pericentromeres and sister chromatids are separated. Modified from (308). **b)** SGO1 is involved in centromere recruitment of CPC (chromosomal passenger complex) composed of Survivin, INCENP (inner centromere protein), Borealin/Dasra and AURORA B. CDK1 phosphorylates Borealin and survivin for their recognition and recruitment by SGO proteins. SGO1 also recruits AURORA B at centromeres for removal of tensionless kinetochore. Modified from (265)

How SGO1 contributes to biorientation as a tension sensor has been explained through different mechanisms. PP2A with its regulatory subunit, RTS1/B' is localized to pericentromeres in SGO1 dependent manner and this interaction is required for biorientation (Figure 1.14a) (309-311). SGO1

association with RTS1 and another PP2A subunit CDC55 (cell division control protein 55) is implicated in removal of SGO1 from pericentromeres upon achieving tension. The depletion of RTS1 or CDC55 increases SGO1 levels on pericentromeres and centromere tethering of RTS1 in SGO1 depleted cells restores biorientation defects of SGO1 depletion suggesting PP2A-RTS1 role in tension sensing and biorientation (308-310). However, a similar study in budding yeast showed that mutants lacking RTS1($\Delta rts1$) had biorientation comparable to wild-type RTS1, thus SGO1-PP2A RTS1 interaction is not required for biorientation (312). In human cells, overexpression of SGO1 leads to enhanced activity of PP2A-B56 subunit that results in downregulation of AURORA B activity yet depletion of SGO1 reduces AURORA B centromere localization suggesting that SGO1 manipulate AURORA B centromere localization via PP2A to achieve initial kinetochore-microtubule binding (313).

SGO1 mediated recruitment of Condensin, a chromosomal complex required for chromosome assembly, and AURORA B kinase, is implied in achieving biorientation (310, 312). CPC is required for kinetochore-microtubule error correction (314-316). Several independent studies have shown requirement of SGO proteins in recruitment of CPC (Figure 1.14b) (302, 308, 317-320). CPC centromere targeting by SGO1 binding is facilitated by phosphorylation of CPC by CDK1 in fission yeast and humans (317). AURORA B phosphorylates its kinetochore substrates DAM1, NDC80 and MCAK (Mitotic associated Kinesin) important for microtubule binding to abolish microtubule attachments on tensionless kinetochore (321-323). Overall, SGO1 mediated achievement of biorientation requires PP2A-RTS1, Condensin and AURORA B.

1.3.11. Protein phosphatase 2A (PP2A)

Phosphorylation is a post-translation modification manifested by transfer of a phosphate group (PO_4^{3-}) usually from ATP to specific amino acids on substrates (324). This changes the net charge on substrates which helps achieve many biochemical functions in a cell (325-327). Protein phosphatases reverse kinase function by dephosphorylation, thus, interplay between the two is important for normal progression of cell cycle (328, 329). Protein phosphatase 2A (PP2A) constitutes about 1% of total protein expression in mammalian cells and performs diverse roles in cells including mitotic

regulation (330). PP2A regulates serine/threonine phosphorylation which is the most abundant form of phosphorylation and thus has an important role in cellular regulation (331).

1.3.11.1. Structure of PP2A

Protein phosphatase 2A has two distinct forms (328). The dimeric form also known as the core enzyme (PP2A_D) is composed of a 65kD scaffold subunit (PP2AA) and a 36kD catalytic subunit (PP2AC) (332). The trimeric form (PP2A_T) is a holoenzyme (Figure 1.15) composed a regulatory subunit (PP2AB) in addition to scaffold and catalytic subunits (331, 333). The subunits have several families and these family members have further isoforms. It is estimated that these variations give rise to approximately 200 different PP2A trimeric holoenzyme complexes (332). PP2AB, the regulatory subunit of PP2A is the key regulator of PP2A holoenzyme (334). The regulatory subunits comprise of 4 different families. These are B, B', B'' and B''' (Figure 1.15).

PP2AB also known as B55 has four distinct isoforms: α , β , γ and δ . These are associated with various cell types and involved in tissue morphogenesis (333, 335). The second family PP2AB' or B56 has five different isoforms: α , β , γ , δ , and ϵ . PP2AB' perform diverse functions hence, present in both nucleus and cytoplasm (336). The PP2AB'' or PR72 family has two isoforms PR70 and PR130 expressed in all tissues and has been observed to regulate the DNA damage checkpoint (337). The PP2A B''' family is a nuclear protein also known as calmoduline binding protein (CaM) and requires ATP and Mg⁺² for its activation (338).

PP2Ac, the catalytic subunit of PP2A, has two isoforms, PP2Ac α and PP2Ac β and their activity is regulated by post-translational modifications including phosphorylation and methylation (339). PP2Ac binds to scaffold and regulatory subunits via its C-terminal region (336, 340, 341).

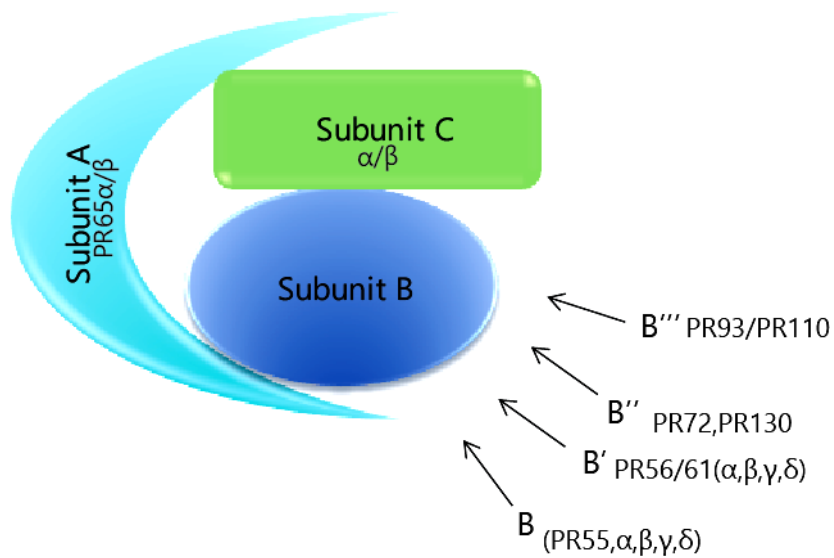


Figure 1.15 PP2A holoenzyme: The core enzyme of PP2A consisting of scaffold subunit (A) and catalytic subunit (C) can bind a variety of regulatory B subunits. At present 4 subfamilies of B subunit have been characterized. These are B, B', B'', B'''. The flexibility of regulatory subunit allows PP2A holoenzyme to form up 200 distinct types, thus permitting PP2A to perform multitude of function in cells. Adapted from (332)

Third subunit, PP2AA/PR65 or the scaffold subunit binds with both catalytic subunit and regulatory subunits. Different types of B subunits can bind on the same region of the scaffolding subunit depending on the type of PP2A (Figure 1.15) (342). PP2AA has two isoforms: PP2AA α and PP2AA β and are expressed in cytoplasm of almost all tissues (343).

1.3.11.2. Role of PP2A during mitosis

PP2A is recruited to centromeres in complex with SGO1 for protection of sister chromatids cohesion and biorientation (270, 292, 309). PP2A is also involved in SAC silencing by removing phosphorylation by MPS1 (180, 181). Recent evidence shows that BUBR1 plays a vital role in recruitment of PP2A-B56 to kinetochores that eventually leads to silencing of SAC (181, 188-190).

1.3.12. PLK1 (Polo-like kinase 1)

Polo-like kinase 1, a serine/threonine kinase belonging to a family of Polo-like kinases, was first identified in *Drosophila* (344, 345). There are five Polo like kinases (PLK 1-5) identified in humans so far (346). PLK5 lacks kinase domain thus is inactive and does not appear to have a role in cell cycle progression. Instead, its functions involve DNA damage response, tumor suppression and neuronal activity in humans and mice (347-349). PLK1-4 have various functions including cell cycle phase transition, DNA damage response, centrosome maturation/duplication and DNA replication (350-353).

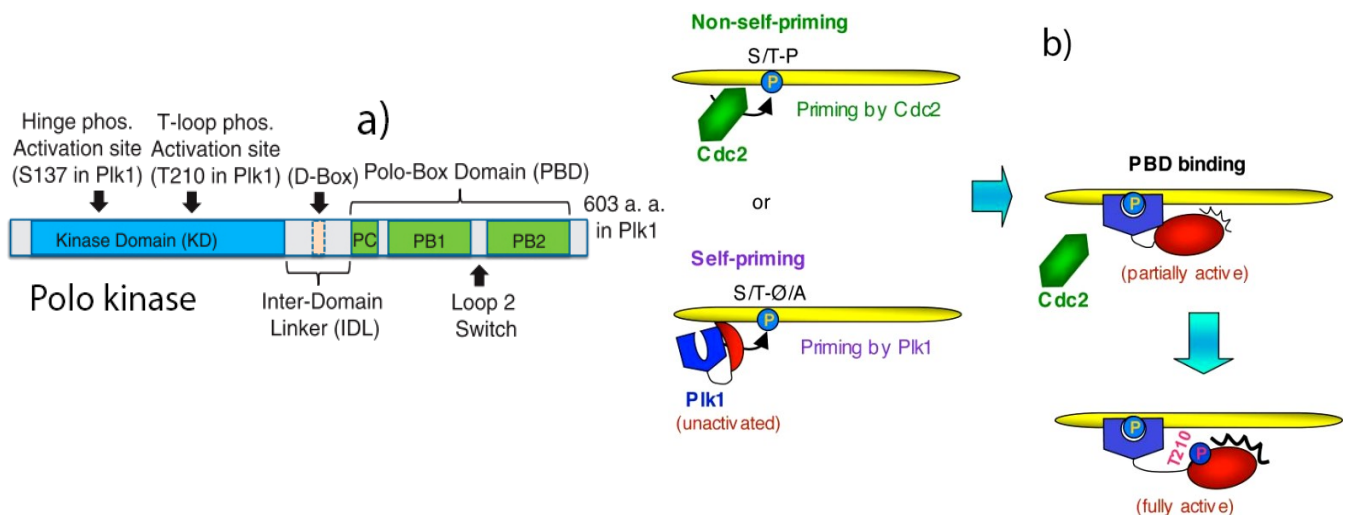


Figure 1.16 PLK1 structure and activation: **a)** Human PLK1 composed of 603 residues has a C-terminus PBD (polo box domain) and N-terminus kinase domain. Kinase domain is phosphorylated at S137 and T210 required for its activation. PBD has two polo boxes, PB1 and PB2 that has a loop 2 switch region between them. A polo cap (PC) is presented adjacent to PBD. Kinase domain and PBD are separated by Inter-domain linker (IDL) which contains a D-Box required for PLK1 degradation. Image from (344). **b)** The modes of activation of PLK1 localization and substrate binding occur through substrate phosphorylation either by other kinases or kinase domain to help activate and localize PLK1. Modified from(354).

PLK1 has two distinct domains (Figure 1.16a) (354, 355). At the N-terminus, a conserved serine/threonine catalytic domain is followed by two polo box motifs forming a functional Polo Box domain (PBD) at C-terminus. The kinase domain and PBD are separated by an inter domain linker (IDL) (356). The PBD is required for PLK1 localization and function during cell cycle (357). In

the absence of PLK1 substrates, the PBD acts as an inhibitor of N-terminal kinase domain(344). Two models have been proposed for regulation and activity of PLK1(354) (Figure 1.16b). According to self priming and binding, PLK1 substrates are phosphorylated by kinase domain of PLK1 to create binding site for PBD and allows for substrate binding (354, 358). Conversely, for non-self priming and binding, other kinases such as CDC2 (CDK1 in humans) create “priming phosphorylation” sites on substrates that promotes PBD binding (116, 356). In both cases, PBD binding with substrates partially activates PLK1 due to alleviation of PBD inhibition of kinase domain, further activation of PLK1 occurs after PLK1 is phosphorylated at residues T210 by Aurora A kinase (359).

1.3.12.1. Functions of PLK1 in cell cycle

PLK1, the most studied kinase of polo family, has been implicated in a number of functions during cell cycle (346). In human cells, PLK1 localizes to centrosomes during G2 and promotes centrosome maturation by increasing the centrosome nucleation activity through phosphorylation of pericentrin protein (PCNT) of pericentriolar matrix (PCM) (360, 361). PLK1 catalytic function has been implicated in nuclear envelope breakdown (NEB) through recruitment of dynactin (362). Furthermore, PLK1 is also involved in DNA damage checkpoint (363). PLK1 activity is abolished in response to DNA damage and cells are arrested at G2/M (364, 365). In normal circumstance, Aurora A kinase with the help of Bora proteins phosphorylates PLK1 at T210 to activate PLK1 for mitotic entry (site shown in Figure 1.16a) (366). In response to DNA damage, Bora is destroyed by E3 ubiquitin ligase SCF- β -TRCP which keeps PLK1 inactivated and halts cell cycle at G2 (364, 367). Finally, PLK1 is implicated in tumor development for it is overexpressed in wide array of cancers including lung, breast, stomach and pancreatic cancer (368).

1.3.12.2. Function of PLK1 during mitosis

BUBR1 hyperphosphorylation by PLK1 is essential for kinetochore-microtubule attachments (369, 370). Moreover, PLK1 phosphorylates BUBR1 for recruitment of PP2A-B56 for correct kinetochore-microtubule attachments (188, 189). In human cells, PLK1 also phosphorylates a protein called SGT1

(Small glutamine-rich tetratricopeptide repeat-containing protein 1) that promotes its stabilization and interaction with MIS12 and later recruitment of NDC80 for stable KT-MT attachments (371).

The inhibition of PLK1 results in unresolved chromatid cohesion which demonstrates essential role of PLK1 in regulating cohesion (296). Mass spectrometry analysis of cohesin showed that SA2 subunit of cohesin is the target of PLK1 and mutations in SA2 phosphorylation sites caused inefficient removal of cohesin from chromosome arms during early mitosis (372). PLK1 SA2 interaction is mediated through sororin, an essential protein for cohesin stability, that binds PLK1 after phosphorylation of its conserved ST¹⁵⁹P site by CDK1, thus allowing for SA2 phosphorylation by PLK1 and removal of cohesin from chromosome arms (373).

A role for PLK1 in SAC has been reported in recent studies. PLK1 inhibition does not override SAC arrest, instead PLK1 has been shown to promote SAC maintenance by AURORA B recruitment possibly through controlling Haspin mediated Histone H3 phosphorylation (H3T3) in U2OS cells (374). Another study defines a separate pathway in which BUB1 acts as scaffold for BUB1-PLK1 kinase complex needed for CDC20 phosphorylation and APC/C inhibition (375). Thus, PLK1 is required for maintaining the SAC.

1.3.13. MPS1 (Monopolar spindle 1)

MPS1 is a dual specificity kinase i.e. acts both as serine/threonine and tyrosine kinase and is a key regulator of the SAC (376, 377). Although present in all other tested eukaryotes, *C. elegans* lack MPS1 (378). It was first identified in budding yeast in which mutation of *mps1* gene (*mps1-1*) had spindle pole body (centrosome in humans) duplication defect resulting in monopolar spindle formation, hence the name MPS1 (379). Later, it was shown to be required for SAC as well (112). MPS1 is autophosphorylated during mitosis and its dimerization leads to trans-autophosphorylation needed for its activation and SAC (380, 381). MPS1 is recruited to kinetochores by NDC80 and AURORA B kinase whose kinase function is required for MPS1 recruitment for SAC function (75, 140).

1.3.13.1. MPS1 functions

1.3.13.1.1. SAC function

MPS1 depletion leads to SAC defects which suggest that it is important for spindle assembly checkpoint (77, 381). MPS1 inhibition by chemical inhibitors causes MAD1 mislocalization from unattached kinetochores (143, 382, 383). Further analyses showed MPS1 kinase activity is needed to recruit O-MAD2 to MAD1-C-MAD2 complex at kinetochores (141, 142). MPS1 inhibition affects SAC proteins recruitment which causes SAC override in human cells (140, 142, 143, 192).

Recently, it has become clear that phosphorylation of KNL1 at specific MELT(Methionine, Glutamic acid, Leucine, Threonine) consensus motifs by MPS1 is essential step in kinetochore recruitment of downstream SAC members including BUB1 and BUBR1 (84, 87, 191). Studies in human cells have demonstrated that KNL1 containing first MELT and KI motifs (shown in Figure 1.17) is sufficient to mount SAC response but inefficient in chromosome biorientation (83). A similar study validated these results and concluded that gradual deletion of MELT results in gradual decrease in BUB1 and BUBR1 signal and a minimal number of four phosphorylated MELTs present between residues 1000-2316 can support SAC and chromosome congression function in MPS1 dependent manner (Figure 1.17) (86).

1.3.13.1.2. Function at Centrosome

In budding yeast, MPS1 localizes to spindle pole bodies and regulates Spindle pole body duplication (384). However, fission yeast and *Drosophila* MPS1 has shown to be dispensable for centrosome duplication (385, 386). *C.elegans* lack MPS1, yet are fully capable of centrosome duplication(387). In humans the role of MPS1 in centrosome duplication is controversial (388). Studies on human MPS1 implicated its requirement for centrosome duplication (389, 390); however, in another study, centromere duplication was unaffected after MPS1 depletion (391).

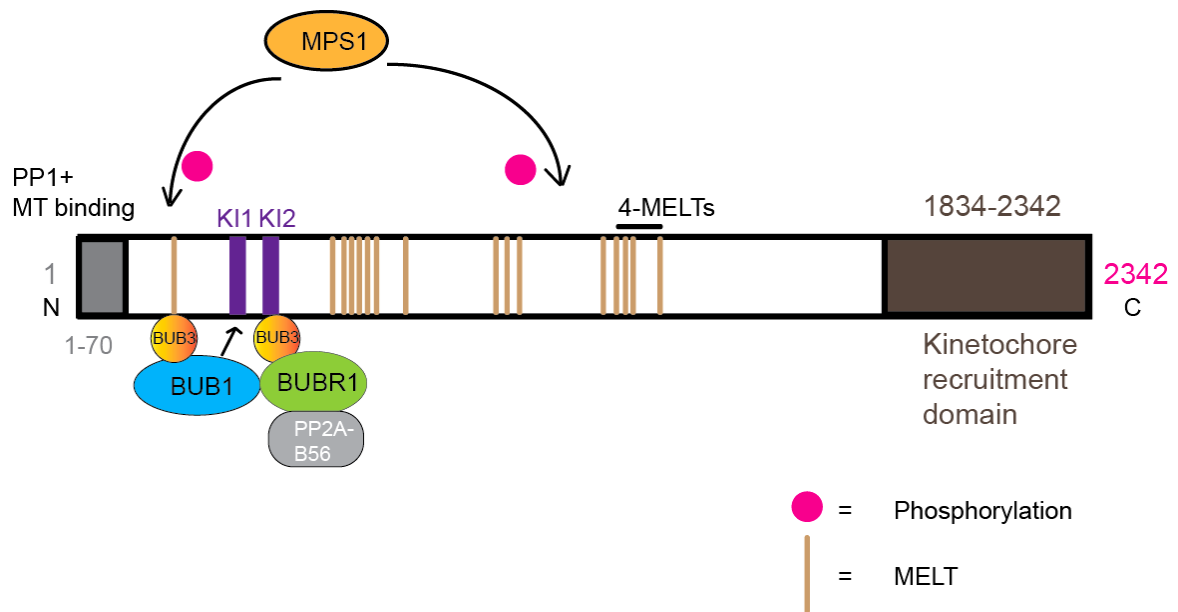


Figure 1.17 MPS1 recruits SAC proteins at KNL1: At N-terminus, KNL1 binds PP1 while C-terminus aa 1834-2342 is required for its kinetochole binding. MPS1 phosphorylates consensus MELT motifs on KNL1. There are at least 19 MELT motifs in humans. BUB3 interacts with phosphorylated MELTs and recruits BUB1. BUB1 then recruits BUBR1 and its downstream targets MAD1, MAD2 and CDC20 (not shown). The 4 MELT motifs sufficient to recruit BUB1 for SAC function are shown. N-terminal region with first MELT and KI motifs are sufficient to sustain SAC. Adapted from (185).

1.4. BUB1 (budding uninhibited by benzimidazole 1)

BUB1 is a serine/threonine kinase required for SAC activity (392-394). BUB1 was identified during a study of a genetic screen for mutants that continued budding after treatment with spindle poisons in budding yeast (110). Thus, revealing BUB1 requirement for SAC. Later, it was characterized as a kinase that binds with another related protein called BUB3 required for its kinetochore localization (113, 198, 395).

1.4.1. Structure of BUB1

In humans, BUB1 kinase consists of N-terminal Tetratricopeptide repeat (TPR) motif that interacts with KNL1 (Figure 1.18) (79). Recent studies have identified a BUB1 "loop region" that follows the TPR region required for BUB3 interaction with KNL1 (85). However, a similar loop region in BUBR1 does not perform this function (85, 396). Proceeding further, BUB3-binding domain or GLEBS (Gle-binding sequence) motif is required for BUB3 binding, BUB1 recruitment to kinetochores and SAC function (113, 397). Next to BUB3 binding domain, the region BUB1R1LM (BUBR1 localization motif) is needed for binding with BUBR1 (398). In the middle region, BUB1 contains conserved motif1 essential for SAC function and recruitment of SAC proteins MAD1, MAD2 and BUBR1 (397, 399). BUB1 contains two KEN boxes needed for CDC20 binding and SAC function (375, 399, 400). Finally, at the C-terminus, the kinase domain is required for kinase activity and chromosome congression (194, 397, 400, 401).

1.4.2. BUB1 kinetochore recruitment

BUB1 kinetochore localization has been studied in different model organisms including yeast (402, 403), *Drosophila* (404), *C.elegans* (148, 405), *Xenopus* (145), mice (198) and human cells (113, 199, 397). Its kinetochore signal is observed from early mitosis till anaphase (145, 198, 199, 406). Fluorescence recovery after photobleaching (FRAP) analyses confirmed these studies and demonstrated that BUB1 is a stable protein at kinetochores (121, 407, 408). Two structural regions essential for BUB1 kinetochore binding have been identified. TPR motif also known as KNL1 binding domain and BUB3 binding domain were implicated in BUB1 recruitment to kinetochores. Mutation in the KNL1 binding domain impaired BUB1 binding to KNL1, indicating its

requirement for BUB1 recruitment at kinetochores (79, 409). However, recent studies have demonstrated that deleting a bulk of residues in TPR region does not affect BUB1 localization although BUB1 localization is enhanced when TPR is present suggesting TPR region stabilizes BUB1 binding at kinetochores (193, 396, 410).

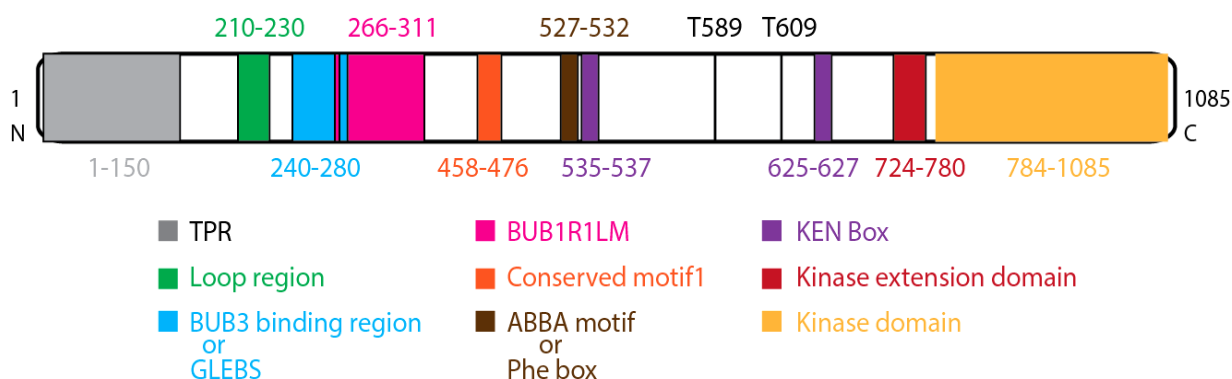


Figure 1.18 Structural domains of human BUB1: The N-terminus of BUB1 contains a TPR region for protein-protein interactions with KNL1. A Loop region follows the TPR region essential for BUB3-BUB1 interaction with KNL1. The BUB3 binding region is required for BUB1 binding to KNL1. R1LM (BUBR1 localization motifs) is needed for direct binding to BUBR1 to BUB1 and its kinetochore recruitment. The middle region contains conserved motif1, ABBA and KEN boxes are required for SAC function and CDC20 binding respectively. T609 is CDK1 phosphorylation site for PLK1 binding (411). The C-terminal region comprises an N-terminal extension domain and serine/threonine kinase domain. BUB1 autophosphorylation T589 required for focused localization is studied in chapter 2. The numbers represent amino acids for each region. "N" and "C" are amino-terminus and Carboxy-terminus respectively. Modified from (412).

BUB3 binding domain or GLEBS is absolutely required for BUB1 kinetochore targeting (393). First studied in yeast for its requirement in recruitment, BUB3 binding domain was later studied in vertebrates where its deletion resulted in a uniform cytoplasmic expression of BUB1 with severe reduction of its kinetochore localization, thus confirming the role of BUB3 binding domain in BUB1 kinetochore localization (113, 397, 413).

1.4.3. Regulation of BUB1 activation

Many kinases require activation segment phosphorylation for their activation (414). The activation segment, present in kinase domain, spans between

consensus tripeptide motifs DFG and APE and contains about 20-35 residues preceded by a catalytic loop (414, 415). Three short motifs constitute the activation segment: a Mg^{+2} binding loop, an activation loop and a P+1 loop. In many kinases, Mg^{+2} binding loop is structurally reorganized to inactivate or activate kinases. The short sequence of P+1 starts with a GT (glycine-threonine) motif forms interactions with catalytic motif required for correct conformation of P+1 loop. The phosphorylated residue of activation loop is stabilized by extensive coordination between adjacent residues in catalytic loop (415). Kang and colleagues resolved the crystal structure of BUB1 kinase domain (400). They also reported the requirement of kinase extension domain in kinase activity of BUB1 as mutations in kinase extension domain cause disruption of kinase activity towards CDC20 hence kinase extension domain promotes BUB1 activation (400). Furthermore, studies on comparison of activated and inactivated BUB1 showed that reorganization of P+1 loop after its phosphorylation is specifically self-regulated through intramolecular rather than intermolecular autophosphorylation and thus has an essential role in BUB1 activation (401). At the N-terminus, the BUB1 TPR region could stimulate BUB1 kinase domain for its activation (410, 413). However, recent analyses do not support this as mutations of TPR do not affect kinase domain activation (401, 412).

Degradation of BUB1 for its inactivation has been proposed by studies in budding yeast and human cells (416-418). BUB1 KEN boxes were shown to be required for its degradation but recent studies have suggested otherwise. Instead, KEN boxes are required for CDC20 binding and SAC signaling (375, 399, 400). Others have shown that BUB1 could be removed from kinetochores either through motor proteins Dynein or by phosphatase action (187, 202). Thus far, the literature is insufficient to fully conclude on how BUB1 is inactivated. Further studies are required for definite understanding of BUB1 inactivation after SAC silencing.

1.4.4. BUB1 Functions

1.4.4.1. BUB1 role in mitosis

BUB1 has been extensively studied for its roles during mitosis and areas of inquiry can be divided into the following categories: BUB1 requirement for SAC, BUB1 kinase activity in SAC and chromosome congression and role of BUB1 as a recruiter of SAC proteins.

1.4.4.2. BUB1 requirement for SAC

Requirement of BUB1 for SAC has been tested in several organisms (Table 1). BUB1 is essential for SAC function in budding yeast and fission yeast (254, 395, 419-422). Similarly, mutations in BUB1 causes premature mitotic exit in *Drosophila* (404). Furthermore, studies in mice have also demonstrated that BUB1 is required for launching SAC response (198, 413, 423). In *C.elegans*, depletion of BUB1 causes SAC defects (424, 425). Thus, BUB1 is indispensable for SAC in these organisms. Earlier studies in human cells disputed the role of BUB1 in SAC (146, 269, 426). These studies suggested that mitotic index i.e. a measure of SAC activity remains unchanged in both BUB1 depleted and control cells when spindle damage is induced suggesting that BUB1 is not required for SAC function. However, overwhelming data from studies in *Xenopus* and humans supported the requirement of BUB1 in SAC. BUB1 depletion or structural mutations lead to abrogation of SAC in these studies (64, 145, 397, 399, 400, 427, 428). The difference in the observation could arise due to difference in BUB1 depletion efficacy, as low levels of BUB1 are sufficient to induce a SAC response (428). For this reason, studies that involved either conditional knockout mice (423) or a strong BUB1 siRNA penetrance demonstrated a functional role of BUB1 in SAC (397, 428).

1.4.4.3. BUB1 kinase activity and SAC

In yeast, the studies to understand the role of BUB1 kinase activity to stimulate SAC response have resulted in contentious outcomes. The seminal work in budding yeast and fission yeast showed that manipulation of BUB1 kinase domain either by individual mutations or by complete removal of the entire kinase domain had deficient mitotic checkpoint, hence showing

requirement of kinase activity for SAC (395, 420). Contrarily, later a study in budding yeast showed that a BUB1 construct lacking its kinase domain still kept the functional checkpoint after spindle damage (403). Another study observed that kinase domain was only needed for SAC on tensionless kinetochores rather than on unattached kinetochores in budding yeast (429). In fission yeast, kinase domain mutants that lacked kinase activity or kinase domain still produced checkpoint response suggesting that kinase function does not stimulate the SAC (274, 421).

In *Xenopus*, BUB1 mutant lacking in its kinase activity still supported mitotic checkpoint suggesting redundancy of kinase domain for SAC activation (145). However, the same group later demonstrated the dependency of kinase activity for SAC in suboptimal SAC conditions i.e. lower doses of spindle poisons in BUB1 kinase deficient mutants (64). In *C.elegans*, mutation in kinase domain severely reduced BUB1 kinase activity and significantly affected SAC signaling (148).

In human and mouse cells, the role of kinase function is not very clear. Abolishing BUB1 catalytic activity by using kinase domain mutant or deletion of kinase domain still produces SAC response suggesting kinase activity of BUB1 is dispensable for the SAC (252, 397, 399, 430). However, similar mice and human studies resulted in opposite conclusion in which BUB1 activity towards CDC20 was measured to determine SAC function (375, 400, 413, 427). BUB1 uses its KEN (shown on BUB1 structure Figure 1.8) boxes to bind and phosphorylate CDC20 required for SAC (375, 400, 427). It is not certain at the moment if discrepancies in the above mentioned studies are due to differences in requirement of BUB1 kinase activity in these different organisms or due to differences in experimental assays and approaches. Interestingly, several studies have suggested that BUB1 structural motifs differentiate SAC functions i.e. non-kinase region of BUB1 is required for SAC whereas kinase region (kinase activity) is required for chromosome congression and cohesion maintenance through SGO1 recruitment (397, 399, 430).

1.4.4.4. BUB1 and recruitment of kinetochore components

BUB1 acts as a recruiter of several checkpoint and non-checkpoint proteins. BUB1 has been shown to recruit all four MCC members i.e. BUBR1, MAD2, BUB3 and CDC20. BUB1 binds and recruits its paralog BUBR1 and its binding partner BUB3 throughout cell cycle and these interactions are important for kinetochore localization of all three proteins (113, 145, 194, 404, 425, 431). The role of BUB1 in BUBR1 recruitment has been studied in several organisms. Fission yeast BUBR1 homolog MAD3 was readily recruited to ectopic sites by BUB1 (408). In mouse cells, BUBR1 levels at kinetochores dropped to almost undetectable after reduced expression of BUB1 (392, 423, 432). Studies in frogs have concluded that immunodepletion of BUB1 in egg extract reduced BUBR1 kinetochore localization (145, 146, 431). Chen and colleagues observed that immunodepletion of BUBR1 can negatively regulate BUB1 kinetochore recruitment (431). This observation is interesting for that fact that at least in human cells BUB1 is recruited at kinetochores before BUBR1 (199).

Human cells studies have demonstrated that while recruitment of BUBR1 is severely reduced after BUB1 depletion or inhibition (146, 151, 398, 426), using similar methods of BUB1 knockdown still localized BUBR1 to the kinetochores normally (428). Mutants of BUB1 conserved region called conserved motif1 (aa 458-476 shown in Figure 1.18) could not recruit BUBR1 to kinetochores and had defective SAC (397). Whether a direct binding exists between this region and BUBR1 was not tested in those assays. Recently, direct BUB1 and BUBR1 interactions have been reported (396, 398). Mutations in the BUB1 region adjacent to BUB3 binding domain, termed as BUBR1 localization motif (R1LM) (Figure1.18) encompassing aa 266-311 greatly reduced BUB1-BUBR1 binding and BUBR1 kinetochore localization compared to control in protein binding assays confirming a direct BUB1 and BUBR1 interaction in human cells (398). A similar study determined a much larger region comprising BUB1 aa 271-409 required for binding and recruitment of BUBR1 (396). Interestingly, the study reported that a BUB1 construct containing aa 1-284 was also not able to recruit BUBR1. Taking BUB1-R1LM region into account, the BUBR1 interaction motif in BUB1 should be placed between aa 284 and 311 in humans.

BUB1 requirement for recruitment of MAD1 and MAD2 have been tested in several organisms that include worms, yeast, frogs, and humans (144-146, 148, 151, 433). In *C.elegans*, mutating individual amino acids in BUB1 kinase domain reduced MAD1 kinetochore localization and abrogated SAC independent of BUB1 kinase function (148). A direct interaction between BUB1 and MAD1 exists in yeast through a basic RLK (Arginine-Leucine-Lysine) motif in MAD1 (150). The same RLK motif is conserved in humans and is required for MAD1 kinetochore targeting (434). Budding yeast BUB1 construct containing first aa 609 is sufficient for MAD1 binding but not BUB1 1-369 (403). Indeed, BUB1 aa 367-608 middle region is required to recruit MAD1 to kinetochores after phosphorylation of its residues by MPS1 in budding yeast. Moreover, in vitro studies have shown that MAD2 binds BUB1 in the presence of MAD1 (144). While MAD2 is required for MAD1 kinetochore targeting in budding yeast, MAD1 is needed for MAD2 recruitment in *Xenopus* (200, 406). Thus, these interactions are conserved in yeast and frogs. In humans, BUB1 conserved motif1 falls within middle region(aa 367-608) and is also required for MAD1 and MAD2 kinetochore targeting (397) but recent data show that depletion of BUB1 does not affect overall MAD1 kinetochore localization and it is only required to accelerate MAD1 loading to kinetochores. Hence, in humans BUB1 is not a major recruiter of MAD1 unlike in yeast and worms (399).

Much of the studies on MCC have extensively reported interaction of CDC20 with BUBR1 (122, 160, 161, 171, 435), however, recent studies have also pointed to an interaction between BUB1 and CDC20 (176, 400). Studies in human cells have identified a CDC20 interacting motif called ABBA in BUB1 (aa 527-532, shown Figure 1.18) containing a consensus sequence of [F/Y] xx [F/Y] x [D/E] (x represents variable amino acid) (161, 177, 399). Vleugel and colleagues have demonstrated that deleting BUB1 amino acids between 501 and 555 containing BUB1 KEN1 and ABBA motifs caused inefficient CDC20 kinetochore localization and defective SAC in human cells (399). In another study cells expressing mutation of the same KEN1-box and Phe-box could not inactivate APC/C compared to WT samples, therefore CDC20 binding to BUB1 is required for SAC (375). In summary, the above studies

clearly show that BUB1 involved in the recruitment of members of MCC therefore, has a key role in SAC in besides its kinase activity.

Studies in frog and human cells have demonstrated the requirement of BUB1 in recruitment and stability of CPC and RZZ complex (151, 398, 436). BUB1 kinase activity is required to recruit Borealin and Survivin in humans and fission yeast respectively (302, 317). Interestingly, BUB1 recruitment itself depends on AURORA B function (146, 437). Analyses of BUB1 in budding yeast have contested its requirement in CPC kinetochore recruitment as depletion of either BUB1 or SGO1 did not impair CPC localization (306). In humans, BUB1 depletion significantly reduces ZW10 and Zwilch components of RZZ, thus BUB1 is required for recruitment of the RZZ complex (398).

Studies in yeast demonstrated that BUB1 is required for SGO recruitment to centromeres during mitosis and meiosis (264, 394, 429, 438). Similarly, in mice, *Xenopus* and human cells, BUB1 depletion caused SGO misrecruitment and cohesion defects (151, 269, 271, 292, 397, 413, 430, 436). Initial studies to learn about the mechanism of SGO recruitment resulted in controversial outcome. Studies in fission yeast showed that BUB1 constructs lacking kinase domain were efficient in recruiting SGO1 to centromeres suggesting that BUB1 kinase activity is dispensable for SGO1 recruitment (439). However, in a similar yeast study, SGO1 was mislocalized from centromeres in cells expressing kinase inactive BUB1 (264).

Data available for budding yeast, mice and human cells have confirmed that BUB1 kinase activity is indeed required for SGO1 (151, 397, 429, 430). Histone H2A was identified as a substrate of BUB1 kinase through experiments in which BUB1 efficiently phosphorylated Histone H2A at S121 (H2AT120 human) (274). This elucidated the missing link between BUB1 and recruitment of SGO to centromeres. Further studies demonstrated that H2A T120 signal was enriched at centromeres in a BUB1 dependent manner as depletion of BUB1 severely reduced H2ApT120 signal (275, 401, 413). Moreover, SGO1 localized primarily at centromere in mice and human cells (268, 270, 430). Two recent reports have studied the role of BUB1 to determine localization pattern of SGO1 during mitosis in human cells (273, 275). SGO1 is phosphorylated by CDK1 at T346 (Figure 1.12) required for

cohesin binding and cohesion protection (273). SGO1 mutagenesis studies showed that SGO1 binding to cohesin rather than its H2ApT120 mediated kinetochore localization is required for cohesion protection (275). Furthermore, BUB1 mediated phosphorylation of H2ApT20 recruits SGO1 predominantly to kinetochores where it binds to cohesin and subsequently to inner centromeres in human cells (275).

Overall, BUB1 is a highly active SAC member needed for recruitment of other kinetochore proteins. BUB1 depletion or its ectopic expression analyses have demonstrated that structural interactions recruit BUB1 targets to kinetochores and its kinase activity is required for chromosome alignment and segregation function (394, 398, 428).

Table. 1. The summary of BUB1 mitotic functions in different organisms

	SAC function	Kinase activity and SAC	Recruitment function
Yeast	✓	✗	✓
C.elegans	✓	✓	✓
Mice	✓	Contentious	✓
Xenopus	✓	✗	✓
Drosophila	✓	Not reported	✓
Human	✓	Contentious	✓

1.4.4.5. BUB1 in chromosome congression, biorientation and segregation

Chromosome congression can facilitate bi-orientation by bringing chromosomes to a metaphase plate. Once biorientation is achieved, cleavage of cohesin leads to normal chromosome segregation (49, 440). Thus,

chromosome congression, biorientation and segregation are tightly connected. Studies on mouse oocytes have described the role of BUB1 in chromosome congression in which BUB1 knockout oocytes had chromosome congression defects (252). Others have confirmed that in yeast, mouse and human cells chromosome alignment and congression defects are increased after BUB1 depletion or mutations in its structure (146, 151, 269, 392, 394, 397, 403, 428, 430). While kinase activity is required in yeast and human cells (397, 421) others have concluded that BUB1 kinase function is not needed for chromosome congression in mice and human cells (151, 252, 430). Interestingly, a single point mutation at non-kinase N-terminus A130S residue causes chromosome congression defects (397). Abolishing BUB1 activity by chemical inhibitors causes mislocalization of SGO, and CPC, however, chromosome segregation is unaffected in human cells (151). This observation is contrary to our understanding that BUB1 kinase function is required for chromosome congression through SGO and CPC localization (179, 413).

BUB1 is implicated in chromosome congression in above studies; therefore, it might also be important for biorientation and kinetochore-microtubule attachments (269, 428). Yeast and vertebrate studies have concluded that BUB1 phosphorylation stimulates H2A to recruit SGO which regulates centromeric loading of CPC and bi-orientation (264, 318, 429, 436). Contrarily, a study in mice has demonstrated that BUB1 is partially needed for kinetochore-microtubule attachments and biorientation (423). In humans, BUB1 and AURORA B have been shown to be required for kinetochore-microtubule attachments and biorientation respectively (426). Yet another study demonstrated that BUB1 is required for chromosome attachments independent of AURORA B kinase (428, 441). Overall, these studies show requirement of BUB1 for chromosome congression, segregation and biorientation.

1.4.4.6. BUB1 in Aneuploidy and Cancer development

The complete loss of SAC leads to early embryo death and the SAC gene deregulation is implicated in aneuploidy and tumor development which is explained in more detail in "Importance of SAC" above. Supporting this

argument, in mouse model complete BUB1 inactivation has been implicated in embryonic lethality due to mitotic defects (423) and hypomorphic expression or catalytically inactive BUB1 leads to aneuploidy and tumor formation (392, 413, 432). Similarly in human cells, BUB1 mutations result in tumor metastasis and progression (442). Chromosome instability leads to aneuploidy (443, 444) and several studies have identified mutation or abnormal *Bub1* expression in chromosomally unstable cancer cells of colon, breast and lungs (115, 236, 445, 446). Thus, BUB1 deregulation contributes to tumorigenesis through cell division regulation.

1.5. Hypothesis and Objectives

BUB1 is one of the core kinases of SAC. It is required for recruitment of other SAC components and its kinase function is needed for chromosome congression. In the past, the kinase function of BUB1 has been studied however; the autophosphorylation function of BUB1 has not been explored in detail. Owing to the importance of kinase function of BUB1, it is imperative to investigate BUB1 autophosphorylation function. This doctoral project particularly sought to understand the role and place of BUB1 autophosphorylation in downstream signaling of BUB1. Objectives were set based on hypotheses and cell based assays were employed to test them which are explained in two parts below.

Aim 1:

An earlier study explored the functional analyses of certain structural domains of BUB1 (397). The structural domains that included TPR, BUB3 binding domain (also known as GLEBS), conserved motif I and kinase extension domain were studied for their role in SAC and chromosome congression (397). However, their role in BUB1 kinase activity and autophosphorylation was not reported. We hypothesized that due to their relevance in the SAC and chromosome congression these domains could also be required for autophosphorylation and kinase activity. Prior to the start of my doctoral project, BUB1 autophosphorylation sites had been identified in Dr. Sabine Elowe's Lab. We decided to use autophosphorylation sites (T589) for this doctoral project due to the fact that it is a highly conserved autophosphorylation site present outside the kinase domain. We set our objectives to understand the role of these domains in kinase activity and autophosphorylation of BUB1 described in chapter 2. We used following methodology to achieve this aim.

- Tested the role of these individual domains by transiently expressing mutants of these domains and evaluated their role in BUB1 kinase activity and autophosphorylation using cell based assays similar to the ones reported by Klebig and colleagues. We used phosphospecific antibodies against T589 and S679 autophosphorylation to elucidate the

role of domains mentioned above in BUB1 autophosphorylation and kinase activity.

- The role TPR domain at N-terminus of BUB1 in its localization has been implied by previous studies (79, 409). However, other relevant studies have not supported this conclusion (193, 410). To definitely test this we used TPR domain mutant (Δ TPR, lacking first 150 amino acids) and utilized in vitro and in vivo cell based experiments shown in chapter 2 to investigate the role of BUB1 TPR domain. We also investigated the contribution of TPR domain in BUB1 kinase activity.

Aim 2:

We chose to study the conserved autophosphorylation site T589 present outside the kinase domain for it is conserved from yeast to humans. We hypothesized that owing to its highly conserved position, this site could be important for BUB1 signaling. We sought to test this by using cells stably expressing BUB1 T589A mutant (replacing Threonine with Alanine) in HeLa cells. Using in vitro and in vivo techniques we tested the localization of BUB1 substrate Histone H2A phosphorylation at T120 (H2ApT120). Previous studies have defined this signaling pathway in which SGO1 is recruited to centromeres after H2ApT120 by BUB1 for proper chromosome cohesion (274).

As explained in Chapter 2 below, we observed the spread of H2ApT120 and SGO1 on chromosomes in T589A mutants. We set our objective to understand the underlying mechanism. In the literature, cells expressing inactive BUB1 have chromosome arm spread of H2ApT120 and SGO1 (269, 275). However, BUB1 T589A mutant is an active kinase and is stably expressed at kinetochores. Could mutation at T589 alter BUB1 turnover that causes abnormal localization of these substrates? To test this hypothesis we performed the following experiments.

- We compared the cytoplasmic expression of BUB1 T589A with controls using fixed cells on cover slips and live cells to avoid permeability artifacts in the fixed cells.
- Used fluorescence recovery after photobleaching (FRAP) and tested the kinetochore turnover of BUB1 T589A and controls.

- To confirm that the abnormal spread of BUB1 substrate H2ApT120 was due to abnormal turnover in BUB1 T589A mutants we stably tethered T589A using MIS12 tag and measured the recovery of H2ApT120 and SGO1 in MIS12 constructs.

2. Chapter2

Bub1 autophosphorylation feeds back to regulate kinetochore docking and promote localized substrate phosphorylation

Adeel Asghar^{1, 2}, Audrey Lajeunesse¹, Kalyan Dulla³, Guillaume Combes^{1,2}, Philippe Thebault², Erich Nigg⁴ and Sabine Elowe^{1,2,5}

- 1 Molecular and Cellular Biology, Faculty of Medicine, Université Laval.
- 2 Axe of reproduction, mother and youth health, Centre de recherche du Centre Hospitalier Universitaire de Québec, Québec, Québec, G1V 4G2, Canada.
- 3 Current address: ProQR Therapeutics N.V., Darwinweg 24, 2333 CR Leiden, Netherlands
- 4 Biozentrum, University of Basel, Klingelbergstrasse 50/70, CH-4056 Basel, Switzerland
- 5 Author for correspondence: sabine.elowe@crchuq.ulaval.ca

Running title: Autoregulation of Bub1 signaling

2.1. ABSTRACT

During mitosis Bub1 kinase phosphorylates Histone H2A-T120 to promote centromere sister chromatid cohesion through recruitment of shugoshin (Sgo) proteins. The regulation and dynamics of H2A-T120 phosphorylation are poorly understood. Using quantitative phosphoproteomics we show that Bub1 is autophosphorylated at numerous sites. We confirm mitosis-specific, autophosphorylation of a several residues, and show that Bub1 activation is primed in interphase but fully achieved only in mitosis. Mutation of a single autophosphorylation site T589 alters kinetochore turnover of Bub1 and results in uniform H2A-T120 phosphorylation and Sgo recruitment along chromosome arms. Consequently, improper sister chromatid resolution and chromosome segregation errors are observed. Kinetochore tethering of Bub1-T589A refocuses H2A-T120 phosphorylation and Sgo1 to centromeres. Recruitment of the Bub1-Bub3-BubR1 axis to kinetochores has recently been extensively studied. Our data provides novel insight into the regulation and kinetochore residency of Bub1, and indicates that its localization is dynamic and tightly controlled through feedback autophosphorylation.

2.2. RÉSUMÉ

Au cours de la mitose la kinase Bub1 phosphoryle Histone H2A-T120 pour promouvoir la cohésion des chromatides sœurs au centromère par le recrutement des protéines Shugoshin (Sgo). La régulation et la dynamique de la phosphorylation de H2A-T120 sont encore mal comprises. En utilisant des techniques phospho-protéomique quantitatives, nous montrons que Bub1 est autophosphorylée à de nombreux sites. Nous confirmons l'autophosphorylation de plusieurs résidus spécifiques de la mitose et montrons que l'activation de Bub1 est commencée en interphase mais est complètement atteinte seulement en mitose. La mutation d'un unique site d'autophosphorylation T589 modifie le renouvellement de Bub1 au kinétochore et a pour effet une phosphorylation de H2A-T120 et un recrutement uniforme de Sgo le long des bras chromosomiques. Par conséquent, une mauvaise résolution des chromatides sœurs et des erreurs dans la ségrégation des chromosomes sont observées. Le rattachement de Bub1-T589A au kinétochore relocalise la phosphorylation de H2A-T120 et SGO1 aux centromères. Récemment le recrutement de l'ensemble Bub1-Bub3-BubR1 aux kinétochores a largement été étudié. Nos données fournissent un nouvel aperçu de la régulation et de la localisation de Bub1 au kinétochore, elles indiquent que sa localisation est dynamique et étroitement contrôlé par un mécanisme de rétrocontrôle de l'autophosphorylation.

2.3. INTRODUCTION

The accurate traverse through mitosis results in equal allocation of duplicated sister chromosomes, and is critical for cellular and organism health. To ensure this, eukaryotes have evolved a safe-guard mechanism known as the spindle assembly checkpoint (SAC) which functions during both meiosis and mitosis ¹⁻⁵, and monitors the correct attachment of kinetochores to microtubules. The activities of both the SAC and the microtubule attachment machinery are orchestrated by a network of kinases and phosphatases. SAC kinases including budding uninhibited by benzamidazole 1 (Bub1), monopolar spindle 1 (Mps1) and Aurora B play a dual and interconnected role in microtubule attachment regulation and SAC signaling ^{6, 7}. Recently, a remarkable body of work has begun to outline how these kinases (and their counteracting phosphatases) monitor the status of attachments and relay this as a diffusible biochemical signal. A clear picture of the recruitment of the checkpoint kinase Bub1 to the kinetochore is beginning to emerge. Mps1 phosphorylation of so-called MELT motifs on the KNL1 subunit of the macromolecular KMN complex together with the KI (Lys-Ile) motifs of KNL1 promote the recruitment of Bub1-Bub3 in a manner that involves multiple cooperative interactions ^{5, 8}. Less well understood is how this recruitment is dynamically regulated although recent evidence supports a role for the protein phosphatases PP2A and PP1 in determining the extent of Bub1 recruitment ^{9, 10}. The current model posits that once at the kinetochore, Bub1 acts as a stable scaffold for recruitment of APC/C inhibitors including BubR1, Mad1 and Mad2, as well as centromere proteins E and F (Cenp-E and Cenp-F, respectively) and the mitotic centromere-associated kinesin (MCAK); this scaffolding function of Bub1 is thought to be kinase independent ^{11, 6, 12}.

Bub1 also has kinase-dependent functions during mitosis. Cdc20 is an in vitro target of Bub1, and this phosphorylation may directly contribute to APC/Cdc20 inhibition ¹³. Bub1 phosphorylation of the conserved histone H2A at T120 (H2A-T120, human numbering) results in a histone mark that mediates the recruitment of MEI-S332/shugoshin (Sgo) proteins to the centromere during both meiosis and mitosis ¹⁴. In mammalian mitosis, Bub1 recruitment of Sgo1 in complex with protein phosphatase 2A (PP2A) protects cohesion at centromeres until the metaphase-anaphase transition ¹⁵⁻¹⁸. The

kinase activity of Bub1 is therefore clearly critical for ensuring faithful chromosome segregation, and recent elegant work has begun to elucidate how Bub1 kinase activity is regulated. Crystal structures and biochemical studies have shown that autophosphorylation of Bub1 in the activation segment results in conformational changes of this region to selectively regulate the activity of Bub1 towards H2A-T120¹⁹. Thus, another important substrate of Bub1, is Bub1 itself.

Here, we use a quantitative proteomics approach to identify Bub1-specific autophosphorylation sites. We show that Bub1 is significantly autophosphorylated outside the activation segment and kinase domain, including at the conserved Threonine 589 (T589). We show the Bub1 activity is primed in interphase but does not fully mature until mitosis. Immunofluorescence with a phosphospecific antibody indicates that autophosphorylation at T589 is prevalent during early mitosis. Alanine substitution of this residue (T589A) results in chromosome missegregation and incomplete sister chromatid arm resolution as a result of non-localized H2A-T120 phosphorylation and ectopic Sgo1 recruitment. Fluorescence recovery after photobleaching (FRAP) experiments reveal that Bub1-T589A and Bub1-kinase dead (D946A, hereafter referred to as KD) exhibit more rapid kinetochore turnover than wild-type (WT) protein. Forced localization of Bub1-T589A to the KT refocuses H2A-T120 phosphorylation and Sgo1 localization to the kinetochore. We propose that spatially-constrained H2A-T120 phosphorylation, and thus sister chromatid cohesion, is promoted by a positive feedback mechanism formed by autophosphorylation of Bub1 at T589 that regulates the dynamics of Bub1 kinetochore docking.

2.4. RESULTS

2.4.1. Identification of Bub1 autophosphorylation sites

To identify Bub1 autophosphorylation sites, we devised an approach based on stable isotope labelling in cell culture (SILAC, Fig. 2.1 a) of Bub1 WT and KD. To enable quantitation of the changes of phosphopeptide abundance by mass spectrometry, cells were labeled by growing them in medium containing either light arginine and lysine (Arg0/Lys0) or the heavy isotopic variants [¹³C₆,¹⁵N₄]arginine and [¹³C₆,¹⁵N₂]lysine (Arg10/Lys8). Immunoprecipitated,

mitotic, Bub1-WT and Bub1-KD expressed in differentially labelled cells were separately subjected to a non-radioactive *in vitro* kinase assay. This autophosphorylation amplification step was introduced to increase the occupancy of phosphorylation sites within Bub1 and thus increase phosphopeptide detection, and importantly, to allow distinction between genuine autophosphorylation sites and phosphorylation incurred by co-precipitating kinases. We also considered this approach superior to an *in vitro* assay of recombinant proteins as Bub1 mitotic modifications, localization and binding partners may all contribute to genuine and physiologically relevant Bub1 autophosphorylation. The experiment was performed in triplicate with minor changes: the amino acid labeling was reversed in one replicate (exp2, Fig. 2.1 b) to control for a potential effect of amino acid labelling, and in the final replicate (exp3, Fig. 2.1 b), a combination of Lys-C, Glu-C and elastase were used instead of trypsin to diversify peptide coverage.

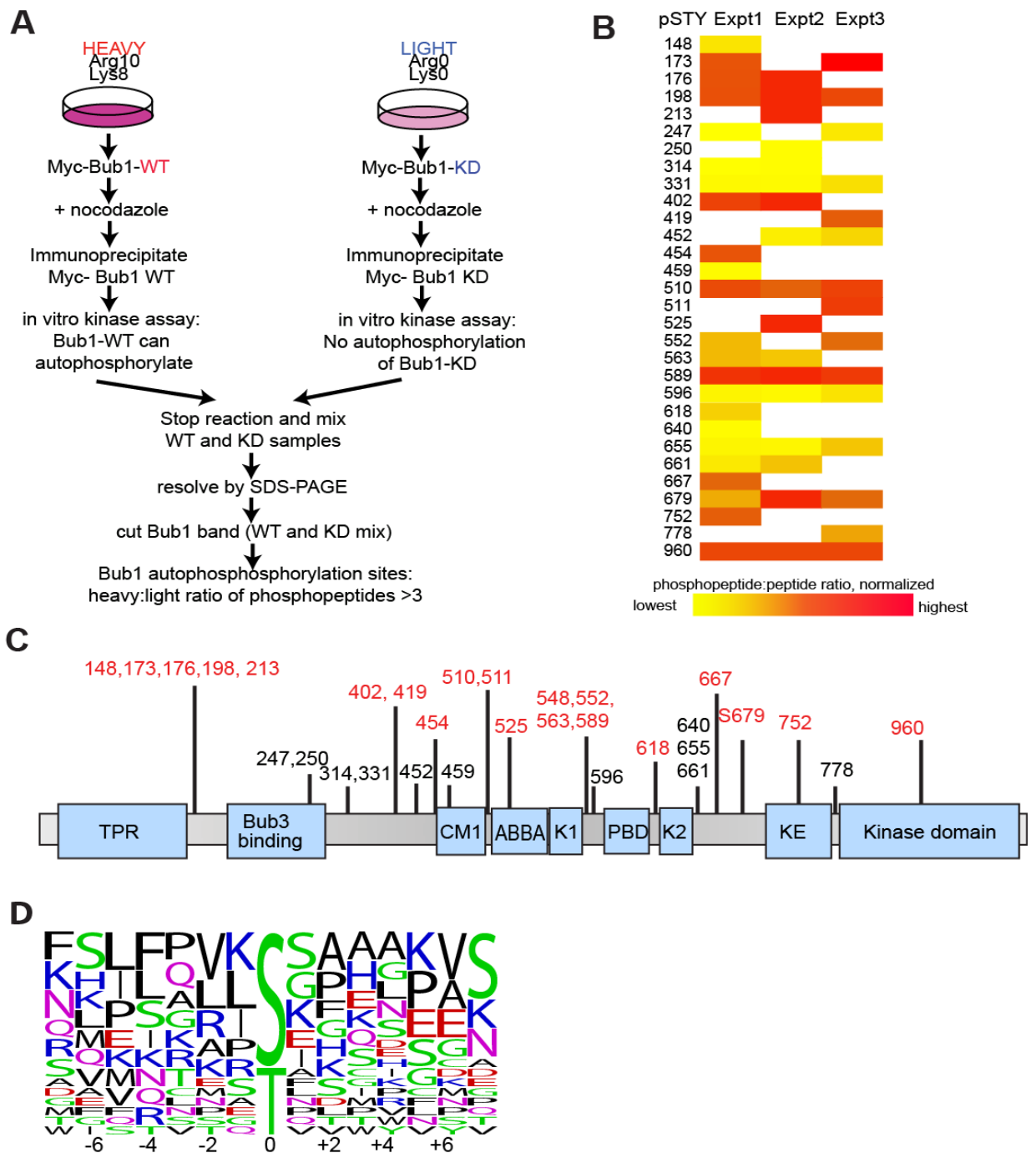


Figure 2.1 Identification of Bub1 autophosphorylation sites: (a) Schematic of the SILAC protocol for identification of Bub1 autophosphorylation sites. (b) Heat map representation of normalized phosphopeptide: peptide ratio of phosphosites identified on Bub1 from 3 independent mass spectrometry experiments. (c) Cartoon illustration of the position of the identified phosphorylation sites relative to the functional domains of Bub1. Autophosphorylation sites are red; other phosphorylation sites are in black. (d) Weblogo representation and amino acid enrichment of Bub1 surrounding phosphorylation sites.

Data from the three independent experiments resulted in a combined coverage of 68% of Bub1, and a total of 38 unique phosphorylation sites (MASCOT score cutoff of ≥ 13 ; Class I sites ²⁰ (table S1), of which 30 sites could be definitively assigned SILAC and protein ratios in at least 1 replicate. Threonine 960 phosphorylation in the activation segment of the kinase domain was identified in all three experiments, was found to have a high phosphopeptide:peptide ratio, and was used as reference for normalization; results of which are shown in Fig 2.1 b. Several additional phosphosites were identified after Lys-C, Glu-C, and elastase digestion but contained neither lysine nor arginine and no SILAC ratio could be assigned. These were thus excluded from further analysis (See Supplementary Data 1).

Of the sites we identified, 19 were novel, whereas 19 have been previously curated in PhosphoSitePlus. The majority of the phosphorylation sites identified were situated in low complexity stretches in between domains (Fig. 2.1c) with the exception of T960 in the kinase activation segment.

20 phosphosites were significantly upregulated in Bub1-WT compared to Bub1-KD, and thus considered potential Bub1 autophosphorylation sites (Fig. 2.1 c, red). These sites exhibited a fold increase in phosphopeptide:peptide ratio of ≥ 3 , considered a conservative cutoff requirement for fold change ²¹. Alignment of these sites, together with H2A-T120 (Fig. 2.1 d) suggested a tendency for basic (mainly K at positions -1 and +5) and small nonpolar (at positions +2, +3) residues relative to the phosphoacceptor, as well as an exclusion of acidic residues surrounding the phosphosites. Of the phosphosites that were not considered to be Bub1 dependent (phosphopeptide:peptide ratio < 3), 50% (residues 452, 459, 596 and 655) were followed by a proline suggesting that they may be targets of a proline-directed kinase such as CDK1 or MAPK, in agreement with previous observations ²²⁻²⁴. S314 and S331 adhered to the consensus for ATM/ATR kinases; S314 was previously identified as an ATM site and may be required for Bub1 activation ^{25, 26}. Two additional sites, S247 and S250 adhered to a Plk1/Mps1 consensus, which have also been shown to phosphorylate Bub1^{27, 24}. Thus, Bub1 is highly phosphorylated by a number of mitotic kinases, including itself.

2.4.2. Regulation of Bub1 activation and autophosphorylation

To investigate Bub1 autophosphorylation at sites outside the activation segment, we generated phosphospecific antibodies towards two potential autophosphorylation sites, T589 and S679. These sites (see Fig. 2.2 a for evolutionary alignment) were consistently autophosphorylated in our MS experiments. They were also preceded by at least one basic residue at the -1 (T589) or -2 (S679) position, and have been independently observed in large scale mitotic mass spectrometry screens ^{21, 28}; we thus reasoned that they were genuine *in vivo* autophosphorylation sites. Anti-pT589 staining of fixed cells clearly decorated kinetochores and overlapped the Bub1 signal in prophase and prometaphase (Supplementary Figure 1a). Anti-pT589 signal was lost upon depletion of Bub1 or phosphatase treatment (Supplementary Figure 1b), demonstrating that the pT589 signal is both Bub1-dependent and phosphospecific. Importantly, depletion and rescue experiments revealed that the pT589 signal was lost in Bub1-KD and Bub1-T589A expressing cells (Supplementary Figure 1c) indicating that phosphorylation at T589 is strictly dependent on Bub1 kinase activity, in agreement with its identification as an autophosphorylation site.

No signal was detected by immunofluorescence with anti-pS679 antibody, although there was a clear signal on Western blots. Anti-pS679 detects Bub1 from mitotic extracts, before but not after phosphatase treatment, demonstrating phosphospecificity of this antibody (Supplementary Figure 1d).

A number of groups have recently reported on the role of the Bub1 TPR domain in regulating kinase activity with conflicting results ^{19, 29, 30}. We thus sought to determine domains of Bub1 required for kinase function as measured by autophosphorylation. We depleted endogenous Bub1 with siRNAs targeting the 3'UTR ³¹, and expressed MYC-tagged Bub1, WT, KD, the Bub3-binding mutant (Δ 229-256), the checkpoint mutant in conserved motif I (Δ 458-476), the kinase extension domain mutant (Δ 740-766)¹², and the Δ TPR in HeLa cells. We then determined phosphorylation at T589 (Fig. 2.2 b, c) and S679 (Fig. 2.2 c).

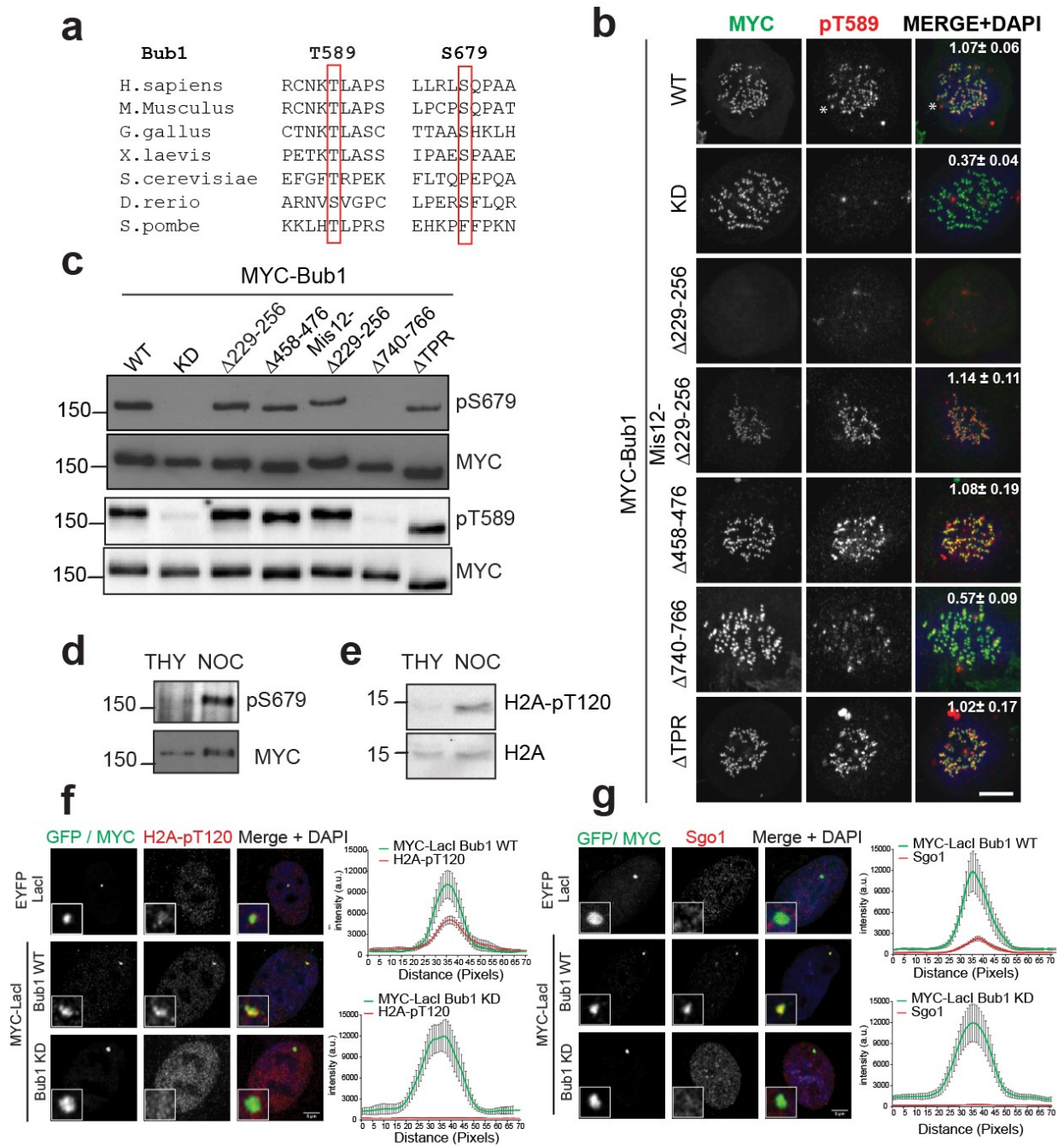


Figure 2.2 Full Bub1 activation is mitotic specific and requires the kinase extension domain: (a) Evolutionary conservation of Bub1 T589 and S679. (b) Bub1 deletion mutants were expressed in HeLa cells depleted of endogenous Bub1. Mitotic cells were stained with Hoechst (Blue in MERGE), anti-MYC (green) and anti-pT589 (red), scale bar= 10 μ m. Quantitation of pT589 signal relative to CREST at kinetochores (mean \pm SE) from a minimum of 10 cells per condition is indicated in the right-most panel. (c) Cells were transfected with Bub1 mutants as in (b) and enriched in mitosis by nocodazole treatment. Anti-pT679 (upper half) and anti-pT589 (bottom half) Western blots were performed with MYC-Bub1 immunoprecipitated from equalized lysates. Anti-MYC blotting (second and fourth panels) reveals equal loading. (d) MYC-Bub1 was immunoprecipitated from HeLa cells stably expressing MYC-Bub1-WT arrested in G1/S or mitosis by thymidine (THY) or nocodazole (NOC)

treatment, respectively, and blotted with Anti-pT679 antibodies (upper panel) or stripped and reprobed with anti-MYC. (e) Western blots of Histones purified from thymidine and nocodazole arrested cells with anti-H2A-pT120 (upper panel) and anti-H2A (lower panel) antibodies. (f) and (g) U2OS cells expressing a 256 copy array of the *lac* operator were transfected with a LacI-GFP, 3XMYC-LacI-Bub1-WT or KD. Fixed cells were stained with Hoechst (blue), anti-MYC or GFP in the control (green) and either anti-H2A-pT120 (red, f), or anti-Sgo1 (red, g). The overlap between the MYC and H2A-pT120 or Sgo1 is shown in the panel on the right of each figure. Error bars represent SE. Scale bar= 5 μ M.

As the Bub3-binding mutant Δ 229-256 does not bind to the kinetochore, we forced kinetochore localization using a Mis12-tag to determine the role of Bub3 binding in Bub1 activation independent of its role in kinetochore recruitment. As expected Bub1-WT expressing cells demonstrated robust pT589 and pS679 signal, whereas little or no signal was observed in cells expressing Bub1-KD or the Bub1 kinase extension domain mutant (Δ 740-766, Fig. 2.2 b, c), confirming the status of these sites as *bona fide* Bub1 autophosphorylation sites. Bub3-binding, conserved motif I and the TPR domain of Bub1 did not significantly contribute to Bub1 kinase activity, as measured by T589 and S679 phosphorylation (Fig. 2.2 b, c). Kinetochore recruitment is therefore not required for Bub1 activation, but serves to focus Bub1 kinase activity to kinetochores. We were also intrigued by the recent suggestion that Bub1 is a constitutively active kinase based on the persistent phosphorylation of the P+1 autophosphorylation site S969 in G1¹⁹. To definitively test this, we verified Bub1 autophosphorylation at S679 (Fig. 2.2d) as well as H2A-T120 (Fig. 2.2e) in extracts from thymidine and nocodazole-arrested cells. We find that neither Bub1-S679 nor H2A-T120 (in agreement with previous results ¹⁴) was apparently phosphorylated in interphase extracts although a clear signal was detected in extracts from mitotic cells, suggesting that Bub1 was not generally active during interphase. Nevertheless, we considered the possibility that the constitutive phosphorylation of S969 may reflect partial Bub1 activity, as has been previously suggested ¹⁹

To test whether Bub1 may be further activated during interphase, we expressed 3xMYC and *Lac* repressor (*LacI*)-fused Bub1 WT and Bub1-KD in cells stably expressing a 256-copy array of the *lac* operator sequence (*LacO*) in an arm of chromosome1³² in an effort to artificially increase the localized

concentration of Bub1. In interphase cells, LacI-tagged Bub1 WT and KD efficiently localized to the *LacO* array as indicated by anti-MYC immunofluorescence. In lacI-Bub1-WT but not LacI-Bub1 KD-expressing cells or control cells, a clear overlapping signal was detected for H2A-pT120 and Sgo1 (Fig. 2.2 f, g). Thus, increasing the local concentration of Bub1 is sufficient to induce its activation, even in the absence of kinetochores in interphase. This is in agreement with our data above showing that Bub1 activity is not dependent on Bub3-binding (Fig.2.2 b, c). Collectively, our results demonstrate that Bub1 phosphorylation at T589 and S679 occurs *in vivo* and establish that these are indeed autophosphorylation sites. Moreover, our data confirm and extend earlier observations demonstrating that Bub1 activation is primed already in interphase. We show that under normal circumstances, Bub1 is not sufficiently active in interphase but can be efficiently activated by increasing the local concentration.

2.4.3. Bub1 T589 autophosphorylation regulates mitotic progression

We next focused on the role of T589 autophosphorylation as this site is highly evolutionarily conserved (Fig 2.2 a). We generated stable isogenic HeLa lines expressing a single copy of triple MYC and GFP-tagged Bub1 WT, KD and T589A¹² (Supplementary Figure S2a, b). In *in vitro* kinase assays, Bub1-T589A supported efficient H2A-T120 phosphorylation and mitotic arrest in the presence of nocodazole or taxol, suggesting that T589 phosphorylation is not implicated in regulation of the kinase activity or the SAC function of Bub1 (Supplementary Figure 2 c, d).

We sought to test whether Bub1 autophosphorylation at T589 contributes to chromosome congression which requires Bub1 kinase activity^{12, 29, 33}. Stable Bub1 lines were depleted of endogenous Bub1, and treated with MG132 to monitor congression. Whereas approximately 50% of Bub1-WT expressing cells aligned metaphase plates, only 23% of Bub1-KD and 26% of Bub1-T589A cells aligned at metaphase (Fig. 2.3 a, b). The misalignment observed in cells expressing Bub1-KD was more severe than that observed in Bub1-T589A cells (71% in Bub1-KD cells versus 39% in Bub1-T589A cells with >12 misaligned kinetochores, Fig.2.3 c), indicating that T589 is not the only Bub1

substrate to contribute to chromosome alignment. We also assessed mitotic defects and progression in the Bub1 cell lines by live-cell imaging of progression through an unperturbed mitosis in cells co-expressing mRFP-Histone H2B to permit chromosome visualization. We found no significant difference in the duration of mitosis between control (GL2 siRNA), Bub1-depleted cells, and cells depleted of endogenous Bub1 but rescued with Bub1-WT and Bub1-KD, in agreement with previous reports ¹². Strikingly, cells expressing Bub1-T589A consistently required more time to complete mitosis, averaging 102 minutes between NEBD and anaphase, whereas cells expressing WT and KD Bub1 required on average 71 and 75 minutes, respectively (Fig. 2.3 d, e, Movies S1-S3, the video files have been submitted separately with this thesis). In agreement with our observations in fixed samples, chromosome attachment defects were less pronounced in Bub1-T589A expressing cells, than in Bub1-KD cells (Fig. 2.3 f). Our data demonstrate that Bub1 autophosphorylation at T589 contributes to proper chromosome congression, and mutation of this residue causes a transient delay in mitosis.

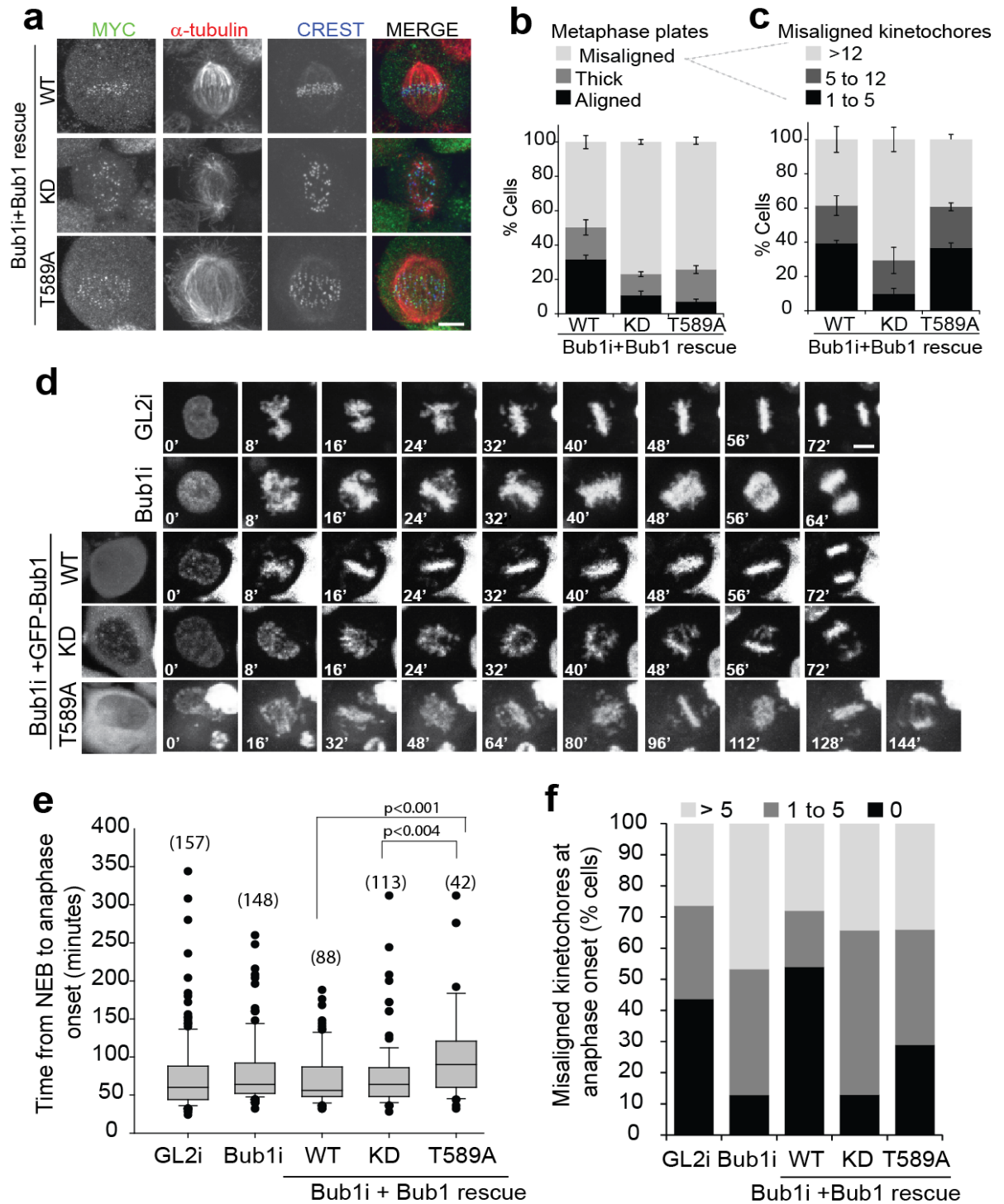


Figure 2.3 Loss of Bub1 phosphorylation at T589 causes chromosome congression defects: (a) Stable cell lines expressing Bub1-WT, Bub1-KD, and Bub1-T589A were generated. See Supplementary Figure 2 for characterization of the cell lines. Cells depleted of endogenous Bub1 were synchronized in mitosis as in Fig 2 (a) and then arrested for a further 2 hours in MG132 before fixation and staining with anti-MYC (green), anti- α -tubulin (red) and anti-CREST (blue). (b) Quantitation of metaphase alignment from (a) was determined as described under materials and methods. A minimum of 100 cells were considered per condition in each of three replicates. Bars represent SE. (c) The number of kinetochores from the "misaligned" category in (b) in the various Bub1 expressing lines. (d) Stills of the live-cell imaging

of the cells lines and treatments indicated. Movies for Bub1-WT, KD and T589A expressing cells are shown in Supplementary Movies 1-3, respectively (the video files have been submitted separately with this thesis). (e) Quantitation of the mitotic timing of the experiment in (d). The number of cells scored is indicated in parentheses. Significance is measured by *t* test (two-tailed). (f) Quantitation of lagging kinetochores at anaphase observed in (d). The number of cells scored per condition is indicated in (e). Scale bar= 10 μ M.

2.4.4. Bub1 autophosphorylation restricts H2A-pT120 to centromeres

The delay in mitotic progression in Bub1-T589A expressing cells was somewhat surprising considering that the more severe KD mutant exhibited normal timing. We reasoned that the effect of the T589A mutation on mitotic timing may be masked in the Bub1-KD, in which all Bub1 phosphorylation and activity is lost. To address this possibility, we sought to determine the effect of the T589A mutant on kinase-dependent Bub1 signaling. The H2A-pT120 centromeric mark generated by Bub1 recruits Sgo1 and Sgo2 to promote chromosome biorientation and proper chromosome segregation¹⁴; lack of Bub1 protein or Bub1 kinase activity has been reported to cause the spread of Sgo1 along the entire length of the chromosome^{15, 34, 35}. In agreement with these observations, we find that Sgo1 is mislocalized to chromosome arms in cells expressing Bub1-KD, whereas Sgo1 is primarily localized to the centromere in cells expressing Bub1-WT^(34, Fig. 2.4 a). Like Bub1-KD, expression of Bub1-T589A, led to relocalization of Sgo1 to chromosome arms, and the Sgo1 signal was more intense than that detected in Bub1-KD cells, an observation that was confirmed by corrected total cell fluorescence measurements directly on the chromosome arms (Fig. 2.4 a and quantification within).

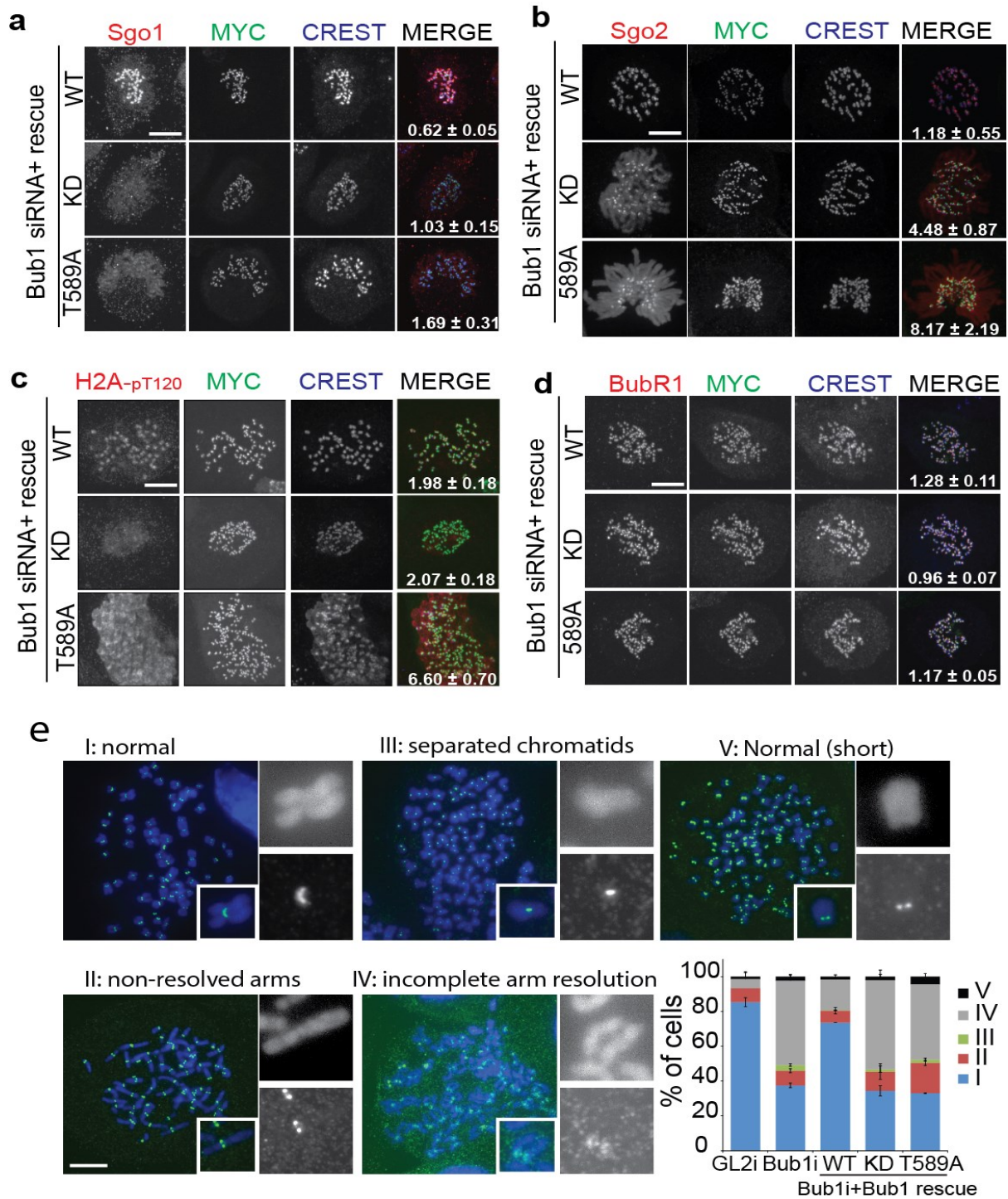


Figure 2.4 Uniform H2A-T120 phosphorylation, ectopic Sgo recruitment and impaired sister chromatid resolution in cells expressing Bub1-T589A: (a-d) Mitotic Bub1-WT, KD, and T589A depleted of endogenous Bub1 were fixed and stained with anti-CREST (blue), anti-MYC (green), and in (a) Sgo1, (b) Sgo2, (c) H2A-pT120, and (d) BubR1 (all in red). Quantitation of immunofluorescence intensity specifically at the chromosome arms (Corrected total cell fluorescence) ± SE of Sgo1, Sgo2 and H2A-pT120 is indicated in the respective MERGE panel. For BubR1, fluorescence intensity relative to the CREST signal ± SE is shown. (e) Stable Bub1 cell lines were depleted of endogenous Bub1, arrested in mitosis using nocodazole and harvested for chromosome spreads before staining with Hoechst (blue) and anti-

GFP (green). The different chromosomal conformations were quantified and indicated in the graph. The data represents the mean \pm SE of 4 independent experiments, with 58-105 cells scored per condition per experiment. Scale bar= 10 μ M.

Similarly, Sgo2 signal was detected at chromosome arms in cells expressing Bub1-KD whereas it localized as expected to the centromere in Bub1-WT cells (Fig. 2.4 b). Like Sgo1, expression of Bub1-T589A led to relocalization of Sgo2 to the chromosome arms (Fig. 2.4 b), at levels considerably higher than seen in Bub1-KD expressing cells. Nevertheless, a significant signal for Sgo2 could be clearly detected at the kinetochore indicating that unlike Sgo1, a pool of Sgo2 remained insensitive to Bub1-KD and Bub1-T589A. We next examined the H2A-T120 phosphorylation under the same conditions. In cells expressing Bub1-WT, H2A-pT120 was clearly localized to the centromere but lost in Bub1-KD expressing cells, as expected. Expression of Bub1-T589A, surprisingly, resulted in H2A-T120 phosphorylation along the entire length of the chromosome (Fig. 2.4 c). Quantitation of the H2A-pT120 signal specifically at chromosome arms revealed a significant increase in cells expressing this mutant compared to the essentially background staining observed Bub1-WT and Bub1-KD expressing cells (Fig 2.4 c).

To test whether the scaffolding function of Bub1 is altered by loss of T589 phosphorylation, we verified the localization of BubR1. We found that at least steady-state levels of BubR1 are unchanged between cells expressing Bub1-WT, KD or T589A (Fig. 2.4 d). Similarly, recent reports have concluded that Bub1 overexpression which leads to H2A-pT120 spread to chromosome arms did not alter the strength of the SAC or the recruitment of mitotic regulators²⁹. Collectively, our data indicate that T589 autophosphorylation limits H2A-pT120 and hence Sgo to centromeres. The extended mitosis observed in Bub1-T589A cells may thus be a result of the longer time required to remove the ectopic cohesion resulting from unchecked H2A phosphorylation.

Sgo1 translocation to the chromosome arms after Bub1 inactivation induces persistent cohesion along mitotic chromosomes¹⁵. We therefore tested whether Bub1-T589A expression also resulted in ectopic cohesion using chromosome spreads. In control GL2-treated cells (85%) and rescued cells expressing Bub1-WT (74%) sister chromatids were predominantly X-shaped with only the centromere connection apparently maintained (Fig. 2.4 e). As

expected, cells depleted of Bub1 or depleted of Bub1 and rescued with Bub1-KD showed a significant increase in the proportion of cells with poor resolution of sister chromatids along the entire chromosome length (57% and 62%, respectively). Similarly, and in agreement with the mislocalization of Sgo proteins, cells expressing Bub1-T589A (61%) mostly displayed incomplete resolution along the length of chromosomes, presumably due to unscheduled protection of cohesion caused by the spread of Sgo along the entire chromosome length. Together, these results suggest that in addition to H2A-T120 phosphorylation itself, Bub1 autophosphorylation at T589 is required to restrict H2A-T120 phosphorylation to the centromere, thereby confining Sgo and cohesion protection to this region.

2.4.5. Bub1-KD and -T589A display increased cytoplasmic residency

Loss of localized H2A-T120 phosphorylation in Bub1-T589A cells was also seen in KNL1-depleted cells¹⁹ and suggested that kinetochore targeting of Bub1 enriches H2A-T120 phosphorylation at centromeres¹⁴. To independently verify these observations, we depleted Bub3, the constitutive binding partner of Bub1 that is strictly required for Bub1 kinetochore binding through interaction with KNL1³⁶⁻³⁸, reviewed in⁸. Bub3 depletion results in efficient relocalization of Bub1 to the cytoplasm, as expected⁽³⁹⁾ and data not shown). Concomitant to this loss, we observed a massive spread of H2A-T120 phosphorylation along chromosome arms and a corresponding recruitment of Sgo1 (Fig. 2.5 a, b). These results are in strong agreement with the observation that Bub3 binding is not required for Bub1 activity *per se*, but rather to focus Bub1 activity to kinetochores (Fig. 2.2b, c), and argue that loss of Bub3-Bub1 concentration at the kinetochore results in ectopic H2A-T120 phosphorylation and Sgo1 recruitment¹⁹, likely through the activity of cytoplasmic Bub1.

The parallels in the phenotype observed in Bub3-depleted cells and Bub1-T589A cells were surprising, considering that Bub1-T589A localized efficiently to the kinetochore, as measured by indirect immunofluorescence, and exhibited normal activity towards H2A *in vitro* (Fig. S2b,c).

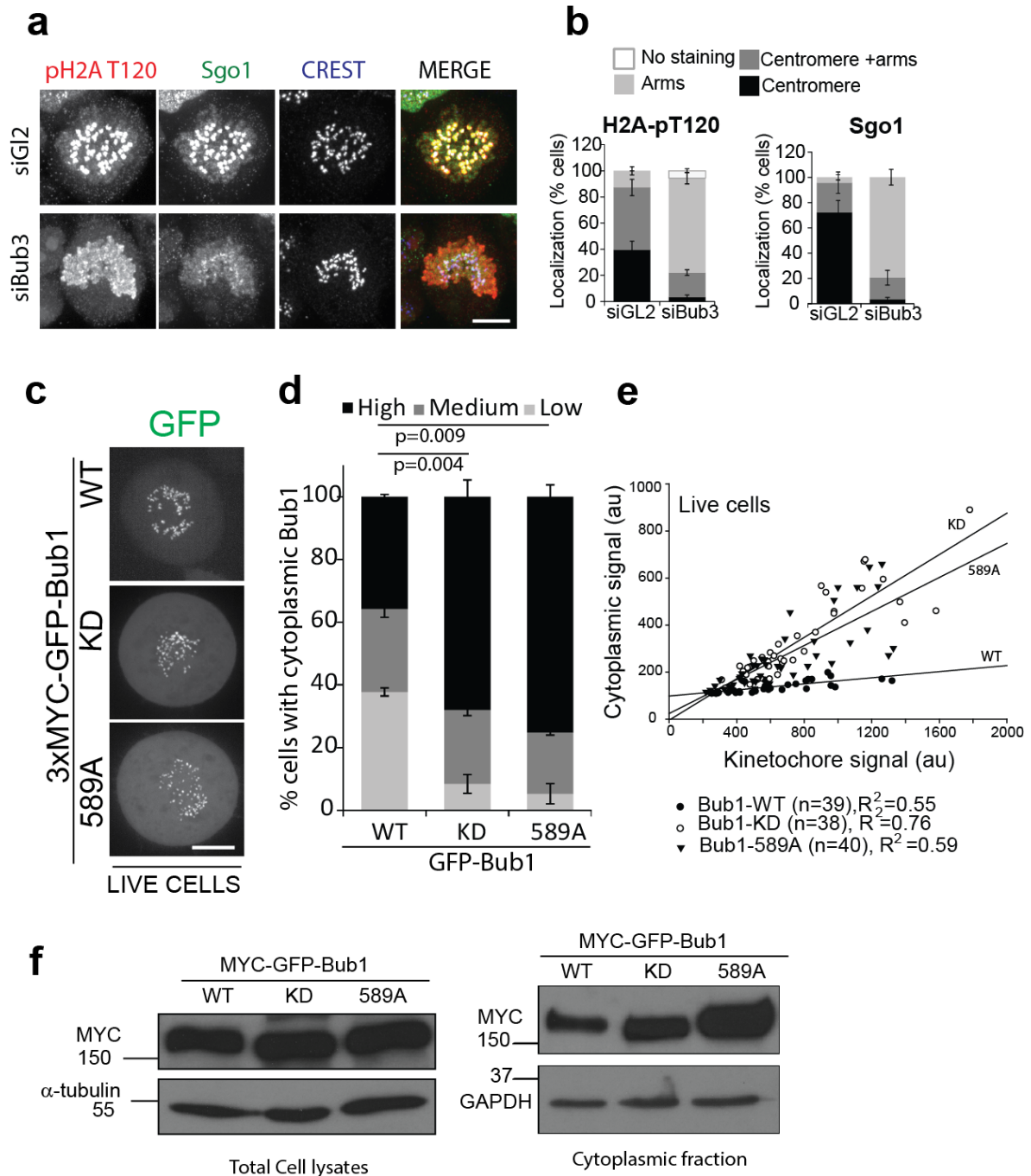


Figure 2.5 Bub1-KD and Bub1-T589A display increased residency in the cytosol: (a) Mitotic control (siGL2) and Bub3 depleted (siBub3) cells were fixed and stained with anti-H2A-pT120 (red), anti-Sgo1 (green) and anti-CREST (blue). (b) Quantitation of the localization of H2A-pT120 and Sgo1 signals. The data represents the mean \pm SE of three independent experiments. 80-300 cells were scored per condition per experiment. (c) Images and (d) quantitation (normalized average pixel intensity) Low (1-1.2), Medium ($>1.2 - \leq 1.3$), and High (>1.3) of 3XMYC-GFP-Bub1 signal and localization in live cells synchronized in mitosis by a thymidine release. The data represents the mean \pm SE of three independent experiments, with 58-61 cells measured per condition. Significance was measured for the high group by 1-way ANOVA and pairwise t-test (Holm-Sidak). (e) Scatter plot of the cytoplasm vs kinetochore GFP levels of individual cells from each of the stable cell lines. The number of cells, R^2 (measure of the goodness-of-fit) and significance (1-way ANOVA)

are indicated. (f) Western blots showing levels of the 3XMYC-GFP-Bub1 proteins in the stable cell lines in whole cell extracts (left) and in cytoplasmic extracts (right). Scale bar= 10 μ M.

To determine directly whether Bub1-T589A resided in the cytoplasm and to avoid potential artifacts from fixation, we monitored the localization of eGFP-tagged Bub1 in our isogenic cell lines in living mitotic cells. We measured the cytoplasmic expression using three independent approaches. First, we monitored Bub1 expression in undisrupted prometaphase cells. Approximately 38% of the cells expressing Bub1-WT showed low or undetectable levels of GFP signal in the cytoplasm, in agreement with Bub1 residency being primarily at the kinetochore. Surprisingly, we found that in Bub1-KD and Bub1-T589A expressing cells, this percentage was much lower with approximately 8% and 5% of cells exhibiting low cytoplasmic GFP levels, respectively. Conversely, proportionally more Bub1-KD and T589A cells displayed high GFP signal in the cytoplasm when compared to Bub1-WT expressing cells (Fig.2.5 c, d). As an alternative approach, we plotted the cytoplasmic versus kinetochore GFP-Bub1 signal of individual cells in a random population of mitotic cells from each of the cell lines. Linear regression analysis indicated that Bub1-KD and Bub1-589A expressing cells tended to display higher cytoplasmic versus kinetochore ratios than Bub1-WT (Fig. 2.5e). While no significant difference was observed between Bub1-KD and Bub1-T589A cells ($P=0.36$), the cytoplasmic: kinetochore GFP ratios in these cells were found to be significantly higher than the cells expressing Bub1-WT ($P<0.001$, 1-way ANOVA, Fig. 2.5e). Finally, we tested the overall expression in these Bub1 cell lines, as well as the proportion of the protein that is found in the cytoplasmic compartment after fractionation. Western blotting indicated that Bub1- WT, KD and T589A are expressed at similar overall levels (Fig 2.5 f, left panel). However, when taking just the cytoplasmic fraction in consideration, both Bub1-KD and Bub1-T589A displayed higher cytoplasmic levels (Fig. 2.5 f), in agreement with our aforementioned results. Taken together, our observations suggest that while Bub1-WT, -KD and -T589A cell lines express similar overall levels of Bub1, Bub1-KD and Bub1-T589A exhibit higher cytoplasmic occupancy than Bub1-WT.

2.4.6. Kinetochores-tethered Bub1-T589A refocuses H2A-pT120 and Sgo

Because Bub1-T589A appeared to localize normally to kinetochores (Supplementary Figure 2a, b), we examined whether an increase in exchange at kinetochores caused aberrant cytoplasmic presence by measuring FRAP. After photobleaching at kinetochores, Bub1-WT recovered to approximately 52% (Fig. 2.6 a) in agreement with previous observations in PtK₂ cells⁴⁰ and fission yeast¹¹, with a half-life of approximately 15 seconds. Recovery of Bub1-KD and Bub1-T589A increased marginally to 55% and 61%, respectively. Recovery occurred with significantly faster kinetics with half-life measurements of 7.44 seconds for Bub1-KD and 5.85 seconds for Bub1-T589A ($P < 0.001$, 1-way ANOVA). In contrast, we found no major difference in cytoplasmic diffusion rates (Fig. 2.6 a). This data suggests that Bub1 kinase activity and in particular autophosphorylation at T589, restricts the kinetics as well as the fraction of Bub1 exchanged between kinetochores and the cytoplasm.

We next reasoned that if increased Bub1-T589A kinetochore turnover was indeed causing uniform H2A-pT120 and Sgo1 recruitment to chromatin, then stable tethering of Bub1-T589A to the kinetochore would refocus H2A-T120 phosphorylation. To test this idea, we expressed MYC-tagged Bub1 WT, the Bub3-binding mutant $\Delta 259-276$, and T589A or their Mis12 chimeras to stably incorporate Bub1 at kinetochores. In the majority of Bub1 WT-expressing cells, H2A-pT120 was centromeric and this proportion was further increased in cells expressing the Mis12-Bub1WT, in accordance with the stable docking of Mis12 at kinetochores (Fig. 2.6 b, c⁴¹). As expected, expression of Bub1- $\Delta 259-276$ and Bub1-T589A caused a significant increase in the proportion of cells with H2A-pT120 staining at chromosome arms. Strikingly, in cells expressing Mis12-Bub1-T589A and Mis12-Bub1- $\Delta 259-276$, the H2A-pT120 signals concentrated at kinetochores in over 90% of the cells, effectively rescuing the aberrant H2A-T120 arm phosphorylation seen in these mutants (Fig. 2.6 b, d). In line with the role of H2A-pT120 as a major receptor for Sgo1 at kinetochores, Mis12-Bub1-T589A efficiently targeted Sgo1 to kinetochores (Fig. 2.6 c, e). Thus, ectopic phosphorylation of H2A-T120 and Sgo1 recruitment resulting from Bub1-T589A (which inappropriately shuttles

between the kinetochore and cytoplasm) and Bub1- Δ 259-276 (which does not localize to the kinetochore at all) can be effectively rescued by artificial tethering of Bub1 to kinetochores.

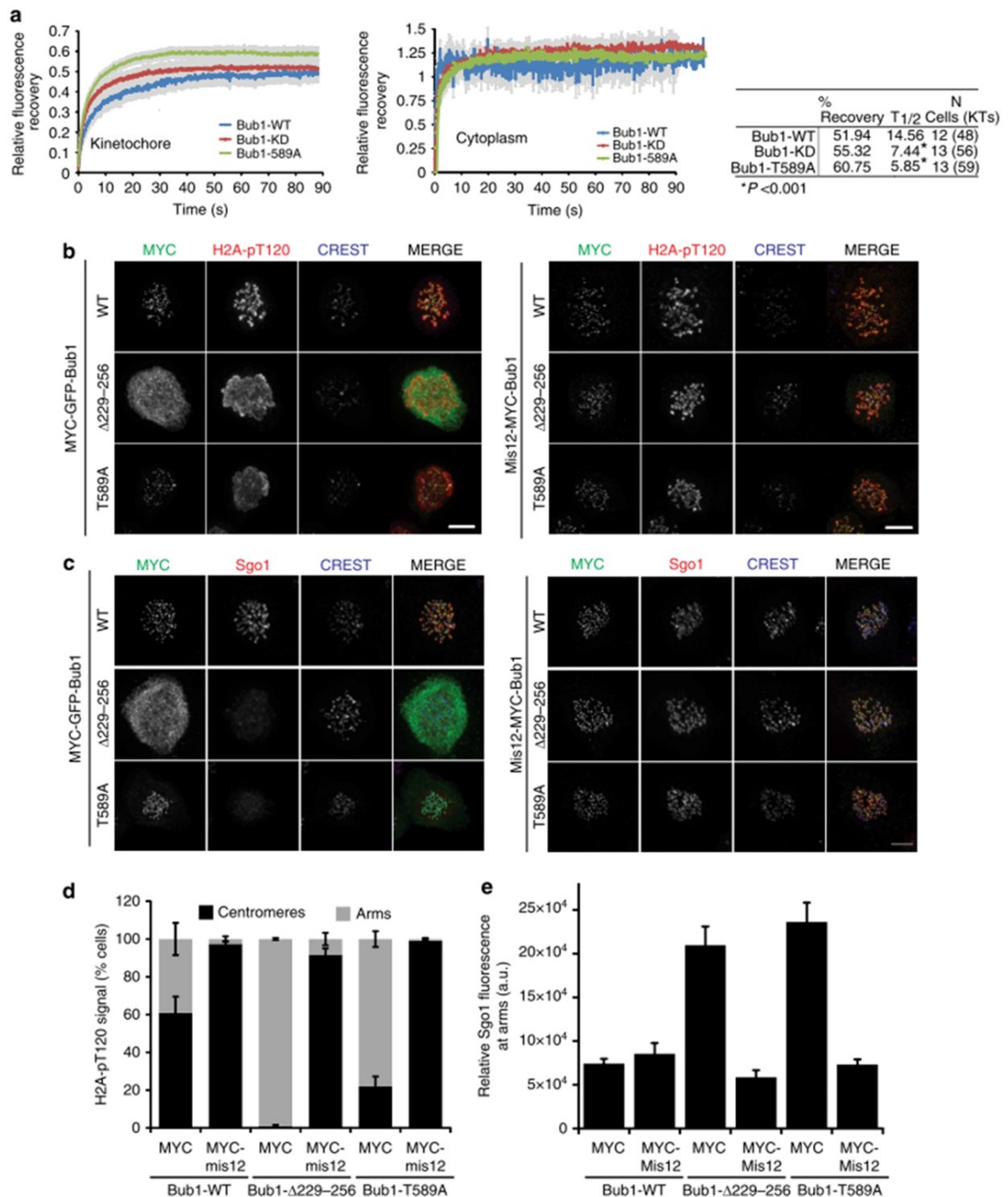


Figure 2.6 Bub1-KD and Bub1-T589A display aberrant kinetochore shuttling dynamics: (a) Recovery analysis of 3XMYC-Bub1 WT, KD, and T589A after FRAP at the kinetochore (left) and cytoplasm (right). Recovery parameters for the kinetochore population are shown in the table on the right. Statistical analysis was performed by ANOVA. (b) Mitotic cells expressing MYC-tagged (left panels) or MYC-Mis12-tagged (right panels) Bub1-WT, T589A, and Δ 229-256 were fixed and stained

with anti-H2A-pT120 (red), anti-MYC (green) and anti-CREST. (c) Cells treated as in B but were stained with Sgo1 (red). (d, e) Quantitation of the phenotypes observed in (b), and (c), respectively. For (d) the data is the mean \pm SE of three independent experiments with 80-100 cells scored per condition per experiment.

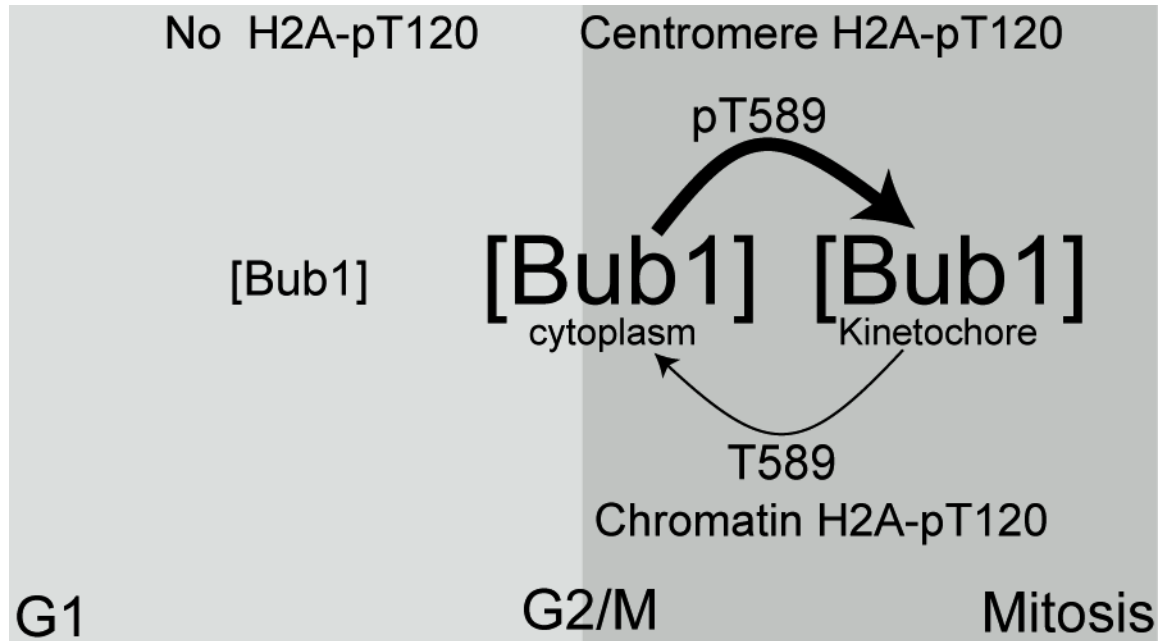


Figure 2.7 Model of Bub1 activation and autoregulation: See text for full discussion of the model.

2.5. DISCUSSION

Many protein kinases undergo autophosphorylation in the course of catalysis. In the activation segment, a conserved structural element within the kinase domain, phosphorylation stabilizes the catalytically active state of many eukaryotic protein kinases⁴² and often occurs through autocatalysis. Although SAC kinases are known to be highly autophosphorylated, the current picture of the function of this autophosphorylation is far from being complete.

Here, we show that Bub1 becomes highly autophosphorylated during mitosis at a number of conserved sites outside the activation segment including T589 and S679. This activity requires the kinase extension domain, but not the TPR domain, kinetochore recruitment or Bub3-binding. Recruitment to the kinetochore by Bub3 instead serves to concentrate Bub1 activity at kinetochores. While it is now clearly established that bulk kinetochore recruitment of Bub1-Bub3 occurs through binding to KNL1 after Mps1 phosphorylation of MELT sequences^{8, 36-38, 43-46}, autophosphorylation at the highly conserved T589 is required for proper Bub1 kinetochore-cytoplasm shuttling, which is in turn required for accurate mitotic progression by ensuring localized H2A-T120 phosphorylation and Sgo recruitment. Kinetochore tethering of either Bub1-T589A or the Bub3-binding mutant Bub1- Δ 229-256 via Mis12, refocuses H2A-T120 phosphorylation and Sgo1 to the centromere. Our study reveals an additional regulatory layer controlling Bub1 localization.

Considerable evidence from the literature supports this model of Bub1 function. Firstly, all conditions in which proper Bub1 kinetochore targeting is impaired result in spread of the H2A-pT120 signal and/or Sgo1 displacement along chromosome arms. Our data here show that depletion of Bub3 or loss of the Bub1-Bub3 interaction result in unchecked H2A-T120 phosphorylation and Sgo recruitment. Similarly, depletion of KNL-1 or ectopic localization of the Bub1 kinase domain to chromosome arms led to uniform H2A-T120 phosphorylation on chromatin^{14, 19}. In fission yeast, expression of Bub1 lacking the N-terminal kinetochore targeting region elevated H2A-S121 phosphorylation along the entire chromosome length¹⁴. Interestingly,

depletion or inhibition of Aurora B kinase also affects Sgo1 localization by causing its redistribution to chromosomes arms during mitosis and meiosis⁴⁷⁻⁵¹. This may be at least in part due to the loss of Bub1 kinetochore targeting in the absence of Aurora B activity^{35, 52, 53}. In addition to our observations with Bub1, both Aurora B and Mps1 have been reported to contribute to their own localization through autophosphorylation. In *S.cerevisiae*, Ipl1 (the budding yeast Aurora B orthologue) and Cdk1 phosphorylation of a number of consensus sites in Sli15/INCENP restricted premature chromosomal passenger complex localization to the spindle^{54, 55} but left Ipl1 activity unchanged. Similarly in vertebrates, Aurora B activity is strictly required for proper loading of the complex at centromeres⁵⁶ and the central spindle^{57, 58}. Mps1 exchange is also dependent on its own kinase activity⁵⁹. More inactive than active Mps1 can be detected at kinetochores by immunofluorescence and FRAP analysis indicated faster recovery (1.5 fold) of inactive Mps1 at the kinetochore⁵⁹. More recently, it has been suggested that Mps1 autophosphorylation at a number of N-terminal sites outside the kinase domain reduces the affinity of Mps1 to kinetochores and may thus underlie this exchange⁶⁰. The ability to regulate their own localization may therefore be a hallmark of the structurally and functionally diverse kinases that orchestrate mitosis.

Crystal structures suggest that Bub1 may be a constitutively active kinase^{19, 61}, and Bub1 is autophosphorylated at S969 in the activation segment throughout the cell cycle. However, it is clear that not all Bub1 phosphorylation events occur during interphase (Fig. 2.2 d, e,¹⁴). To reconcile these results we propose that a critical concentration of Bub1 must be reached before activation (see model in Fig. 2.7). In interphase, the concentration of Bub1 is low and thus the kinase remains effectively inactive. In agreement with this, Bub1 is degraded at the end of mitosis in an APC/Cdh1-dependent manner and its levels drop rapidly upon entry into G1^{24, 62}. Indeed increased local concentration of Bub1 is sufficient for activation and H2A-T120 phosphorylation and Sgo1 recruitment during interphase (Fig 2.2 f, g). At G2/M Bub1 protein expression increases and the critical threshold would be achieved resulting in Bub1 activation. In support of this idea, H2A-S121 is phosphorylated and Sgo2 is recruited along the entire

chromosome length in G2 in a Bub1-dependent manner in fission yeast ¹⁴. Upon mitotic entry and the establishment of kinetochores, this activity becomes concentrated in the vicinity of its targets through Bub3-Bub1 binding to KNL1. Because cytoplasmic Bub1 remains capable of phosphorylating H2A-T120 during mitosis albeit ectopically (Fig. 2.5 a, 2.6 b and ¹⁴), kinetochore targeting spatially restricts, rather than activates Bub1 ¹⁹. T589 autophosphorylation further restricts Bub1 shuttling between the cytoplasm and kinetochore. This is necessary because the increased cellular concentration of Bub1 during mitosis is sufficient to activate it and induce otherwise indiscriminate H2A-T120 phosphorylation and Sgo recruitment in these mutants. The effect of this dynamic exchange in Bub1-KD cells is masked due to the lack of H2A-T120 phosphorylation altogether. Loss of this autoregulatory phosphorylation results in ectopic cohesion protection due to mislocalized Sgo and a significant prolongation of mitosis, perhaps reflecting the additional time required to remove Sgo and cohesion from along chromosome arms. In support of this notion, a similar transient delay in exit was reported in cells depleted of WAPL, a protein required for the timely removal of cohesion in prophase⁵⁰. Thus the role of Bub1 in Sgo localization and cohesion protection is two-fold: Firstly, Bub1 directly phosphorylates H2A-T120 to mediate Sgo recruitment and secondly, through feedback autophosphorylation at T589, Bub1 ensures that H2A-pT120 and Sgo are restricted to kinetochores. Constitutive autophosphorylation of S969 in the P+1 loop of Bub1 (which occurs by intramolecular phosphorylation and is independent of Bub1 concentration¹⁹), may function as a priming event to ensure rapid and efficient H2A-T120 (and T589) phosphorylation upon mitotic entry. Activation of Bub1 may thus not be switch-like, and may involve intermediate states that exhibit varying degrees of activity ⁶¹.

The H2A-pT120-Sgo1 pathway serves as an adaptor to facilitate Aurora B inner centromeric accumulation ⁶³⁻⁶⁵. We therefore checked both localization and activation of Aurora B. We found that neither Aurora B protein levels, nor Aurora B activity, as measured by autophosphorylation on T232, or phosphorylation of the canonical substrate CENPA-S7 was appreciably different between Bub1-WT and Bub1-T589A cells, although all three signals were diminished in Bub-KD cells, as expected (Supplementary Figure 3).

Considering that depletion of both Sgo1 and Sgo2 is necessary to mislocalize Aurora B ⁶³, that we observed appreciable levels of Sgo2 at kinetochore, and that we found no effect of Bub1 autophosphorylation on the Haspin generated pH3T3 marker that recruits survivin to centromeres⁶⁵, it is likely that sufficient Aurora B is recruited and activated at centromeres in the Bub1-T589A expressing cells. Although we cannot rule out a minor effect on Aurora B activity that is beyond the resolution offered by the phosphospecific antibodies used in this study, the congression defects observed may be due to a reduction in centromeric Sgo2, which is required for MCAK recruitment ⁶⁶. We also found that steady-state BubR1 levels as measured by IF are unchanged in the Bub1-T589A mutant. However, considering that BubR1 kinetochore binding occurs directly through Bub1 ⁶⁷, it may well be that BubR1 kinetochore turnover (rather than bulk levels) is also altered in the Bub1 T589A mutant. Answering this question will require further investigation.

How T589 phosphorylation changes the dynamics of Bub1 shuttling remains unclear. One possibility is that phosphorylation may induce conformational changes that alter affinity of Bub1 to kinetochores. Binding of Bub3 as measured by immunoprecipitation revealed no difference between this mutant and Bub1-WT however, and any change caused by this mutation might be small and restricted to the shuttling pool of Bub1 (~ 50%) and thus not easily detected by such steady-state assays. Alternatively, it is possible the pT589 motif forms a docking site for a protein interaction motif, which would allow for the dynamic exchange of Bub1 between the cytoplasm and kinetochores. For example, 14-3-3 binding to pThreonine motifs has been shown to control the nucleocytoplasmic exchange of a number of proteins ⁶⁸. Whether a similar mechanism regulates Bub1 exchange remains to be explored.

2.6. Materials and Methods

2.6.1. Cell culture and transfection

All cell lines were grown at 37°C with 5% CO₂ in DMEM (Dulbecco's Modified Eagle Medium, Hyclone) supplemented with 10% FBS or BGS (fetal bovine serum or supplemented bovine growth serum PAA). HeLa cells for the generation of stable isogenic cell lines were a generous gift of Patrick Meraldi¹². Stable lines were generated by electroporation essentially (Flp-In system, Life technologies) and were selected for and grown in the presence of hygromycin (300µg/mL). U2OS cells expressing a 256 copy array of the Tet operator sequences were a kind gift of David Spector (CSHL,³²) and were maintained in the presence of 100µg/ml of hygromycin. Drug treatments were performed at the following concentrations and durations unless otherwise indicated: thymidine (Acros Organics, 2 mM for 16 h); MG132 (Calbiochem, 20 µM for 2h); nocodazole (Sigma, as indicated, 16 h). Transient plasmid transfections (Fig. 2, 6) were performed with jetPRIME or TransIT (Polyplus) according to the manufacturer's instructions. Protein depletion was performed with DsiRNAs (IDT) unless otherwise indicated, using either oligofectamine (Invitrogen) or INTERFERin (Polyplus) and analyzed at 48-72 h after transfection. The Bub1 siRNA pool targeting the 3'-UTR region has been previously reported³¹. The DsiRNA equivalent was generated and correspond to the following sequences: Bub1-3'UTR-1: 5'-UCCCAUGGAAUAUUUCCAUGUAAAA; Bub1-3'UTR-2: 5'-UCACACUGUAAAUAUGAAUCUGCTC; Bub1-3'UTR-3: 5'-AAAAACAGGUUUAAGUGAGCAGAUU; and Bub1-3'UTR-4: 5'-UUUAAGGACUGUCUAUAUCCAAUUUU. The Bub3-siRNAs used target the following sequences: siBub3-1: UGACAGAUGCAGAAACAAAdTdT, DsiBub3-2: 5' AGGGUUAUGUAUUAAGCUCUAUUGA

2.6.2. Chromosome Spreads

The Bub1 stable cell lines were split into 6-well plates and transfected with Bub1 3'UTR DsiRNA. At 36h post-transfection, cells are synchronized with 330 nM nocodazole overnight. Mitotic cells were shaken off, washed 3 times

in PBS and incubated for 15 min at 37°C with rotation in 55mM KCl to swell the cells. 20000 cells were subsequently resuspended in 200 µl of 55 mM KCl, 0.1 % Tween 20, and chromosomes were spread onto coverslips by centrifugation at 500xg in a cytospin with slow acceleration and deceleration. Cells attached on slide were fixed in PTEMF for 10 min as before ⁶⁹. Spread chromosomes were then stained as indicated in the figure legends.

2.6.3. Cloning and mutagenesis

Bub1 WT was cloned into the pcDNA5/FRT/TO expression vector modified to include an N-terminal triple MYC tag (HindIII-KpnI) followed directly in-frame by EYFP (KpnI-BamHI), generated by PCR amplification from pEGFP-N1 (Clontech). For artificial kinetochore targeting of Bub1-T589A and Bub1- Δ 229-256, the EGFP sequence was substituted for hMis12. For construction of the LacI expressing plasmid, *LacI* was amplified from pSV2-YFP-LacI (David Spector) and subcloned into the KpnI site of pcDNA3.1-3xMYC ⁷⁰. Bub1-WT and Bub1-KD were subsequently cloned into this vector using BamHI and XhoI. Bub1 KD (D946A), T589A and S679A were generated by QuickChange site-directed mutagenesis. Bub1- Δ 150 lacking the first 150 amino acids was generated by PCR. Bub1 plasmids for mutants Δ 229-256, Δ 740-766 and Δ 458-476 were a gift from Patrick Meraldi ¹².

2.6.4. Immunofluorescence and antibodies

Cells were grown on cover slips and were arrested in mitosis either by nocodazole (330 nM) or by 10-12 hour release from thymidine block. Fixation was performed by incubation with PTEMF (0.2% Triton X-100, 20mM PIPES pH6.8, 1mM MgCl₂, 10mM EGTA and 4% formaldehyde) ⁶⁹ before blocking in 3% BSA in PBS-T. Coverslips were incubated with primary and secondary antibodies for 1 hour at room temperature except for CENP-A pS7, which was incubated at 4°C overnight. Rabbit polyclonal phosphospecific antibodies against T589 and S679 were generated against phosphopeptides CIRCnkpTLAPS and CLLRLpSQPAAG, respectively. Antibodies were affinity purified with the phosphopeptide for all experiments shown here and used at 1µg/ml. Other antibodies were used at 1µg/ml unless otherwise indicated, as follows: Anti-MYC (9E10, Thermo scientific), anti-Bub1 ⁷⁰, anti-GFP (11814460001, Roche), anti-SgoL1 (H00151648-M01, Abnova), anti-

H2ApT120 (61195, Active motif and a generous gift of Y. Watanabe), anti- α -tubulin (DM1A, Santa Cruz), anti-Sgo2 (Kind gift of Tim Yen), anti-GAPDH (used at 1:2000, NB300-221, Novusbio), CENP-A pS7(used at 1:100, 2187, Cell Signaling Technology), anti-Aurora B (611082, BD transduction laboratories), anti-Aurora pT232 (600-401-677, Rockland), Anti-Histone H2A (07-146, Millipore) and CREST anti-centromere serum (HCT-0100, Immunovision). Dylight series secondary antibodies (Thermo) were used for immunofluorescence (1/1000) and HRP-coupled secondary antibodies (Jackson ImmunoResearch were used for Western blotting (1/10000).

2.6.5. Fractionation, immunoprecipitation and Western Blotting

For Immunoblotting and immunoprecipitations, cells were lysed with RIPA buffer containing 150mM Tris-HCL pH7.5, 150mM NaCl, 10mMNaF, 1% NP-40, 0.1% Na Deoxycholate, and a protease and phosphatase inhibitor cocktail that included 20mM B-glycerophosphate, 0.1mM sodium vanadate, 10mM sodium pyrophosphate, 1ug/mL leupeptin, 1ug/mL aprotinin, 1mM AEBSF. Cells were lysed on orbital shaker at 4°C for at least 30min; lysates were centrifuged at 14000 rpm for 15min at 4°C. The supernatant was collected and protein concentrations were measured using the BCA assay (Thermo Scientific). For isolation of the cytoplasmic and cytoskeletal fraction of Bub1, mitotic cells stably expressing Bub1-WT, KD or T589A were harvested by shake-off after thymidine release, washed twice in PBS and lysed for 10 minutes on ice in cytoskeletal buffer (CSK, 0.5% TRITONX-100, 100mM PIPES pH 6.8, 100 mM NaCl, 1.5mM MgCl₂, 300mM sucrose, protease inhibitor cocktail (1 μ g/ml aprotinin, 1 μ g/ml leupeptin, 1mM AEBSF, 10mM NaF), and 1 mM ATP). The lysate was spun down for 4 minutes at 3200 rpm and the resulting supernatant (S1) constituted the cytoplasmic fraction. The original, non-cropped blots for all Westerns in this manuscript are shown in Supplementary Figure 4

2.6.6. Microscopy, Live cell imaging, and FRAP

Cells were imaged by confocal microscopy on an inverted Olympus IX80 microscope equipped with a WaveFX-Borealin-SC Yokagawa spinning disc (Quorum Technologies) and an Orca Flash4.0 camera (Hamamatsu). Image acquisition was performed using Metamorph software (Molecular devices).

Optical sections were acquired with identical exposure times for each channel within an experiment and then projected into a single picture using ImageJ (rsb.info.nih.gov). Image processing was performed in Image J or Photoshop, and images shown in the same figure have been identically scaled.

For FRAP experiments, the cells were grown in glass-bottom lab-tek chambered slides (thermoscientific). FRAP was performed on Leica DMI600B equipped with a heated chamber (37°C) and a Mosaic active illumination system (Spectral applied research), that allowed for simultaneous bleaching and acquisition, and an ImageEM (512x512) camera (Hamamatsu). The microscope and Mosaic were operated by Metamorph. The GFP-tagged Bub1 protein at both kinetochores and the cytoplasm was bleached using a 405 nm laser (diode 475mW power at 100%) and excited at 491nm (detection filters 536/40 nm). Individual kinetochores or cytoplasmic regions were bleached by a 400 msec laser pulse. Image acquisition (every 150 msec) began 15 frames before bleaching and continued for an additional 750 frames post bleaching. The bleached region in each case was a circular region of 15 pixel diameter, and only kinetochores that remained visible within this region for the length of the experiment were included in the analysis. Quantification of fluorescence recovery was obtained using the FRAP profiler plugin of ImageJ, which accounts for correction of overall bleaching. Recovery rates for cytoplasmic and kinetochore Bub1 WT, KD and T589A were determined after fitting a single exponential curve (which showed the best fit) using the formula $F(t)=A(1-e^{-t/\tau})$, where, A= fraction recovery. Half-time recovery was determined using the formula $T_{1/2} = \ln 0.5 / -\tau$.

Live cell imaging was performed on the above indicated microscopy system that is also equipped with a motorized stage (ASI) and an incubator with atmospheric CO₂ heated to 37°C. Bub1 stable cell lines were subjected to depletion of endogenous Bub1 for 48 hours, then synchronized in mitosis after a further 16h block with thymidine. Image acquisition was started 12h after release. Only cells visibly expressing the GFP-tagged Bub1 were included in subsequent analysis.

2.6.7. SILAC labelling and Mass spectrometry

293T cells were cultured in heavy or light amino acid containing medium for 5 generations before transfection with 3xMYC-tagged Bub1-WT or Bub1-KD. Cells were incubated for 36 hours, after which nocodazole was added for an additional 16 hours. Cells were harvested, lysed in RIPA lysis buffer and 3XMYC-tagged Bub1 WT or KD were immunoprecipitated with anti-MYC antibodies for 2 hours. The immunoprecipitated Bub1 was washed 3X with RIPA lysis buffer, 1X with RIPA buffer including 300mM NaCl, and a final buffer exchange with kinase reaction buffer lacking ATP and MgCl₂. The immunoprecipitates were then subjected to a cold in vitro kinase assay (20 mM TRIS pH 7.4, 10mM EGTA, 100 mM Na Orthovanadate, 10 mM MgCl₂, 4 mM MnCl₂, 1 mM DTT, 5 mM NaF, and 100 uM ATP) at 30°C for 30 minutes. The reaction was stopped by the addition of SDS PAGE sample buffer. The Bub1-WT and Bub1 KD immunoprecipitates were then mixed, resolved by SDS-PAGE, and visualized by coomassie brilliant blue staining. The band corresponding to the size of 3XMYC-Bub1 was excised and processed for mass spectrometry⁶⁹. In-gel digestion was performed using either 15 ng/ml of trypsin or was added in an enzyme/substrate ratio of 1:50 of each Lys-C, Glu-C, and elastase.

2.6.8. Nano-LC-MS/MS Analysis

All peptide samples were separated by online reverse phase nano-LC and analyzed by electrospray MS/MS. Using a nanoACQUITY ultra performance liquid chromatography system (Waters), samples were injected onto a 14-cm fused silica capillary column with an inner diameter of 75 µm and a tip of 8 µm (New Objective) packed in-house with 3-µm ReproSil-Pur C18-AQ (Dr. Maisch GmbH). The LC setup was connected to a LTQ-Orbitrap MS (Thermo Fisher Scientific) equipped with a nanoelectrospray ion source (Proxeon Biosystems). Peptides were separated and eluted by a stepwise 180 min gradient of 0–100% between buffer A (0.2% formic acid in water) and buffer B (0.2% formic acid in acetonitrile). Data-dependent acquisition was performed on the LTQ-Orbitrap using Xcalibur 2.0 software in the positive ion mode. Survey full scan MS spectra (from m/z 300 to 2000) were acquired in the FT-Orbitrap with a resolution of 60 000 at m/z 400. A maximum of five peptides were sequentially isolated for fragmentation in the linear ion trap using collision induced dissociation (CID). The Orbitrap lock mass feature was

applied to improve mass accuracy. To improve phosphopeptide analysis, the multistage activation option in the software was enabled, and the neutral loss species at 97.97, 48.99, or 32.66 m/z below the precursor ion were activated for 30 ms during fragmentation (pseudo-MS³).

2.6.9. Data processing and analyses

Raw data files including SILAC quantitation were processed using the MaxQuant software suite (version 1.0.12.5). Generation of peak lists was performed with the following MaxQuant parameters; top 12 MS/MS peaks for 100 Da, 3 data points for centroid, Gaussian centroid determination, slice peaks at local minima. During the peak list generation MaxQuant identified potential SILAC pairs based on mass differences of specified labeled amino acids, intensity correlation over elution time etc. Mascot (version 2.2.0, Matrix Science) was used for peptide identifications. The initial precursor mass tolerance was set to ± 7 ppm, whereas an accuracy of ± 0.5 Da was used for MS/MS fragmentation spectra. Carbamidomethylation was set as fixed modification and methionine oxidation, protein N-terminal acetylation, and phosphorylation (STY) were considered as variable modifications. Putative SILAC pairs were searched with their respective labeled amino acids as fixed modification whereas peaks which were not assigned to any of the SILAC pairs were searched using R10 and K8 as variable modifications. Enzyme specificity was set to Trypsin/P i.e. allowing cleavage N-terminal to proline in the context of [KR]P. Up to two missed cleavages were allowed. The minimum required peptide length was set to 6 amino acids. Searches were performed against IPI human (version 3.48; 71,400 protein entries) that was concatenated with reverse database sequences (142,800 protein entries in total). Further, MaxQuant filtered Mascot results using additional parameters, such as the number of labeled amino acids (max of 3) in the identified peptide sequence and the measured mass accuracy as a function of intensity. As an additional quality measure to increase identification stringencies,

we only accepted phosphorylation site identifications with Mascot scores of at least 12 or PTM scores of at least 30. Quantitation of SILAC pairs was performed with the following parameters; re-quantify, for protein quantitation discard unmodified counterpart peptides except for oxidation and acetyl protein N-terminal, use razor and unique peptides, minimum ratio count of 1, minimum score 0, minimum peptides 1. The initial maximum false-discovery rates (FDR) were set to 0.02, and 0.05 for peptides and proteins, respectively, and further reduced by Mascot score filtering as described above. FDR's were calculated as (number of hits in the reversed database/number of hits in the forward database) × 100%. Whenever the set of identified peptides in one protein was equal to or completely contained in the set of identified peptides of another protein these two proteins were joined in a single protein group. In cases where the peptides have more than one phosphorylation site, some of these phosphorylation sites are identified as multiply phosphorylated peptides whereas others are identified on multiple singly phosphorylated peptides.

2.6.10. Phosphopeptide analysis

A summary of all quantifiable SILAC pairs identified on Bub1 from each of the three independent experiments is shown in Supplementary Data 1. Note that for experiment 2, in a certain number of cases, peptides corresponding to Bub1-KD were identified but lacked phosphorylation all together. In these cases, we marked the phosphopeptide:peptide ratio as 100%. Weblogo analysis was performed on the 15mer peptides corresponding to the 20 autophosphorylation sites identified in this study together with H2A-T120 using the default settings.

2.6.11. Quantification and statistical analysis

Unless otherwise stated, all experiments were performed in triplicate. Image quantification was performed using Image J. For quantification of signal intensities at kinetochores, the CREST/MYC signal was used to generate a binary mask to include kinetochore and centromere signals. Integrated signal intensity was measured in all relevant channels and intensities indicated are

values relative to CREST or MYC. Unless otherwise indicated, a minimum of 10 cells were quantified per condition for all experiments involving kinetochore quantification. For H2A-pT120 and Sgo1 signal intensity at chromosome arms, the following formula was used to measure the corrected total cellular fluorescence. $CTCF = \text{Integrated Density} - (\text{Area of selected cell} \times \text{Mean fluorescence of background readings})$. For Figs.2F, G, signal overlap was measured by drawing a 70 pixel line across the MYC-Bub1 signal and the intensity of the colocalized Sgo1 and Histone H2A-pT120 was measured along the line. To determine chromosome congression, chromatids were counted as incorrectly aligned if they were outside of a rectangular area encompassing the central 30% of the spindle, a volume that generously encompasses wild-type metaphase plates. To determine this region accurately, we only considered cells aligned along the plane of the coverslips, where both spindle poles could be easily distinguished. Cells were considered misaligned when ≥ 1 kinetochore fell outside this central region; thick when kinetochores occupied $>$ half of this volume; and aligned when kinetochores occupied \leq half the volume. In Fig. 3C, we considered only misaligned (ie. falling outside the equatorial 30% volume) kinetochores and counted the number of these per condition.

For the statistical analysis for significance of FRAP data, the relationship between Bub1 WT, KD and T589A were compared among treatments by testing the equality of a set of parameters using F-tests, derived from the error sum of squares of the null model and the full model in SAS. All other statistical analysis was performed with Sigmaplot. Data are expressed as means \pm the standard errors of the mean (SEM). The data were analyzed by analysis of variance or *t* tests (two-tailed) for determination of significance of the differences or as otherwise indicated. A *P* value of <0.05 was considered to be statistically significant.

2.7. ACKNOWLEDGEMENTS:

We would like to thank Julie-Christine Lévesque for assistance with FRAP, the Université Laval statistical consultation service, Maria Fernandes for use of her microscope during the early stages of this study, and Patrick Meraldi, Tim Yen, Yoshi Watanabe and David Spector for sharing valuable reagents. We

also acknowledge the support of the Max Planck Society during the early stages of this study. We thank Mary Herbert, Anna Santamaria, and Lily Wang for critical reading of the manuscript. This research was supported by grants to SE from the Canadian Institutes for Health Research (MOP244442) and the Canadian Cancer Research Society. EAN acknowledges support from the Swiss National Science Foundation (310030B_149641). SE is a Canadian Institutes for Health Research junior investigator.

2.8. Author Contributions:

A.A., A.L, performed the majority of the experiments with assistance from P.T. and G.C. Initial identification of autophosphorylation sites was done by S.E. and K.D. S.E. designed the experiments and wrote the manuscript with assistance from A.A. and K.D. The authors declare no competing interests as defined by Nature Publishing Group, or other interests that might be perceived to influence the results and/or discussion reported in this article.

2.9. REFERENCES:

1. Sacristan, C. & Kops, G.J. Joined at the hip: kinetochores, microtubules, and spindle assembly checkpoint signaling. *Trends in cell biology* (2014).
2. Jia, L., Kim, S. & Yu, H. Tracking spindle checkpoint signals from kinetochores to APC/C. *Trends in biochemical sciences* **38**, 302-311 (2013).
3. Foley, E.A. & Kapoor, T.M. Microtubule attachment and spindle assembly checkpoint signalling at the kinetochore. *Nature reviews. Molecular cell biology* **14**, 25-37 (2013).
4. Musacchio, A. Spindle assembly checkpoint: the third decade. *Philosophical transactions of the Royal Society of London. Series B, Biological sciences* **366**, 3595-3604 (2011).
5. London, N. & Biggins, S. Signalling dynamics in the spindle checkpoint response. *Nature reviews. Molecular cell biology* **15**, 736-748 (2014).
6. Elowe, S. Bub1 and BubR1: at the interface between chromosome attachment and the spindle checkpoint. *Molecular and cellular biology* **31**, 3085-3093 (2011).
7. Funabiki, H. & Wynne, D.J. Making an effective switch at the kinetochore by phosphorylation and dephosphorylation. *Chromosoma* **122**, 135-158 (2013).
8. Ghongane, P., Kapanidou, M., Asghar, A., Elowe, S. & Bolanos-Garcia, V.M. The dynamic protein Knl1 - a kinetochore rendezvous. *Journal of cell science* **127**, 3415-3423 (2014).
9. Espert, A. *et al.* PP2A-B56 opposes Mps1 phosphorylation of Knl1 and thereby promotes spindle assembly checkpoint silencing. *The Journal of cell biology* **206**, 833-842 (2014).
10. Nijenhuis, W., Vallardi, G., Teixeira, A., Kops, G.J. & Saurin, A.T. Negative feedback at kinetochores underlies a responsive spindle checkpoint signal. *Nature cell biology* **16**, 1257-1264 (2014).
11. Rischitor, P.E., May, K.M. & Hardwick, K.G. Bub1 is a fission yeast kinetochore scaffold protein, and is sufficient to recruit other spindle checkpoint proteins to ectopic sites on chromosomes. *PloS one* **2**, e1342 (2007).

12. Klebig, C., Korinth, D. & Meraldi, P. Bub1 regulates chromosome segregation in a kinetochore-independent manner. *The Journal of cell biology* **185**, 841-858 (2009).
13. Tang, Z., Shu, H., Oncel, D., Chen, S. & Yu, H. Phosphorylation of Cdc20 by Bub1 provides a catalytic mechanism for APC/C inhibition by the spindle checkpoint. *Molecular cell* **16**, 387-397 (2004).
14. Kawashima, S.A., Yamagishi, Y., Honda, T., Ishiguro, K. & Watanabe, Y. Phosphorylation of H2A by Bub1 prevents chromosomal instability through localizing shugoshin. *Science* **327**, 172-177 (2010).
15. Kitajima, T.S., Hauf, S., Ohsugi, M., Yamamoto, T. & Watanabe, Y. Human Bub1 defines the persistent cohesion site along the mitotic chromosome by affecting Shugoshin localization. *Curr Biol* **15**, 353-359 (2005).
16. Kitajima, T.S. *et al.* Shugoshin collaborates with protein phosphatase 2A to protect cohesin. *Nature* **441**, 46-52 (2006).
17. Tang, Z., Sun, Y., Harley, S.E., Zou, H. & Yu, H. Human Bub1 protects centromeric sister-chromatid cohesion through Shugoshin during mitosis. *Proceedings of the National Academy of Sciences of the United States of America* **101**, 18012-18017 (2004).
18. Tang, Z. *et al.* PP2A is required for centromeric localization of Sgo1 and proper chromosome segregation. *Developmental cell* **10**, 575-585 (2006).
19. Lin, Z., Jia, L., Tomchick, D.R., Luo, X. & Yu, H. Substrate-specific activation of the mitotic kinase Bub1 through intramolecular autophosphorylation and kinetochore targeting. *Structure (London, England : 1993)* **22**, 1616-1627 (2014).
20. Olsen, J.V. *et al.* Global, in vivo, and site-specific phosphorylation dynamics in signaling networks. *Cell* **127**, 635-648 (2006).
21. Kettenbach, A.N. *et al.* Quantitative phosphoproteomics identifies substrates and functional modules of Aurora and Polo-like kinase activities in mitotic cells. *Science signaling* **4**, rs5 (2011).
22. Chen, R.H. Phosphorylation and activation of Bub1 on unattached chromosomes facilitate the spindle checkpoint. *The EMBO journal* **23**, 3113-3121 (2004).

23. Yamaguchi, S., Decottignies, A. & Nurse, P. Function of Cdc2p-dependent Bub1p phosphorylation and Bub1p kinase activity in the mitotic and meiotic spindle checkpoint. *The EMBO journal* **22**, 1075-1087 (2003).
24. Qi, W., Tang, Z. & Yu, H. Phosphorylation- and polo-box-dependent binding of Plk1 to Bub1 is required for the kinetochore localization of Plk1. *Molecular biology of the cell* **17**, 3705-3716 (2006).
25. Yang, C. *et al.* Aurora-B mediated ATM serine 1403 phosphorylation is required for mitotic ATM activation and the spindle checkpoint. *Molecular cell* **44**, 597-608 (2011).
26. Matsuoka, S. *et al.* ATM and ATR substrate analysis reveals extensive protein networks responsive to DNA damage. *Science* **316**, 1160-1166 (2007).
27. London, N. & Biggins, S. Mad1 kinetochore recruitment by Mps1-mediated phosphorylation of Bub1 signals the spindle checkpoint. *Genes & development* **28**, 140-152 (2014).
28. Olsen, J.V. *et al.* Quantitative phosphoproteomics reveals widespread full phosphorylation site occupancy during mitosis. *Science signaling* **3**, ra3 (2010).
29. Ricke, R.M., Jeganathan, K.B., Malureanu, L., Harrison, A.M. & van Deursen, J.M. Bub1 kinase activity drives error correction and mitotic checkpoint control but not tumor suppression. *The Journal of cell biology* **199**, 931-949 (2012).
30. Krenn, V., Wehenkel, A., Li, X., Santaguida, S. & Musacchio, A. Structural analysis reveals features of the spindle checkpoint kinase Bub1-kinetochore subunit Knl1 interaction. *The Journal of cell biology* **196**, 451-467 (2012).
31. Niikura, Y., Dixit, A., Scott, R., Perkins, G. & Kitagawa, K. BUB1 mediation of caspase-independent mitotic death determines cell fate. *The Journal of cell biology* **178**, 283-296 (2007).
32. Janicki, S.M. *et al.* From silencing to gene expression: real-time analysis in single cells. *Cell* **116**, 683-698 (2004).
33. Fernius, J. & Hardwick, K.G. Bub1 kinase targets Sgo1 to ensure efficient chromosome biorientation in budding yeast mitosis. *PLoS Genet* **3**, e213 (2007).

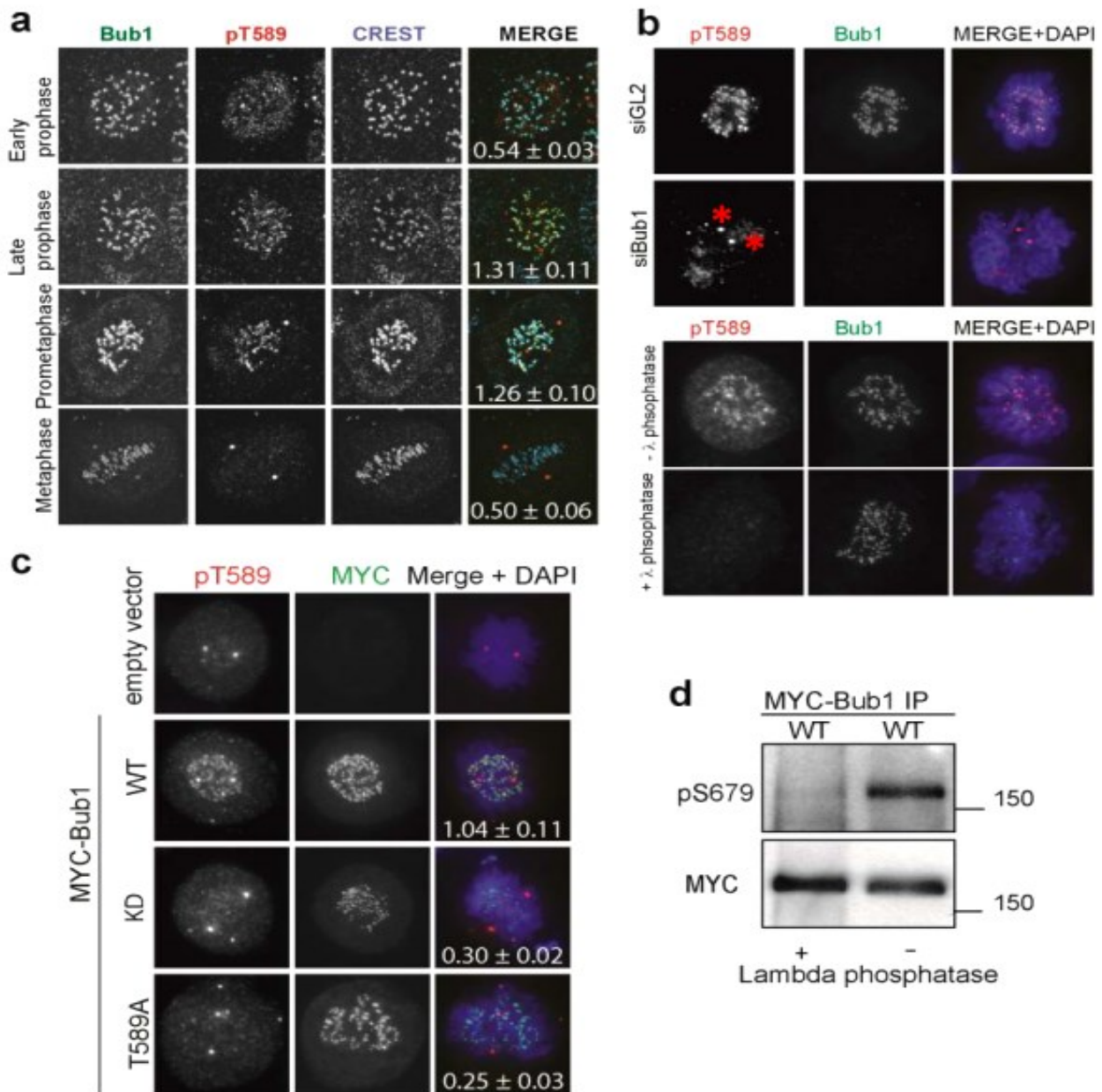
34. Liu, H., Jia, L. & Yu, H. Phospho-H2A and cohesin specify distinct tension-regulated Sgo1 pools at kinetochores and inner centromeres. *Curr Biol* **23**, 1927-1933 (2013).
35. Boyarchuk, Y., Salic, A., Dasso, M. & Arnaoutov, A. Bub1 is essential for assembly of the functional inner centromere. *The Journal of cell biology* **176**, 919-928 (2007).
36. Yamagishi, Y., Yang, C.H., Tanno, Y. & Watanabe, Y. MPS1/Mph1 phosphorylates the kinetochore protein KNL1/Spc7 to recruit SAC components. *Nature cell biology* **14**, 746-752 (2012).
37. Shepperd, L.A. *et al.* Phosphodependent recruitment of Bub1 and Bub3 to Spc7/KNL1 by Mph1 kinase maintains the spindle checkpoint. *Curr Biol* **22**, 891-899 (2012).
38. Primorac, I. *et al.* Bub3 reads phosphorylated MELT repeats to promote spindle assembly checkpoint signaling. *eLife* **2**, e01030 (2013).
39. Taylor, S.S., Ha, E. & McKeon, F. The human homologue of Bub3 is required for kinetochore localization of Bub1 and a Mad3/Bub1-related protein kinase. *The Journal of cell biology* **142**, 1-11 (1998).
40. Howell, B.J. *et al.* Spindle checkpoint protein dynamics at kinetochores in living cells. *Curr Biol* **14**, 953-964 (2004).
41. Hemmerich, P. *et al.* Dynamics of inner kinetochore assembly and maintenance in living cells. *The Journal of cell biology* **180**, 1101-1114 (2008).
42. Nolen, B., Taylor, S. & Ghosh, G. Regulation of protein kinases; controlling activity through activation segment conformation. *Molecular cell* **15**, 661-675 (2004).
43. Vleugel, M. *et al.* Sequential Multisite Phospho-Regulation of KNL1-BUB3 Interfaces at Mitotic Kinetochores. *Molecular cell* **57**, 824-835 (2015).
44. Zhang, G., Lischetti, T. & Nilsson, J. A minimal number of MELT repeats supports all the functions of KNL1 in chromosome segregation. *Journal of cell science* **127**, 871-884 (2014).
45. London, N., Ceto, S., Ranish, J.A. & Biggins, S. Phosphoregulation of Spc105 by Mps1 and PP1 regulates Bub1 localization to kinetochores. *Curr Biol* **22**, 900-906 (2012).

46. Vleugel, M. *et al.* Arrayed BUB recruitment modules in the kinetochore scaffold KNL1 promote accurate chromosome segregation. *The Journal of cell biology* **203**, 943-955 (2013).
47. Tanno, Y. *et al.* Phosphorylation of mammalian Sgo2 by Aurora B recruits PP2A and MCAK to centromeres. *Genes & development* **24**, 2169-2179 (2010).
48. Dai, J., Sullivan, B.A. & Higgins, J.M. Regulation of mitotic chromosome cohesion by Haspin and Aurora B. *Developmental cell* **11**, 741-750 (2006).
49. Resnick, T.D. *et al.* INCENP and Aurora B promote meiotic sister chromatid cohesion through localization of the Shugoshin MEI-S332 in *Drosophila*. *Developmental cell* **11**, 57-68 (2006).
50. Kueng, S. *et al.* Wapl controls the dynamic association of cohesin with chromatin. *Cell* **127**, 955-967 (2006).
51. Lee, N.R. *et al.* Regulation of the subcellular shuttling of Sgo1 between centromeres and chromosome arms by Aurora B-mediated phosphorylation. *Biochemical and biophysical research communications* **454**, 429-435 (2014).
52. Vigneron, S. *et al.* Kinetochore localization of spindle checkpoint proteins: who controls whom? *Molecular biology of the cell* **15**, 4584-4596 (2004).
53. Johnson, V.L., Scott, M.I., Holt, S.V., Hussein, D. & Taylor, S.S. Bub1 is required for kinetochore localization of BubR1, Cenp-E, Cenp-F and Mad2, and chromosome congression. *Journal of cell science* **117**, 1577-1589 (2004).
54. Nakajima, Y. *et al.* Ipl1/Aurora-dependent phosphorylation of Sli15/INCENP regulates CPC-spindle interaction to ensure proper microtubule dynamics. *The Journal of cell biology* **194**, 137-153 (2011).
55. Makrantoni, V. *et al.* Phosphorylation of Sli15 by Ipl1 is important for proper CPC localization and chromosome stability in *Saccharomyces cerevisiae*. *PloS one* **9**, e89399 (2014).
56. Honda, R., Korner, R. & Nigg, E.A. Exploring the functional interactions between Aurora B, INCENP, and survivin in mitosis. *Molecular biology of the cell* **14**, 3325-3341 (2003).

57. Xu, Z. *et al.* INCENP-aurora B interactions modulate kinase activity and chromosome passenger complex localization. *The Journal of cell biology* **187**, 637-653 (2009).
58. Murata-Hori, M., Tatsuka, M. & Wang, Y.L. Probing the dynamics and functions of aurora B kinase in living cells during mitosis and cytokinesis. *Molecular biology of the cell* **13**, 1099-1108 (2002).
59. Jelluma, N., Dansen, T.B., Sliedrecht, T., Kwiatkowski, N.P. & Kops, G.J. Release of Mps1 from kinetochores is crucial for timely anaphase onset. *The Journal of cell biology* **191**, 281-290 (2010).
60. Wang, X. *et al.* Dynamic autophosphorylation of mps1 kinase is required for faithful mitotic progression. *PloS one* **9**, e104723 (2014).
61. Bayliss, R., Fry, A., Haq, T. & Yeoh, S. On the molecular mechanisms of mitotic kinase activation. *Open biology* **2**, 120136 (2012).
62. Taylor, S.S., Hussein, D., Wang, Y., Elderkin, S. & Morrow, C.J. Kinetochores localisation and phosphorylation of the mitotic checkpoint components Bub1 and BubR1 are differentially regulated by spindle events in human cells. *Journal of cell science* **114**, 4385-4395 (2001).
63. Kawashima, S.A. *et al.* Shugoshin enables tension-generating attachment of kinetochores by loading Aurora to centromeres. *Genes & development* **21**, 420-435 (2007).
64. Tsukahara, T., Tanno, Y. & Watanabe, Y. Phosphorylation of the CPC by Cdk1 promotes chromosome bi-orientation. *Nature* **467**, 719-723 (2010).
65. Yamagishi, Y., Honda, T., Tanno, Y. & Watanabe, Y. Two histone marks establish the inner centromere and chromosome bi-orientation. *Science* **330**, 239-243 (2010).
66. Huang, H. *et al.* Tripin/hSgo2 recruits MCAK to the inner centromere to correct defective kinetochore attachments. *The Journal of cell biology* **177**, 413-424 (2007).
67. Overlack, K. *et al.* A molecular basis for the differential roles of Bub1 and BubR1 in the spindle assembly checkpoint. *eLife* **4**, e05269 (2015).
68. Reinhardt, H.C. & Yaffe, M.B. Phospho-Ser/Thr-binding domains: navigating the cell cycle and DNA damage response. *Nature reviews. Molecular cell biology* **14**, 563-580 (2013).

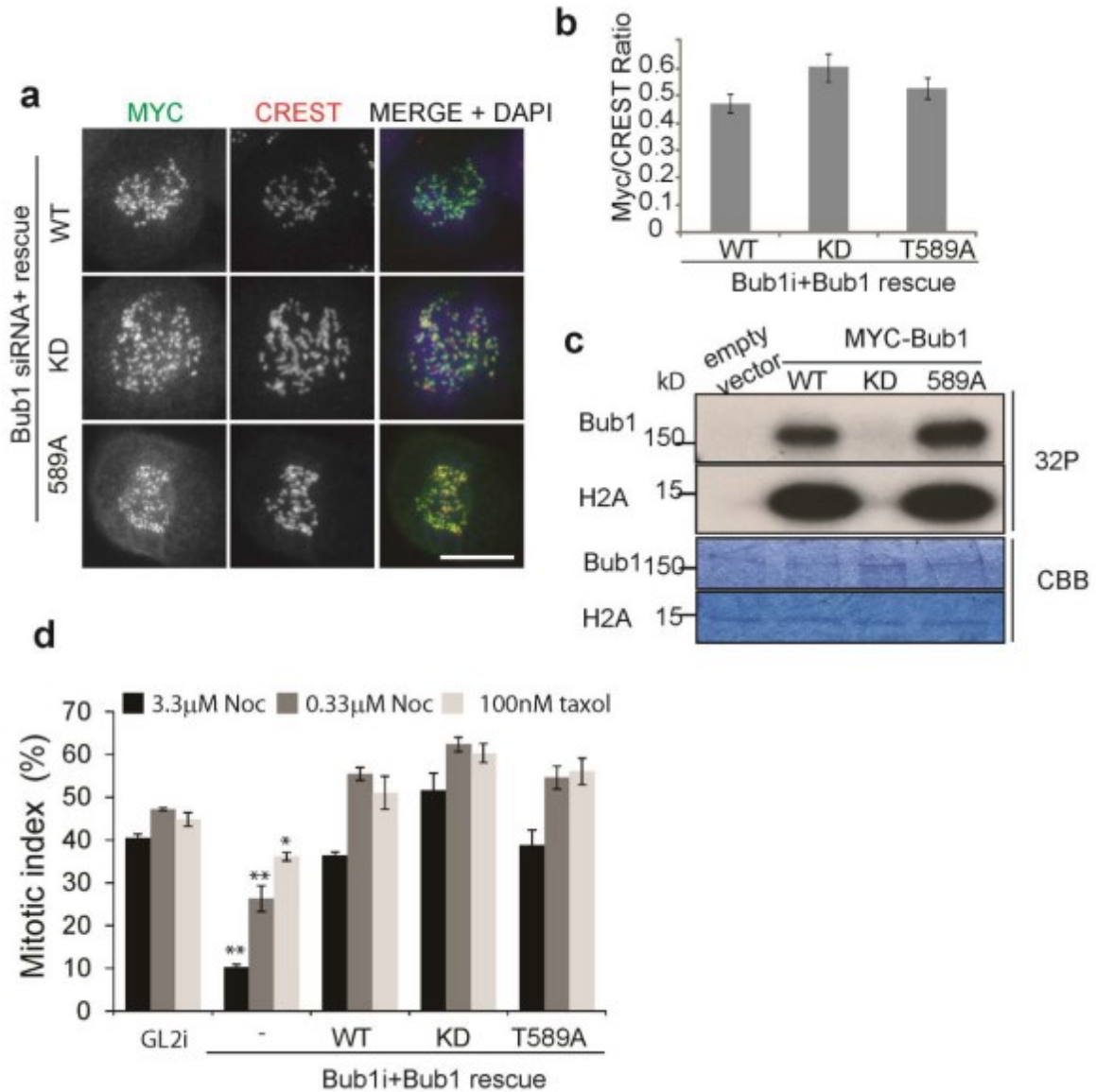
69. Elowe, S., Hummer, S., Uldschmid, A., Li, X. & Nigg, E.A. Tension-sensitive Plk1 phosphorylation on BubR1 regulates the stability of kinetochore microtubule interactions. *Genes & development* **21**, 2205-2219 (2007).
70. Elowe, S. *et al.* Uncoupling of the spindle-checkpoint and chromosome-congression functions of BubR1. *Journal of cell science* **123**, 84-94 (2010).

2.10. Supplementary Information



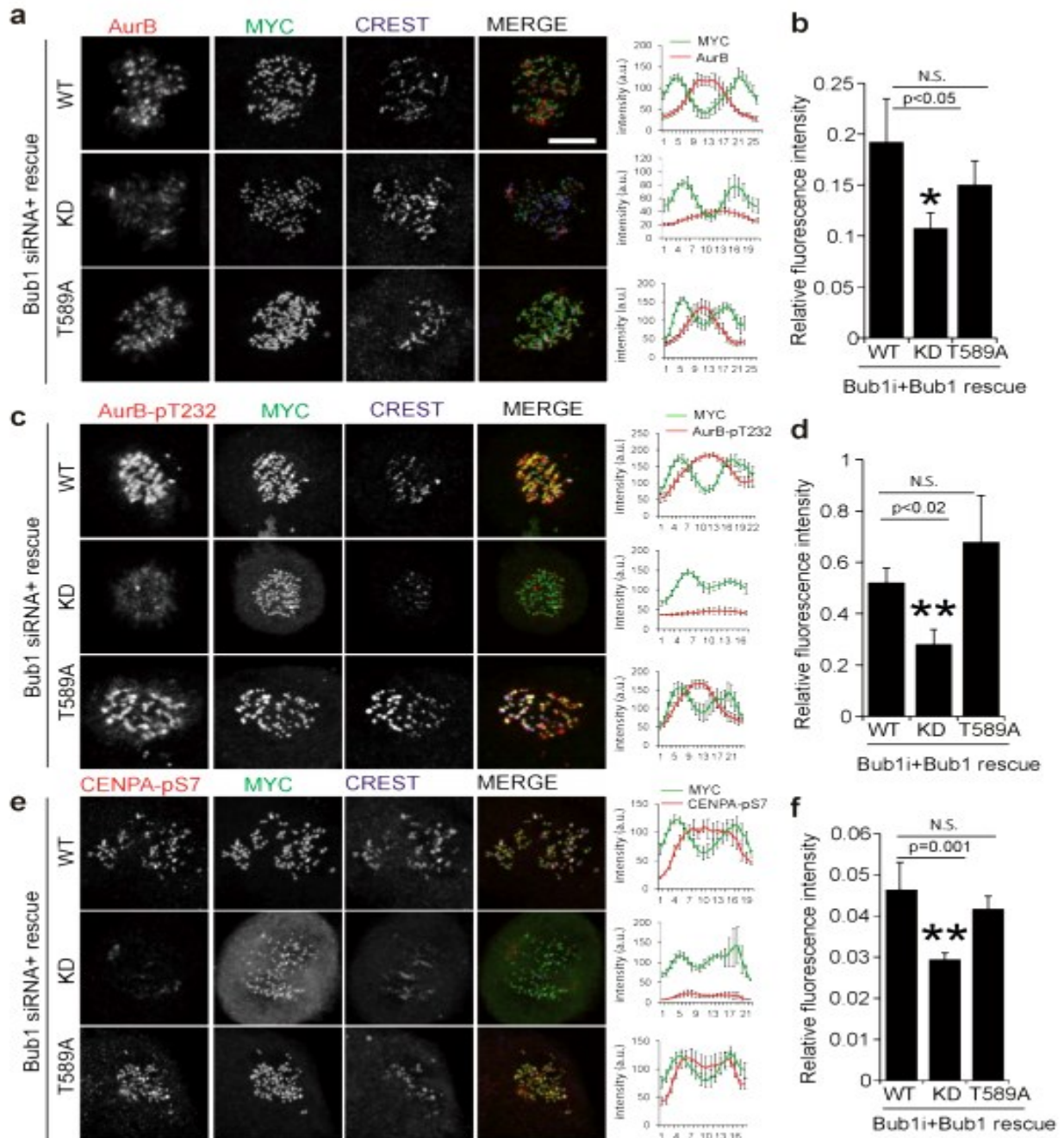
Supplementary Figure 1 Characterization of the pT589 and pS679 Bub1 antibodies: (a) Asynchronous HeLa S3 cells were fixed and stained with the Bub1 anti-pT589 antibody (red) as well as Bub1 (green) and CREST (blue). (b) Bub1-specificity (upper panels) and phosphospecificity (lower panels) of the Bub1 T589A antibody. Asterisk indicates non-specific centrosomal staining that is not lost upon Bub1 depletion. (c) Cells depleted of endogenous Bub1 were rescued with either an empty vector plasmid, or plasmids carrying Bub1 WT, KD, T589A and synchronized in mitosis before fixation and immunofluorescence with anti-pT589 antibody (red) and MYC-Bub1 (green). DNA was counterstained with Hoechst (blue). (d) MYC-tagged Bub1-WT was expressed and immunoprecipitated from 293T cells, before the sample was equally divided and either treated with λ -phosphatase or buffer as a control. The immunoprecipitates were separated by SDS-PAGE and immunoblotted with the Bub1 anti-pS679 antibody (Upper panel) and re-probed with anti-MYC (bottom panel).

For (a) and (c), the quantification in the MERGE panel represents the relative pT589 intensity normalized to CREST in arbitrary units. Scale bar= 5 μ M.



Supplementary Figure 2 Characterization of the isogenic MYC-GFP Bub1 WT, KD and T589A HeLa cell lines: (a) Immunofluorescence of the 3MYC-GFP Bub1-WT, KD, and T589A cell lines. Cells were stained with anti-MYC (green), anti-CREST (red) and Hoechst 33342 (blue) to mark the DNA. Scale bar=10 μ M. (b) Quantitation of kinetochore fluorescence intensity of the MYC signal relative to CREST from (a), n=10 cells. Note the slightly higher kinetochore levels of Bub1-KD in the isogenic cell line which likely explains the slight increase in the mitotic index in (d) (c) In vitro kinase assay of Bub1-WT, KD, and T589A as well as an empty vector control. Cells were transfected with MYC-tagged Bub1-WT, KD, or T589A and the immunoprecipitated MYC-tagged Bub1 proteins were subjected to an in vitro kinase assay to monitor autophosphorylation of Bub1-WT, KD, and T89A (1st panel) as well their ability to phosphorylate histone H2A (2nd Panel). Coomassie-stained gels to

demonstrate protein loading are indicated below the autoradiograms (panels 3 and 4).(d) Bub1-WT, KD and T589A expressing cells or parental cells were depleted of endogenous Bub1 and treated overnight with nocodazole (Noc, 3.3 μ M or 0.33 μ M) or 100nM taxol to arrest the cells. GL2 siRNA cells were used as controls. The mitotic index was counted in each condition. The data represent the mean \pm SE of three independent experiments with 100-600 cells counted per condition. Significance was calculated by one-way ANOVA relative to the Bub1 siRNA condition. ** $p < 0.001$, * $p < 0.03$.



Supplementary Figure 3 Aurora recruitment and activation are normal in Bub1-T589A expressing cells: Bub1 WT, KD and T589A expressing cells were depleted of endogenous Bub1 and localization (a,b), phosphorylation of the activation loop T232 (c,d) and of the canonical substrate CENPA-S7 (e,f) were verified by

immunofluorescence. Signal profile across sister kinetochores showing signal presence and/or overlap is indicated to the right of each set of images and represent the mean profile \pm SE of 7-15 kinetochore pairs. Quantitations (b,d,f) represent normalized kinetochore signals of 8-13 cells per condition. Error bars represent SE and significance was measured by the t-test. Scale bar = 5 μ M.

Figure 2C

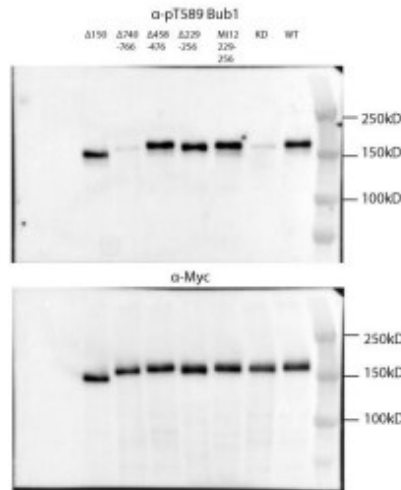
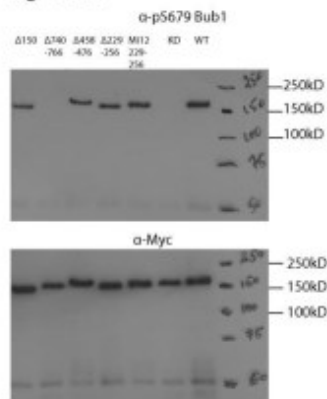


Figure 2D

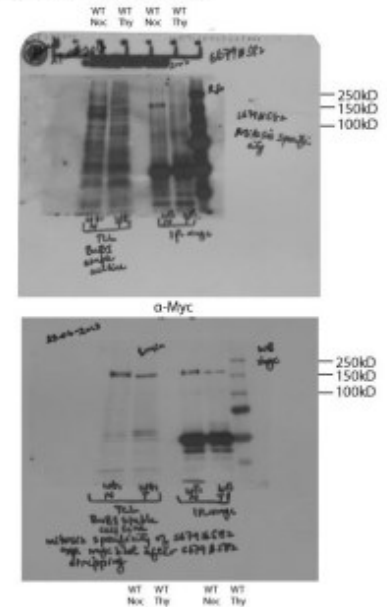


Figure 2e

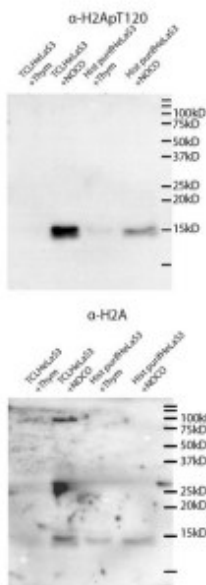
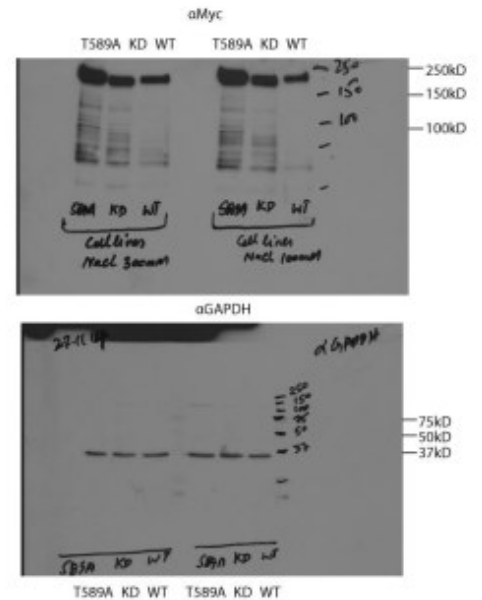
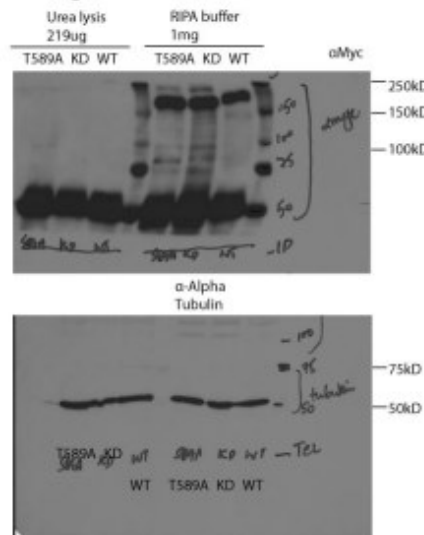


Figure 5F



Supplementary Figure 4. Original non-cropped Western Blots presented in this manuscript: Figure labelling corresponds to the figure in the main manuscript.

Table S1

PTM score_E1	PTM score_E2	PTM score_E3	Phosphopeptide ratio (WT:KD) Normalized by	Protein ratio (WT:KD)_E1	Phosphopeptide ratio (WT:KD) Normalized by	Protein ratio (WT:KD)_E2	Phosphopeptide ratio (WT:KD) Normalized by	Protein ratio (WT:KD)_E3	Phospho sitePlus
63.88			3.69	1.04					N
56.67		52.77	40.53	1.04			30.98	1.5	N
85.46	91.57	41.85	42.03	1.04	100%	1.6			Y
111.87	96.66	92.11	43.89	1.04	100%	1.6	13.00	1.5	N
		81.51							N
	16.1				100%	1.6			N
		3.65							N
94.59		37.98	0.74	1.04			0.84	1.5	N
	56.1				1.31	1.6			N
23.41	23.6	39.19	0.88	1.04	1.31	1.6			Y
71.8	5.46	62.3	1.47	1.04	1.52	1.6	1.06	1.5	Y
		43.32							Y
		73.26							N
107.82	74.81	48.6	58.09	1.04	100%	1.6			N
		58.87					7.75	1.5	N
	35.73	127.99			3.03	1.6	1.30	1.5	Y
23.71			39.95	1.04					N
37.98			1.39	1.04					Y
		18.28							Y
83.81	97.24	65	49.36	1.04	312.5	1.6	14.47	1.5	Y
		54.78					16.18	1.5	Y
	144.98	81.57			100%	1.6			Y
31.97		35.8	8.34	1.04			4.20	1.5	N
27.69	18.28		8.38	1.04	8.12	1.6			Y
39.19	69.17	4.22	73.63	1.04	100%	1.6	16.63	1.5	Y
	114.22	72.16			1.82	1.6	0.97	1.5	Y
112.44			1.97	1.04					N
39.82			5.86	1.04					N
15.8		81.51	1.2	1.04					Y
54.78	83.81	93.69	1.86	1.04	2.06	1.6	1.78	1.5	Y
96.01	56.1		3.22	1.04	8.68	1.6			Y
87.76			22.63	1.04					Y
78.82	31.98	78.4	9.92	1.04	100%	1.6	4.87	1.5	Y
61.19			30	1.04					N
		31.72							N
		77.93							N
		25.44					2.67	1.5	N
35.44	26.52	52.77	53.34	1.04	625	1.6	13.36	1.5	N
		61.5							Y

3. Chapter 3

The role of PLK1 in targeting cytosolic Bub1 to kinetochores

3.1. Introduction

BUB1 is a serine/threonine kinase that forms heterodimeric interaction with a related protein BUB3 throughout cell cycle (1-3). Deleting BUB3 binding domain also known as GLEBS (Gle binding sequence) causes BUB1 kinetochore mislocalization whereas immunodepletion of BUB1 mislocalizes BUB3 from kinetochores (4-7). Thus, BUB1/B

UB3 binding is required for localization of both BUB1 and BUB3. At kinetochores, BUB1 binds to KNL1 which is a scaffold component of a protein complex called KNL1-MIS12C-NDC80C (KMN) network (8, 9). Recent studies have pointed to a KNL1-BUB3-BUB1 pathway for BUB1 recruitment (10-12). BUB3 in complex with BUB1 is able to recognize specific repeats called MELTS (Met-Glu-Lys-Thr) on KNL1 (11, 12). At least 19 of these MELT motifs identified in humans are phosphorylated primarily by MPS1 kinase to create favorable interaction between specific binding pockets on BUB3 and phosphorylated MELT that allows for BUB1 localization (11, 13-15). At kinetochores, stable binding between BUB1 and KNL1 requires interaction between TPR region of BUB1 and Lys-Ile (KI) motif of KNL1 which also promotes MELT motifs ability for SAC signaling (16-18).

BUB1 also makes direct interactions with Polo like kinase 1 (PLK1) after it is phosphorylated at T609 by CDK1 which creates attachment for Polo box domain (PBD) of PLK1 and recruits PLK1 to kinetochores (19). A recent study has shown that BUB1-PLK1 complex at kinetochores is required for efficient CDC20 phosphorylation and BUB1 non-kinase region facilitates this interaction and subsequent phosphorylation (20). Recent and past studies mentioned above have focused on regulation of Bub1 recruitment but details and exact mechanism remains unclear. Here, we show that chemical inhibition of PLK1 enhances localization of BUB1 at kinetochores from cytosol in BUB3 depleted cells.

3.2. Hypothesis and objectives

Earlier we reported the identification of a novel BUB1 autophosphorylation site T589 through mass spectrometry analyses (21). The functional analyses of this site revealed that BUB1 T589 site is required for proper turnover and localization of H2ApT120 and SGO1 at kinetochores. To elucidate the mechanism we hypothesized that PLK1 and AURORA B kinases could play a role since these kinases regulate SGO1 localization at chromosomes during early mitosis in addition to being recruited by BUB1. Our aim was to test this hypothesis by using chemical inhibition of PLK1 and AURORA B in cells stably expressing BUB1 T589A after RNAi mediated knockdown of endogenous BUB1. We observed that BUB1 was also recruited to kinetochores from cytoplasm in HeLa cells which suggested that BUB1 localization is regulated by PLK1. This regulatory pathway is currently being investigated and is described below.

3.3. Results

Stable expression of a non-phosphorylatable mutant BUB1 T589A caused mislocalization of Shugoshin1 (SGO1), a cohesion protector, from centromeres to chromosome arms and cohesion defect was observed in T589A cells. BUB1 phosphorylates Histone H2A at T120 (H2ApT120) to regulate SGO1 recruitment at kinetochores. We also observed H2ApT120 spread over chromosomes arms in BUB1 T589A cells. Our FRAP analysis confirmed that change in turnover of BUB1 T589A at kinetochores had caused SGO1 and H2ApT120 mislocalization.

3.3.1. PLK1 inhibition causes rescue of SGO1 localization in BUB1 T589A

In an effort to understand the mechanism behind mislocalization of BUB1 substrates we used selective and specific inhibitor BI2536 (22) to inhibit PLK1 in BUB1 T589A cells and performed Immunofluorescence staining for SGO1 and H2ApT120. PLK1 inhibition rescued SGO1 centromere localization however a bulk of H2ApT120 still remained at chromosome arms (Figure 3.1).

3.3.2. PLK1 inhibition enhances BUB1 localization in Bub3 depleted HeLa cells

We observed that SGO1 localization is rescued on centromeres after PLK1 inhibition in T589A cells and to further explore this, we next asked if SGO1 mislocalized at chromosome arms can be relocated to centromeres by PLK1 inhibition in HeLa cells. To test this, we depleted BUB3 using siRNA to mislocalize BUB1. The depletion of BUB3 caused a massive reduction in BUB1 levels at kinetochores (Figure 3.2b DMSO-siBUB3). As expected, BUB3 depletion also caused spread of SGO1 and H2ApT120 all over chromosome arms compared to control cells due to BUB1 mislocalization (Figure 3.2a DMSO-siBUB3 vs. DMSO-siGL2). We then added BI2536 which rescued SGO1 and H2ApT120 to centromeres (Figure 3.2a BI-siBUB3).

Interestingly, cytosolic BUB1 recruitment to kinetochores was also enhanced after PLK1 inhibition in BUB3 depleted cells (Figure 3.2b BI-siBUB3). This demonstrated that PLK1 inhibition enhances BUB1 recruitment to kinetochores which refocuses SGO1/H2ApT120 at centromeres at least in BUB3-depleted cells.

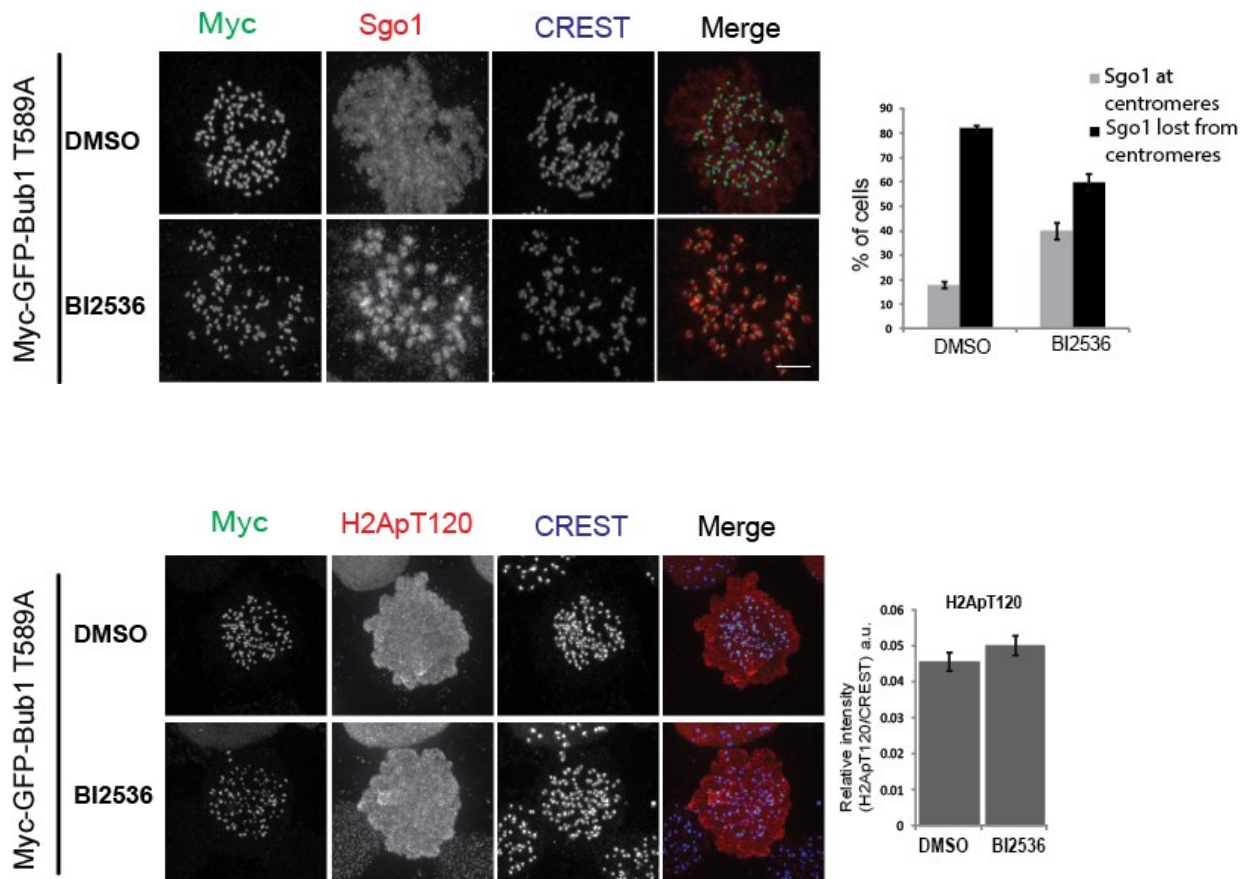


Figure 3.1 PLK1 inhibition recovers SGO1 loss from centromeres while H2ApT120 remains unchanged in BUB1 T589A cells: (a, b) HeLa cells stably expressing Myc-GFP-BUB1 T589A were transfected with BUB1 siRNA targeting 3'UTR of endogenous described in chapter 2 "materials and methods" for 72hrs to deplete endogenous BUB1, synchronized with Thymidine and treated with PLK1 inhibitor for 30min. before fixation. Immunofluorescence (IF) was performed for MYC (green) to detect BUB1 T589A, SGO1 (red), H2ApT120 (red) and CREST (blue). (c) The graph shows percentage (%) of mitotic cells with SGO1 signal at centromeres and signal lost from centromeres for each condition. The data was compiled from three independent experiments (n= approx.300 cells). (d) The graph with mean signal intensity of H2ApT120 of each sample from centromere relative to CREST. (n=12 cells). Error bars in both (c) and (d) show standard error (\pm s.e). Scale bars= 5 μ m. The figure show data from one of at least three replicates.

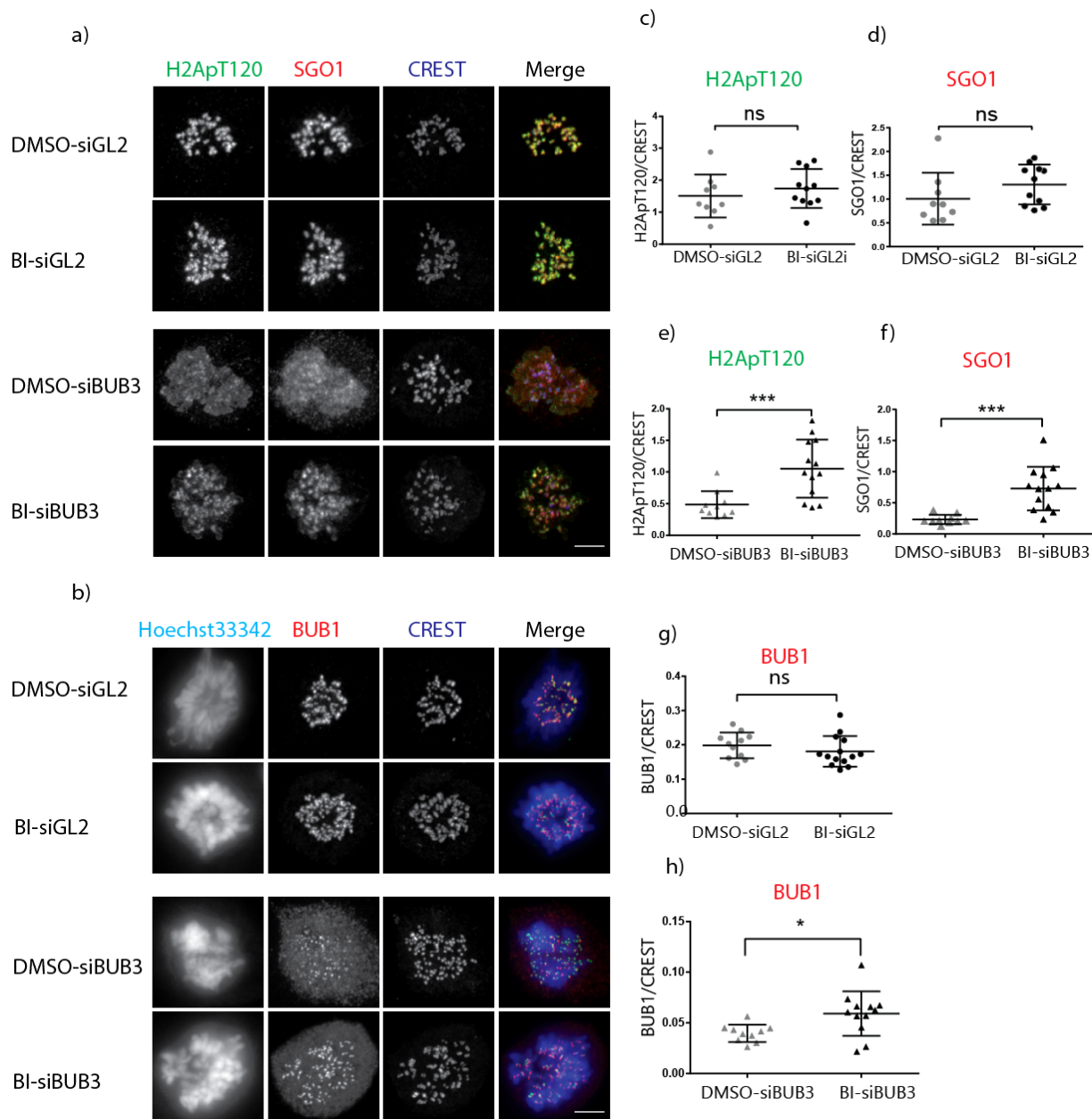


Figure 3.2 PLK1 inhibition recruits cytosolic BUB1, SGO1 and H2ApT120 in BUB3 depleted cells: (a, b) HeLa cells were transfected with control (GL2 siRNA) or BUB3 siRNA (siBub3) for 72hrs, synchronized with Thymidine and released into fresh medium with DMSO or BI 2536 for 10hrs and fixed. BUB1 signal at kinetochore was severely reduced in DMSO-siBUB3 (3b) indicating depletion of BUB3. IF was performed for SGO1 (red), H2ApT120 (green), BUB1 (red), CREST (blue) and Hoechst33342 for DNA staining. (c-h) quantification of a & b shown as mean signal intensity of each protein relative to CREST signal. n= at least 10 cells. Each dot represents one cell. Significance was calculated using t test (ns= not significant, *= $P \leq 0.05$, **= $P \leq 0.01$, ***= $P \leq 0.001$). Error bars represent \pm s.e. Scale bar= 5 μ m. The figure show data from one of at least three replicates.

3.3.3. PLK1 regulates BUB1 localization through KNL1

In our experiments (Figure 3.2), PLK1 inhibition alone does not affect BUB1 localization (siGL2-DMSO Vs. siGL2-BI) which is in agreement with a recent report (23). To understand how PLK1 inhibition promoted BUB1 localization from cytosol, we asked if BUB1 recruitment in PLK1 inhibited cells occurs through KNL1 as BUB1 is recruited at kinetochores by binding to KNL1. We incubated HeLa cells with control (DMSO) and BI 2536 to inhibit PLK1 and immunostained for a conserved residue of KNL1 MELT at T875 as described by previous reports (14, 24, 25) and for KNL1 and BUB1. We observed a significant decrease in signal for both KNL1 and phosphorylation of MELT (pT875) which suggested that PLK1 is required for assembly of KNL1 and phosphorylation of MELT at T875 (Figure 3.3 a, b). We also observed a decrease in BUB1 recruitment at kinetochores. However, in earlier experiments (Figure 3.2), we did not observe a significant BUB1 localization difference after BI 2536 treatment (siGL2-DMSO Vs. siGL2-BI).

The discrepancy in observation above could arise due to difference in inhibitor incubation period between the two experiments. In Figure 3.3, cycling cells were treated with BI 2536 for at least 16 hrs compared to cells release after Thymidine block and incubated with BI2536 for at least 10hrs in the Figure 3.2. We cannot rule out a prolonged PLK1 inhibition causing differences in our observations. These experiments need to be further repeated to fully determine the role of PLK1 inhibition on BUB1 localization in the absence of any further perturbation.

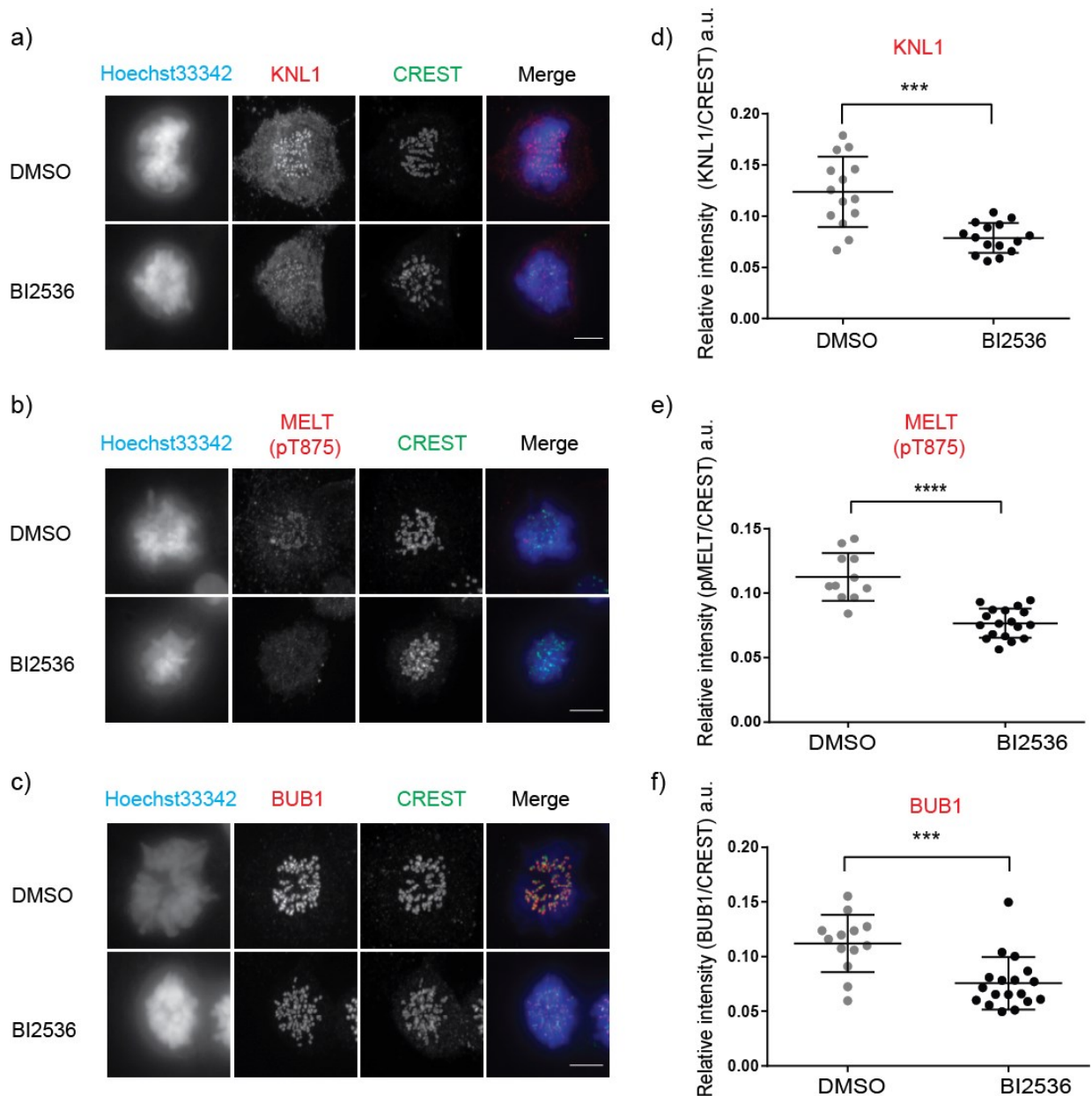


Figure 3.3 PLK1 inhibition impairs KNL1 binding and MELTs phosphorylation at kinetochores: (a-c) HeLa cells were treated with DMSO or BI 2536 for 16hrs and fixed. IF was performed for KNL1 (red), KNL1 MELT (pT875) (red), BUB1 (red), CREST (green) and Hoechst33342 for DNA staining. (d-f) quantification of (a-c) represented as mean of each protein relative to CREST signal of at least 10 cells with error bars showing \pm s.e. Significance was calculated as described in Figure 2. Scale bar= 5μm. The figure show data from one of at least three replicates.

After confirming that PLK1 is absolutely required for KNL1 assembly, we next tested if PLK1 regulates BUB1 localization through KNL1. We reasoned if BUB1 localization is regulated by PLK1 through any scaffold other than KNL1, we would observe a difference in BUB1 localization in control and BI 2536

treated cells after KNL1 depletion. To test this hypothesis, we used HeLa cells and depleted KNL1 using siRNA, treated with control or BI2536 and performed IF.

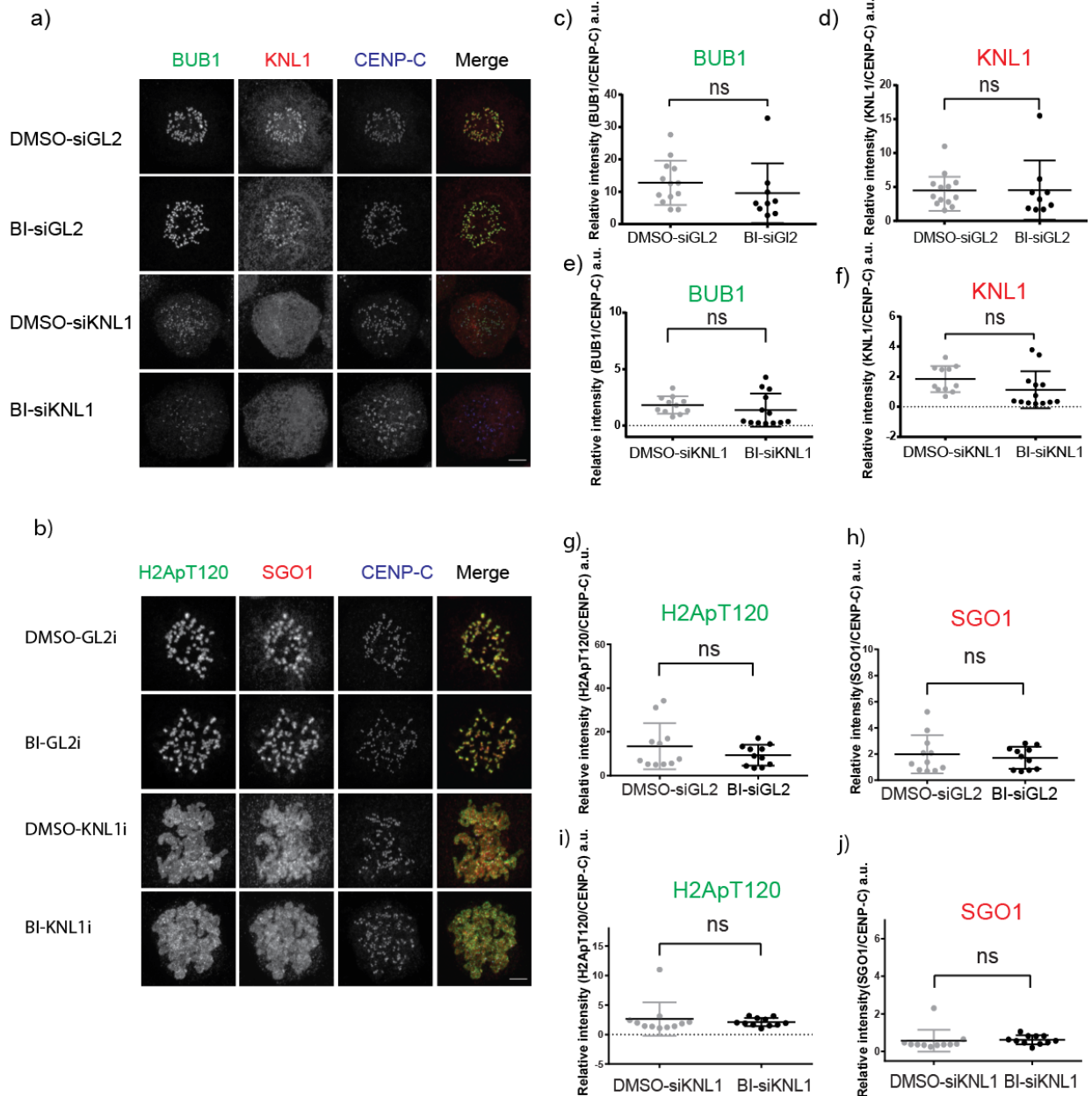


Figure 3.4 BUB1 localization is regulated by PLK1 at KNL1: (a,b) HeLa cells were transfected with control (GL2 siRNA) or KNL1 siRNA (siKNL1) for 72 hrs and synchronized with Thymidine and released into medium containing DMSO or BI 2536 for 10hrs and fixed. IF was performed for BUB1 (green) and KNL1 (red), H2ApT120 (green), SGO1 (red), CENP-C (blue) and Hoechst33342 for DNA staining (not shown). (c-j) Quantification of a & b shows signal intensity of each protein relative to CENP-C of at least 10 cells. Error bars showing \pm s.e. Significance was calculated as described in Figure 2. ns= not significant). Scale bar= 5μm. The figure show data from one of the three replicates.

We observed a massive reduction in KNL1 and BUB1 signal confirming importance of KNL1 for BUB1 kinetochore localization (Figure 3.4a). We quantified and compared BUB1 signal in control and BI 2536 treated cells after KNL1 depletion. The statistical analyses revealed no significant change in BUB1 localization in these cells suggesting that PLK1 can regulate BUB1 recruitment via KNL1. We also stained for SGO1 and H2ApT120 which had signal all over chromosome arms consistent with the fact that KNL1 depletion mislocalizes BUB1 which causes uniform spread of SGO1 and H2ApT120 on chromosomes.

3.4. Discussion and Perspectives

Our experiments show that BUB1 localization is enhanced at kinetochores after PLK1 inhibition by BI 2536 in BUB3 depleted cells. We also report that PLK1 regulate phosphorylation of MELT and assembly of KNL1. Also BUB1 localization is regulated by PLK1 through KNL1 at kinetochores. How this happens is not clear yet. Answering the following questions will help understand the mechanism.

As explained above, BUB1 forms a heterodimer complex with BUB3 for its recruitment. It is important to demonstrate if BUB1 is recruited independent of BUB3 binding after PLK1 inhibition in BUB3 depleted cells. To clarify this, cells should be grown and treated as in Figure 3.2 and immunostained for BUB3. The recruitment of residual BUB3 in PLK1 inhibited cells will confirm that BUB1 is recruited is regulated in heterodimer with BUB3 [Figure 3.5 (1)].

Several studies have reported that PLK1 is present on centrosomes, spindle poles and kinetochores during cell cycle for various functions including chromosome alignment and accurate mitotic progression during mitosis (26, 27). BUB1 is phosphorylated at T609 by CDK1 which allows for PLK1 binding to BUB1 through its PBD for its recruitment. Whether a BUB1 bound PLK1 pool is involved in BUB1 localization has not been studied so far. To determine this, using a Bub1 mutant (BUB1-PBD mutant) unable to bind PLK1 in BUB3 depleted cells and treatment with control or PLK1 inhibitor BI2536 will reveal if BUB1-PLK1 complex is recruited after PLK1 inhibition. The increase in centromere signal of BUB1-PBD mutant and/or

SGO/H2ApT120 after PLK1 inhibition compared to control will suggest that BUB1 is recruited independent of PLK1 binding [Figure 3.5 (2)].

Our experiments so far have shown that PLK1 inhibition causes a decrease in KNL1 phosphorylation at MELT T875. Recently, it was shown that by phosphorylating 13 of 19 MELT motifs PLK1 kinase activity overlaps with MPS1 (24). Whether PLK1 have additional phosphorylation targets at KNL1 that can regulate BUB1 localization is not known. Further structural analyses of KNL1 by Mass spectrometry can reveal those potential PLK1 phosphorylation site (s) [Figure 3.5 (3)]. Mutation of potential PLK1 phosphorylation sites and study of BUB1 recruitment could provide a better understanding of the mechanism behind our observations.

Several reports have shown that BUB1 localization is important for chromosome congression and SAC signaling. However, studies on regulation of BUB1 localization are not complete. It is imperative to understand role of BUB1 localization to fully understand regulation and progression of mitosis. PLK1 has been shown to support MPS1 and AURORA B for SAC activity but also promotes APC/C activation (24, 28, 29). It is yet to be determined if regulation of BUB1 localization by PLK1 contributes to chromosome segregation and SAC signaling. To fully understand this will require answering above questions and further investigation based on acquired results.

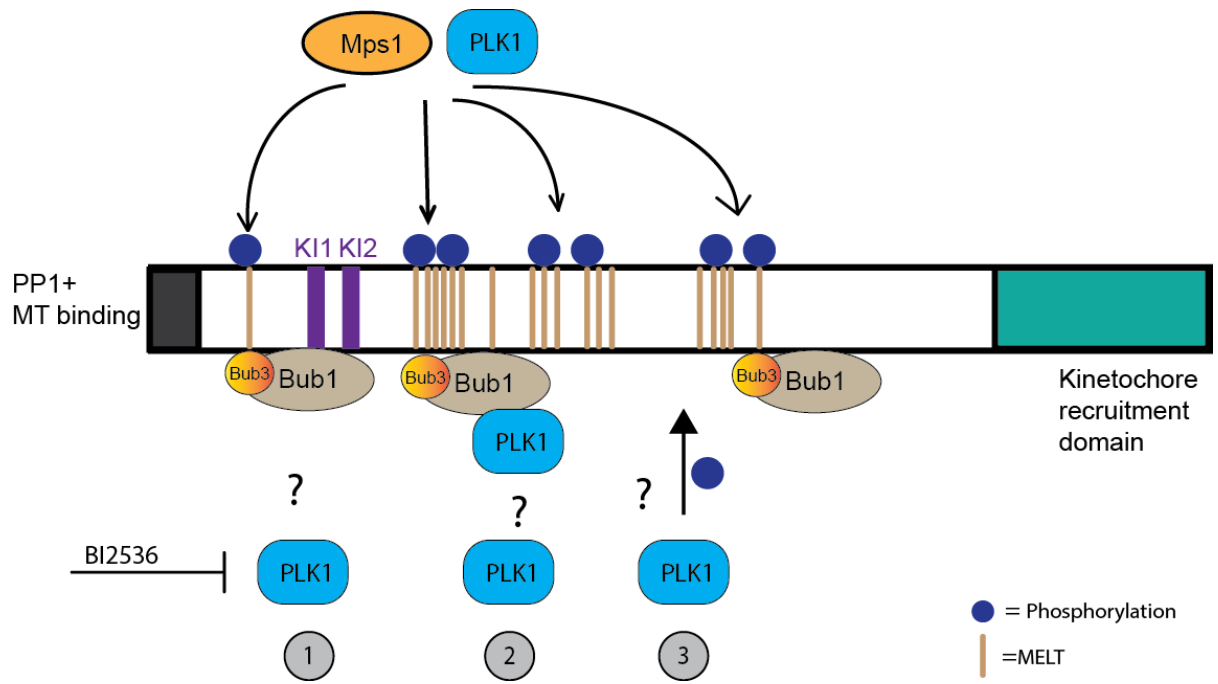


Figure 3.5. Perspective experiments of BUB1 regulation by PLK1. For details see discussion and perspectives

3.5. Materials and Methods

3.5.1. Cell culture, transfection and drug treatment

Cells were grown in DMEM supplemented with 10% fetal bovine serum or bovine growth serum (PAA). Bub1 T589A cells were generated and maintained as described in (21). All cells were grown at 37°C and 5% CO₂. Cells were incubated with drugs at following concentrations and duration: BI2536 (Reagents Direct) 100nM for 16hrs and 10 hrs for Figure 2 and Figure 3 respectively, ZM 447439 (TOCRIS bioscience) 10µM for 30min, Nocodazole (Sigma) 100ng/mL for 16hrs, Thymidine(Acros Organics) 2 mM for 16hrs.

Bub1 and Bub3 siRNA/DisRNA were used as described in (21). For KNL1 following siRNA from ref (8): 5'-AAGAUCUGAUUAAGGAUCCACGAAA-3' was used at 100nM/35mm well. For siRNA transfection reagent INTERFERin (Polyplus) with volume ranging from 8-16uL/35mm well for at least 72 hours was used.

3.5.2. Immunofluorescence and Microscopy

For Immunofluorescence cells were grown on glass cover slips and fixed either after arrest in mitosis by nocodazole or after release from Thymidine block. Cell fixation solution PTEMF (0.2% Triton X-100, 20 mM PIPES pH 6.8, 1 mM MgCl₂, 10 mM EGTA and 4% formaldehyde) was applied for 10min and washed with 1XPBS. Primary and secondary antibodies were prepared in blocking solution (3%-BSA in 1XPBS-Tween 0.2%) and applied on cells for at least 1hr with gentle washing with 1XPBS-Tween 0.2% between primary and secondary antibodies. Following primary antibodies were used for experiments at 1ugmL⁻¹: anti-MYC (9E10, Thermo Scientific), anti-Bub1 described in (30), anti-SgoL1 (H00151648-M01, Abnova), anti-H2ApT120 (61195, Active Motif), anti-KNL1 (AB70537 abcam), CREST anti-centromere (HCT-0100, Immunovision) and CENP-C (MBL life science). Anti-H2ApT120 (Figure1) and anti-KNL1^{T875} were gifts from Y. Watanabe. Secondary antibodies (DyLight® series from Thermo) were used for immunofluorescence (1:1,000).

For confocal microscopy an inverted Olympus IX80 microscope with a WaveFX-Borealin-SC Yokagawa spinning disc (Quorum Technologies) and an

Orca Flash4.0 camera (Hamamatsu) were used. To acquire images Metamorph software (Molecular Devices) was used. Same exposure time in each channel was used and Z stacks were generated with same distance between them. Image stacks were merged into a single projection image and analysed for signal intensity in each channel using ImageJ (rsb.info.nih.gov). Figures and scale bars were created using ImageJ. Final images were prepared using PhotoshopCS6 and Adobe Illustrator softwares.

3.6. Refernces

1.

Larsen NA, Al-Bassam J, Wei RR, Harrison SC. Structural analysis of Bub3 interactions in the mitotic spindle checkpoint. *Proc Natl Acad Sci U S A*. 2007;104(4):1201-6.

2.

Chang L, Zhang Z, Yang J, McLaughlin SH, Barford D. Molecular architecture and mechanism of the anaphase-promoting complex. *Nature*. 2014;513(7518):388-93.

3.

Elowe S. Bub1 and BubR1: at the interface between chromosome attachment and the spindle checkpoint. *Molecular and cellular biology*. 2011;31(15):3085-93.

4.

Taylor SS, Ha E, McKeon F. The human homologue of Bub3 is required for kinetochore localization of Bub1 and a Mad3/Bub1-related protein kinase. *The Journal of cell biology*. 1998;142(1):1-11.

5.

Sharp-Baker H, Chen RH. Spindle checkpoint protein Bub1 is required for kinetochore localization of Mad1, Mad2, Bub3, and CENP-E, independently of its kinase activity. *The Journal of cell biology*. 2001;153(6):1239-50.

6.

Klebig C, Korinth D, Meraldi P. Bub1 regulates chromosome segregation in a kinetochore-independent manner. *The Journal of cell biology*. 2009;185(5):841-58.

7.

Kim T, Moyle MW, Lara-Gonzalez P, De Groot C, Oegema K, Desai A. Kinetochore-localized BUB-1/BUB-3 complex promotes anaphase onset in *C. elegans*. *The Journal of cell biology*. 2015;209(4):507-17.

8.

Kiyomitsu T, Obuse C, Yanagida M. Human Blinkin/AF15q14 is required for chromosome alignment and the mitotic checkpoint through direct interaction with Bub1 and BubR1. *Dev Cell*. 2007;13(5):663-76.

9.

Ghongane P, Kapanidou M, Asghar A, Elowe S, Bolanos-Garcia VM. The dynamic protein Knl1 - a kinetochore rendezvous. *Journal of cell science*. 2014;127(Pt 16):3415-23.

10.

Shepperd LA, Meadows JC, Sochaj AM, Lancaster TC, Zou J, Buttrick GJ, et al. Phosphodependent recruitment of Bub1 and Bub3 to Spc7/KNL1 by Mph1

kinase maintains the spindle checkpoint. *Current biology* : CB. 2012;22(10):891-9.

11.

Primorac I, Weir JR, Chiroli E, Gross F, Hoffmann I, van Gerwen S, et al. Bub3 reads phosphorylated MELT repeats to promote spindle assembly checkpoint signaling. *Elife*. 2013;2:e01030.

12.

Faesen AC, Musacchio A. The (phospho) needle in the (MELT) Haystack. *Molecular cell*. 2015;57(5):765-6.

13.

Vleugel M, Tromer E, Omerzu M, Groenewold V, Nijenhuis W, Snel B, et al. Arrayed BUB recruitment modules in the kinetochore scaffold KNL1 promote accurate chromosome segregation. *The Journal of cell biology*. 2013;203(6):943-55.

14.

Yamagishi Y, Yang CH, Tanno Y, Watanabe Y. MPS1/Mph1 phosphorylates the kinetochore protein KNL1/Spc7 to recruit SAC components. *Nat Cell Biol*. 2012;14(7):746-52.

15.

London N, Ceto S, Ranish JA, Biggins S. Phosphoregulation of Spc105 by Mps1 and PP1 regulates Bub1 localization to kinetochores. *Current biology* : CB. 2012;22(10):900-6.

16.

Krenn V, Wehenkel A, Li X, Santaguida S, Musacchio A. Structural analysis reveals features of the spindle checkpoint kinase Bub1-kinetochore subunit Knl1 interaction. *The Journal of cell biology*. 2012;196(4):451-67.

17.

Krenn V, Overlack K, Primorac I, van Gerwen S, Musacchio A. KI motifs of human Knl1 enhance assembly of comprehensive spindle checkpoint complexes around MELT repeats. *Current biology* : CB. 2014;24(1):29-39.

18.

Kiyomitsu T, Murakami H, Yanagida M. Protein interaction domain mapping of human kinetochore protein Blinkin reveals a consensus motif for binding of spindle assembly checkpoint proteins Bub1 and BubR1. *Molecular and cellular biology*. 2011;31(5):998-1011.

19.

Qi W, Yu H. KEN-box-dependent degradation of the Bub1 spindle checkpoint kinase by the anaphase-promoting complex/cyclosome. *J Biol Chem*. 2007;282(6):3672-9.

20.

Jia L, Li B, Yu H. The Bub1-Plk1 kinase complex promotes spindle checkpoint signalling through Cdc20 phosphorylation. *Nat Commun*. 2016;7:10818.

21.

Asghar A, Lajeunesse A, Dulla K, Combes G, Thebault P, Nigg EA, et al. Bub1 autophosphorylation feeds back to regulate kinetochore docking and promote localized substrate phosphorylation. *Nat Commun.* 2015;6:8364.

22.

Lenart P, Petronczki M, Steegmaier M, Di Fiore B, Lipp JJ, Hoffmann M, et al. The small-molecule inhibitor BI 2536 reveals novel insights into mitotic roles of polo-like kinase 1. *Current biology : CB.* 2007;17(4):304-15.

23.

Espeut J, Lara-Gonzalez P, Sassine M, Shiau AK, Desai A, Abrieu A. Natural Loss of Mps1 Kinase in Nematodes Uncovers a Role for Polo-like Kinase 1 in Spindle Checkpoint Initiation. *Cell Rep.* 2015;12(1):58-65.

24.

von Schubert C, Cubizolles F, Bracher JM, Sliedrecht T, Kops GJ, Nigg EA. Plk1 and Mps1 Cooperatively Regulate the Spindle Assembly Checkpoint in Human Cells. *Cell Rep.* 2015;12(1):66-78.

25.

Zhang G, Lischetti T, Nilsson J. A minimal number of MELT repeats supports all the functions of KNL1 in chromosome segregation. *Journal of cell science.* 2014;127(Pt 4):871-84.

26.

Zitouni S, Nabais C, Jana SC, Guerrero A, Bettencourt-Dias M. Polo-like kinases: structural variations lead to multiple functions. *Nat Rev Mol Cell Biol.* 2014;15(7):433-52.

27.

Archambault V, Lepine G, Kachaner D. Understanding the Polo Kinase machine. *Oncogene.* 2015;34(37):4799-807.

28.

O'Connor A, Maffini S, Rainey MD, Kaczmarczyk A, Gaboriau D, Musacchio A, et al. Requirement for PLK1 kinase activity in the maintenance of a robust spindle assembly checkpoint. *Biol Open.* 2015;5(1):11-9.

29.

Hansen DV, Loktev AV, Ban KH, Jackson PK. Plk1 regulates activation of the anaphase promoting complex by phosphorylating and triggering SCFbetaTrCP-dependent destruction of the APC Inhibitor Emi1. *Mol Biol Cell.* 2004;15(12):5623-34.

30.

Elowe S, Dulla K, Uldschmid A, Li X, Dou Z, Nigg EA. Uncoupling of the spindle-checkpoint and chromosome-congression functions of BubR1. *Journal of cell science.* 2010;123(Pt 1):84-94.

4. Chapter 4

4.1. Discussion and Perspectives

BUB1 is a stable protein at kinetochores and has a slower turnover compared to other SAC proteins BUBR1, BUB3 and MAD2 (1). During its stay at kinetochores BUB1 phosphorylates Histone H2ApT120 to recruit SGO1 at kinetochores. In chapter 2, we described the identification and characterization of novel BUB1 autophosphorylation at T589. The mutation at this site changes BUB1 turnover at kinetochores and subsequently causes SGO1 and H2ApT120 spread on chromosome arms. We showed that altered turnover changes BUB1 substrate localization. The governing mechanism is still elusive however; the discussion section of the chapter sheds some light on how T589 might regulate SGO1 and H2ApT120 localization.

Recent studies have shown that phosphatase activity in particular PP1 activity regulates BUB1 localization at kinetochores and that mutations in the RVSF motif needed for PP1 binding enhances BUB1 localization (2-4). Further analyses have suggested that PP1 activity is not exclusively required during SAC silencing rather it could also play a role in maintaining BUB1/BUBR1 turnover at kinetochore (5). In this pathway, MPS1 repeatedly phosphorylates MELT motifs to recruit BUB3:BUB1/BUBR1 to kinetochores whereas PP1 dephosphorylates them to antagonize MPS1. This cycle of repeated phosphorylation and dephosphorylation of KNL1 MELT contributes in BUB1 and BUBR1 turn over. The fact that PP1 is active during SAC and is a regulator of BUB1 localization makes it a good candidate for further investigation on regulation of BUB1 turnover in situation where BUB1 already lacks autophosphorylation at T589. It is possible that lack in phosphorylation at T589 (T589A) leads to susceptibility to PP1 activity and faster turnover observed in Bub1 T589A cells.

We also observed that restricting BUB1 T589A at kinetochores refocuses SGO1/H2ApT120 from chromosome arms to centromeres pointing to the fact that turnover change caused the spread of phosphorylation at chromosome arms (Chapter 2 Figure 2.6 b, c & d). In chapter 3 we observed that T589A

cells had SGO1 localization recovery to centromeres after PLK1 inhibition. Whether PLK1 is involved in BUB1 T589A turnover has not been tested so far. It is possible that PLK1 contributes to T589A turnover and inhibition of it recovers it. To test that FRAP analyses can be employed to determine change in turnover after PLK1 inhibition in BUB1 T589A cells.

Another recently studied BUB1 autophosphorylation site S969 is present in the activation segment of BUB1 (6). The study revealed that S969 is an intramolecular autophosphorylation site. This study utilized BUB1 kinase active and kinase dead fragments and determined that kinase active fragment of BUB1 could not phosphorylate kinase dead at S969 thus, showing that S969 is regulated by intramolecular autophosphorylation. So far, we have not defined whether T589 autophosphorylation site is inter- or intra-molecular autophosphorylation site. The nature of T589 autophosphorylation residue can be determined using the similar technique mentioned above.

Our study also showed that BUBR1 levels at kinetochores are not affected by mutation at T589. Recently it was shown that BUB1-BUB3 and -BUBR1-BUB3 form a heterotetramer and recruits BUBR1 at kinetochores (7). We did not test whether BUBR1 turnover is also changed in BUB1 T589 cells. A Similar FRAP analyses used to measure BUB1 T589A turnover can be applied to determine BUBR1 turnover in BUB1 T589A cells. Although this may not help in deciphering the mechanism of altered turnover, this could very well tell if BUBR1 has turnover independent of BUB1 in these cells.

In chapter 3 we have shown that PLK1 regulated BUB1 localization. Further studies on the project will demonstrate how PLK1 can affect BUB1 localization regulation. The project will also tell us if PLK1 can regulate SAC signaling and chromosome segregation via Bub1 localization.

4.2. Current understanding of Bub1 activity in SAC

BUB1 kinase takes on the role of a scaffold for SAC proteins like BUBR1, BUB3 and PLK1. A number of studies have shown that BUB1 kinase activity is partially required for SAC and non-kinase region is need for SAC and at least two studies described that middle region (aa 450-550 approx.) is required for

kinase function(8, 9). One study demonstrating the requirement of BUB1 kinase function for SAC argued that low level spindle damage induces BUB1 kinase activity for SAC suggesting kinase function is needed at the end of prometaphase when only few unattached kinetochores are present (10). Recently a study on BUB1 kinase function revealed an “unconventional catalytic” role of non-kinase domains of BUB1 which recruits PLK1 for CDC20 phosphorylation(11). The recruitment of another kinase might also promote an early kinase activity in addition to late kinase activity for SAC.

So far, the evidence from literature have suggested that BUB1 kinase activity is required for SAC activation by recruiting other mitotic kinases to kinetochores e.g. PLK1 recruitment for CDC20 phosphorylation for inhibition of APC or by promoting AURORA B localization that plays a role in SAC signaling. As described in chapter 1, several studies have shown that BUB1 kinase function is also dedicated to recruitment of SGO1 through H2ApT120 for achieving bi-orientation between kinetochores and microtubules. How this integrates with non-kinase function of scaffolding will require further investigation.

Several studies have addressed BUB1 activation and its role during SAC but not many have focused on its inactivation and how it might contribute to SAC silencing. Recent literature shows that phosphatases play a crucial role in BUB1 regulation. PP2A and PP1 are shown to remove BUB1 from kinetochores and antagonize the activity of MPS1. Recently it is shown that a complex FIN1-PP1 removes BUB1 from kinetochores in yeast (4). Existence of a parallel system in humans may provide a better understanding of regulation of BUB1 activity. A recent study shows that deletion of a BUB1 region that binds BUBR1 causes increase in SAC strength suggesting that BUB1 binds a BUBR1-B56 pool that could play a role in SAC silencing (12). In fact, a recent study in *C.elegans* suggested that BUB1 depletion delays anaphase onset independent of its SAC function (13). Understanding on how BUB1 is required for SAC silencing is still in its early stages. An interesting question regarding this will be about the triggers that switch BUB1 from SAC activator to promoter of SAC silencing.

In summary, this thesis work describes a novel autophosphorylation site i.e. T589 on BUB1 required for concentrating BUB1 and its substrates on centromeres and proper chromosome congression. We have also shown that kinase extension domain is required for this autophosphorylation and TPR domain is dispensable for Bub1 localization. The preliminary results of the second project so far have shown that cytosolic BUB1 recruitment could be regulated by PLK1 and could be helpful in further our understanding about the regulatory mechanisms exist among SAC proteins.

4.3. References

1.

Howell BJ, Moree B, Farrar EM, Stewart S, Fang G, Salmon ED. Spindle checkpoint protein dynamics at kinetochores in living cells. *Current biology* : CB. 2004;14(11):953-64.

2.

London N, Ceto S, Ranish JA, Biggins S. Phosphoregulation of Spc105 by Mps1 and PP1 regulates Bub1 localization to kinetochores. *Current biology* : CB. 2012;22(10):900-6.

3.

Maton G, Edwards F, Lacroix B, Stefanutti M, Laband K, Lieury T, et al. Kinetochores are required for central spindle assembly. *Nat Cell Biol*. 2015;17(7):953.

4.

Bokros M, Gravenmier C, Jin F, Richmond D, Wang Y. Fin1-PP1 Helps Clear Spindle Assembly Checkpoint Protein Bub1 from Kinetochores in Anaphase. *Cell Rep*. 2016;14(5):1074-85.

5.

Zhang G, Lischetti T, Nilsson J. A minimal number of MELT repeats supports all the functions of KNL1 in chromosome segregation. *Journal of cell science*. 2014;127(Pt 4):871-84.

6.

Lin Z, Jia L, Tomchick DR, Luo X, Yu H. Substrate-specific activation of the mitotic kinase Bub1 through intramolecular autophosphorylation and kinetochore targeting. *Structure*. 2014;22(11):1616-27.

7.

Breit C, Bange T, Petrovic A, Weir JR, Muller F, Vogt D, et al. Role of Intrinsic and Extrinsic Factors in the Regulation of the Mitotic Checkpoint Kinase Bub1. *PloS one*. 2015;10(12):e0144673.

8.

Klebig C, Korinth D, Meraldi P. Bub1 regulates chromosome segregation in a kinetochore-independent manner. *The Journal of cell biology*. 2009;185(5):841-58.

9.

Vleugel M, Hoek TA, Tromer E, Sliedrecht T, Groenewold V, Omerzu M, et al. Dissecting the roles of human BUB1 in the spindle assembly checkpoint. *Journal of cell science*. 2015;128(16):2975-82.

10.

Chen RH. Phosphorylation and activation of Bub1 on unattached chromosomes facilitate the spindle checkpoint. *The EMBO journal*. 2004;23(15):3113-21.

11.

Jia L, Li B, Yu H. The Bub1-Plk1 kinase complex promotes spindle checkpoint signalling through Cdc20 phosphorylation. *Nat Commun.* 2016;7:10818.

12.

Zhang G, Lischetti T, Hayward DG, Nilsson J. Distinct domains in Bub1 localize RZZ and BubR1 to kinetochores to regulate the checkpoint. *Nat Commun.* 2015;6:7162.

13.

Kim T, Moyle MW, Lara-Gonzalez P, De Groot C, Oegema K, Desai A. Kinetochore-localized BUB-1/BUB-3 complex promotes anaphase onset in *C. elegans*. *The Journal of cell biology.* 2015;209(4):507-17.

4.4. References- Introduction

1.

Daignan-Fornier B, Sagot I. Proliferation/quiescence: the controversial "aller-retour". *Cell Div.* 2011;6:10.

2.

Yao G. Modelling mammalian cellular quiescence. *Interface Focus.* 2014;4(3):20130074.

3.

Schafer KA. The cell cycle: a review. *Vet Pathol.* 1998;35(6):461-78.

4.

Vermeulen K, Van Bockstaele DR, Berneman ZN. The cell cycle: a review of regulation, deregulation and therapeutic targets in cancer. *Cell Prolif.* 2003;36(3):131-49.

5.

Sancar A, Lindsey-Boltz LA, Unsal-Kacmaz K, Linn S. Molecular mechanisms of mammalian DNA repair and the DNA damage checkpoints. *Annu Rev Biochem.* 2004;73:39-85.

6.

Bertoli C, Skotheim JM, de Bruin RA. Control of cell cycle transcription during G1 and S phases. *Nat Rev Mol Cell Biol.* 2013;14(8):518-28.

7.

Pines J. Cyclins: wheels within wheels. *Cell Growth Differ.* 1991;2(6):305-10.

8.

Kousholt AN, Menzel T, Sorensen CS. Pathways for genome integrity in G2 phase of the cell cycle. *Biomolecules.* 2012;2(4):579-607.

9.

Lim S, Kaldis P. Cdks, cyclins and CKIs: roles beyond cell cycle regulation. *Development*. 2013;140(15):3079-93.

10.

Hartwell LH, Weinert TA. Checkpoints: controls that ensure the order of cell cycle events. *Science*. 1989;246(4930):629-34.

11.

Langerak P, Russell P. Regulatory networks integrating cell cycle control with DNA damage checkpoints and double-strand break repair. *Philos Trans R Soc Lond B Biol Sci*. 2011;366(1584):3562-71.

12.

Kastan MB, Bartek J. Cell-cycle checkpoints and cancer. *Nature*. 2004;432(7015):316-23.

13.

Weinberg RA. The retinoblastoma protein and cell cycle control. *Cell*. 1995;81(3):323-30.

14.

Brehm A, Miska EA, McCance DJ, Reid JL, Bannister AJ, Kouzarides T. Retinoblastoma protein recruits histone deacetylase to repress transcription. *Nature*. 1998;391(6667):597-601.

15.

Alberts B. *Molecular biology of the cell*. 4th ed. New York: Garland Science; 2002. xxxiv, 1463, [86] p. p.

16.

Johnson A, Skotheim JM. Start and the restriction point. *Curr Opin Cell Biol*. 2013;25(6):717-23.

17.

Foster DA, Yellen P, Xu L, Saqcena M. Regulation of G1 Cell Cycle Progression: Distinguishing the Restriction Point from a Nutrient-Sensing Cell Growth Checkpoint(s). *Genes Cancer*. 2010;1(11):1124-31.

18.

Zetterberg A, Larsson O, Wiman KG. What is the restriction point? *Curr Opin Cell Biol*. 1995;7(6):835-42.

19.

Malumbres M, Barbacid M. Cell cycle, CDKs and cancer: a changing paradigm. *Nat Rev Cancer*. 2009;9(3):153-66.

20.

Ezhevsky SA, Ho A, Becker-Hapak M, Davis PK, Dowdy SF. Differential regulation of retinoblastoma tumor suppressor protein by G(1) cyclin-

- dependent kinase complexes in vivo. *Molecular and cellular biology*. 2001;21(14):4773-84.
21.
- Ho A, Dowdy SF. Regulation of G(1) cell-cycle progression by oncogenes and tumor suppressor genes. *Curr Opin Genet Dev*. 2002;12(1):47-52.
22.
- Bartek J, Lukas J. Mammalian G1- and S-phase checkpoints in response to DNA damage. *Curr Opin Cell Biol*. 2001;13(6):738-47.
23.
- Dyson N. The regulation of E2F by pRB-family proteins. *Genes Dev*. 1998;12(15):2245-62.
24.
- Lunn CL, Chrivia JC, Baldassare JJ. Activation of Cdk2/Cyclin E complexes is dependent on the origin of replication licensing factor Cdc6 in mammalian cells. *Cell cycle*. 2010;9(22):4533-41.
25.
- Hu B, Mitra J, van den Heuvel S, Enders GH. S and G2 phase roles for Cdk2 revealed by inducible expression of a dominant-negative mutant in human cells. *Molecular and cellular biology*. 2001;21(8):2755-66.
26.
- Coverley D, Laman H, Laskey RA. Distinct roles for cyclins E and A during DNA replication complex assembly and activation. *Nat Cell Biol*. 2002;4(7):523-8.
27.
- Xu M, Sheppard KA, Peng CY, Yee AS, Piwnicka-Worms H. Cyclin A/CDK2 binds directly to E2F-1 and inhibits the DNA-binding activity of E2F-1/DP-1 by phosphorylation. *Molecular and cellular biology*. 1994;14(12):8420-31.
28.
- Hochegger H, Takeda S, Hunt T. Cyclin-dependent kinases and cell-cycle transitions: does one fit all? *Nat Rev Mol Cell Biol*. 2008;9(11):910-6.
29.
- Oakes V, Wang W, Harrington B, Lee WJ, Beamish H, Chia KM, et al. Cyclin A/Cdk2 regulates Cdh1 and claspin during late S/G2 phase of the cell cycle. *Cell cycle*. 2014;13(20):3302-11.
30.
- Wang Y, Ji P, Liu J, Broaddus RR, Xue F, Zhang W. Centrosome-associated regulators of the G(2)/M checkpoint as targets for cancer therapy. *Mol Cancer*. 2009;8:8.
31.
- Gavet O, Pines J. Activation of cyclin B1-Cdk1 synchronizes events in the

nucleus and the cytoplasm at mitosis. *The Journal of cell biology*. 2010;189(2):247-59.
32.

Boutros R, Dozier C, Ducommun B. The when and wheres of CDC25 phosphatases. *Curr Opin Cell Biol*. 2006;18(2):185-91.
33.

Xu B, Kim ST, Lim DS, Kastan MB. Two molecularly distinct G(2)/M checkpoints are induced by ionizing irradiation. *Molecular and cellular biology*. 2002;22(4):1049-59.
34.

Yarden RI, Pardo-Reoyo S, Sgagias M, Cowan KH, Brody LC. BRCA1 regulates the G2/M checkpoint by activating Chk1 kinase upon DNA damage. *Nat Genet*. 2002;30(3):285-9.
35.

Lindqvist A, Rodriguez-Bravo V, Medema RH. The decision to enter mitosis: feedback and redundancy in the mitotic entry network. *The Journal of cell biology*. 2009;185(2):193-202.
36.

Nasmyth K. Disseminating the genome: joining, resolving, and separating sister chromatids during mitosis and meiosis. *Annu Rev Genet*. 2001;35:673-745.
37.

Nigg EA. Mitotic kinases as regulators of cell division and its checkpoints. *Nat Rev Mol Cell Biol*. 2001;2(1):21-32.
38.

Coschi CH, Martens AL, Ritchie K, Francis SM, Chakrabarti S, Berube NG, et al. Mitotic chromosome condensation mediated by the retinoblastoma protein is tumor-suppressive. *Genes Dev*. 2010;24(13):1351-63.
39.

Peters JM, Tedeschi A, Schmitz J. The cohesin complex and its roles in chromosome biology. *Genes Dev*. 2008;22(22):3089-114.
40.

Nakajima M, Kumada K, Hatakeyama K, Noda T, Peters JM, Hirota T. The complete removal of cohesin from chromosome arms depends on separase. *Journal of cell science*. 2007;120(Pt 23):4188-96.
41.

Buheitel J, Stemmann O. Prophase pathway-dependent removal of cohesin from human chromosomes requires opening of the Smc3-Scc1 gate. *The EMBO journal*. 2013;32(5):666-76.
42.

Waizenegger IC, Hauf S, Meinke A, Peters JM. Two distinct pathways remove

mammalian cohesin from chromosome arms in prophase and from centromeres in anaphase. *Cell*. 2000;103(3):399-410.
43.

Job D, Valiron O, Oakley B. Microtubule nucleation. *Curr Opin Cell Biol*. 2003;15(1):111-7.
44.

Nigg EA, Stearns T. The centrosome cycle: Centriole biogenesis, duplication and inherent asymmetries. *Nat Cell Biol*. 2011;13(10):1154-60.
45.

Heald R, Khodjakov A. Thirty years of search and capture: The complex simplicity of mitotic spindle assembly. *The Journal of cell biology*. 2015;211(6):1103-11.
46.

Mimori-Kiyosue Y, Tsukita S. "Search-and-capture" of microtubules through plus-end-binding proteins (+TIPs). *J Biochem*. 2003;134(3):321-6.
47.

Gatlin JC, Bloom K. Microtubule motors in eukaryotic spindle assembly and maintenance. *Semin Cell Dev Biol*. 2010;21(3):248-54.
48.

O'Connell CB, Khodjakov AL. Cooperative mechanisms of mitotic spindle formation. *Journal of cell science*. 2007;120(Pt 10):1717-22.
49.

Kapoor TM, Lampson MA, Hergert P, Cameron L, Cimini D, Salmon ED, et al. Chromosomes can congress to the metaphase plate before biorientation. *Science*. 2006;311(5759):388-91.
50.

Tanaka TU. Bi-orienting chromosomes: acrobatics on the mitotic spindle. *Chromosoma*. 2008;117(6):521-33.
51.

de Gramont A, Cohen-Fix O. The many phases of anaphase. *Trends Biochem Sci*. 2005;30(10):559-68.
52.

Hayashi T, Sano T, Kutsuna N, Kumagai-Sano F, Hasezawa S. Contribution of anaphase B to chromosome separation in higher plant cells estimated by image processing. *Plant Cell Physiol*. 2007;48(10):1509-13.
53.

Mitchison TJ, Salmon ED. Mitosis: a history of division. *Nat Cell Biol*. 2001;3(1):E17-21.
54.

Brust-Mascher I, Civelekoglu-Scholey G, Scholey JM. Mechanism for

- Anaphase B: Evaluation of "Slide-and-Cluster" versus "Slide-and-Flux-or-Elongate" Models. *Biophys J*. 2015;108(8):2007-18.
55.
- Cheeseman IM, Desai A. Molecular architecture of the kinetochore-microtubule interface. *Nat Rev Mol Cell Biol*. 2008;9(1):33-46.
56.
- Van Hooser AA, Heald R. Kinetochore function: the complications of becoming attached. *Current biology : CB*. 2001;11(21):R855-7.
57.
- Cheeseman IM. The kinetochore. *Cold Spring Harb Perspect Biol*. 2014;6(7):a015826.
58.
- Yamagishi Y, Sakuno T, Goto Y, Watanabe Y. Kinetochore composition and its function: lessons from yeasts. *FEMS Microbiol Rev*. 2014;38(2):185-200.
59.
- Foltz DR, Jansen LE, Black BE, Bailey AO, Yates JR, 3rd, Cleveland DW. The human CENP-A centromeric nucleosome-associated complex. *Nat Cell Biol*. 2006;8(5):458-69.
60.
- Okada M, Cheeseman IM, Hori T, Okawa K, McLeod IX, Yates JR, 3rd, et al. The CENP-H-I complex is required for the efficient incorporation of newly synthesized CENP-A into centromeres. *Nat Cell Biol*. 2006;8(5):446-57.
61.
- Westermann S, Drubin DG, Barnes G. Structures and functions of yeast kinetochore complexes. *Annu Rev Biochem*. 2007;76:563-91.
62.
- Johnson MK, Wise DA. Distribution of kinetochore fragments during mitosis with unreplicated genomes. *Cytoskeleton (Hoboken)*. 2010;67(3):172-7.
63.
- Santaguida S, Musacchio A. The life and miracles of kinetochores. *The EMBO journal*. 2009;28(17):2511-31.
64.
- Chen RH. Phosphorylation and activation of Bub1 on unattached chromosomes facilitate the spindle checkpoint. *The EMBO journal*. 2004;23(15):3113-21.
65.
- Biggins S, Walczak CE. Captivating capture: how microtubules attach to kinetochores. *Current biology : CB*. 2003;13(11):R449-60.
66.

- Cleveland DW, Mao Y, Sullivan KF. Centromeres and kinetochores: from epigenetics to mitotic checkpoint signaling. *Cell*. 2003;112(4):407-21. 67.
- McEwen BF, Dong Y, VandenBeldt KJ. Using electron microscopy to understand functional mechanisms of chromosome alignment on the mitotic spindle. *Methods Cell Biol*. 2007;79:259-93. 68.
- Petrovic A, Pasqualato S, Dube P, Krenn V, Santaguida S, Cittaro D, et al. The MIS12 complex is a protein interaction hub for outer kinetochore assembly. *The Journal of cell biology*. 2010;190(5):835-52. 69.
- Maiato H, DeLuca J, Salmon ED, Earnshaw WC. The dynamic kinetochore-microtubule interface. *Journal of cell science*. 2004;117(Pt 23):5461-77. 70.
- Varma D, Salmon ED. The KMN protein network--chief conductors of the kinetochore orchestra. *Journal of cell science*. 2012;125(Pt 24):5927-36. 71.
- Suzuki A, Badger BL, Wan X, DeLuca JG, Salmon ED. The architecture of CCAN proteins creates a structural integrity to resist spindle forces and achieve proper Intrakinetochore stretch. *Dev Cell*. 2014;30(6):717-30. 72.
- Rago F, Gascoigne KE, Cheeseman IM. Distinct organization and regulation of the outer kinetochore KMN network downstream of CENP-C and CENP-T. *Current biology : CB*. 2015;25(5):671-7. 73.
- Ciferri C, Pasqualato S, Screpanti E, Varetto G, Santaguida S, Dos Reis G, et al. Implications for kinetochore-microtubule attachment from the structure of an engineered Ndc80 complex. *Cell*. 2008;133(3):427-39. 74.
- Cheeseman IM, Chappie JS, Wilson-Kubalek EM, Desai A. The conserved KMN network constitutes the core microtubule-binding site of the kinetochore. *Cell*. 2006;127(5):983-97. 75.
- Martin-Lluesma S, Stucke VM, Nigg EA. Role of Hec1 in spindle checkpoint signaling and kinetochore recruitment of Mad1/Mad2. *Science*. 2002;297(5590):2267-70. 76.
- McClelland ML, Gardner RD, Kallio MJ, Daum JR, Gorbsky GJ, Burke DJ, et al. The highly conserved Ndc80 complex is required for kinetochore assembly, chromosome congression, and spindle checkpoint activity. *Genes Dev*. 2003;17(1):101-14.

77.

Stucke VM, Baumann C, Nigg EA. Kinetochore localization and microtubule interaction of the human spindle checkpoint kinase Mps1. *Chromosoma*. 2004;113(1):1-15.

78.

Burke DJ, Stukenberg PT. Linking kinetochore-microtubule binding to the spindle checkpoint. *Dev Cell*. 2008;14(4):474-9.

79.

Kiyomitsu T, Obuse C, Yanagida M. Human Blinkin/AF15q14 is required for chromosome alignment and the mitotic checkpoint through direct interaction with Bub1 and BubR1. *Dev Cell*. 2007;13(5):663-76.

80.

Rosenberg JS, Cross FR, Funabiki H. KNL1/Spc105 recruits PP1 to silence the spindle assembly checkpoint. *Current biology : CB*. 2011;21(11):942-7.

81.

Meadows JC, Shepperd LA, Vanoosthuyse V, Lancaster TC, Sochaj AM, Buttrick GJ, et al. Spindle checkpoint silencing requires association of PP1 to both Spc7 and kinesin-8 motors. *Dev Cell*. 2011;20(6):739-50.

82.

Espeut J, Cheerambathur DK, Krenning L, Oegema K, Desai A. Microtubule binding by KNL-1 contributes to spindle checkpoint silencing at the kinetochore. *The Journal of cell biology*. 2012;196(4):469-82.

83.

Vleugel M, Tromer E, Omerzu M, Groenewold V, Nijenhuis W, Snel B, et al. Arrayed BUB recruitment modules in the kinetochore scaffold KNL1 promote accurate chromosome segregation. *The Journal of cell biology*.

2013;203(6):943-55.

84.

Yamagishi Y, Yang CH, Tanno Y, Watanabe Y. MPS1/Mph1 phosphorylates the kinetochore protein KNL1/Spc7 to recruit SAC components. *Nat Cell Biol*. 2012;14(7):746-52.

85.

Primorac I, Weir JR, Chirolì E, Gross F, Hoffmann I, van Gerwen S, et al. Bub3 reads phosphorylated MELT repeats to promote spindle assembly checkpoint signaling. *Elife*. 2013;2:e01030.

86.

Zhang G, Lischetti T, Nilsson J. A minimal number of MELT repeats supports all the functions of KNL1 in chromosome segregation. *Journal of cell science*. 2014;127(Pt 4):871-84.

87.

London N, Ceto S, Ranish JA, Biggins S. Phosphoregulation of Spc105 by

Mps1 and PP1 regulates Bub1 localization to kinetochores. *Current biology : CB.* 2012;22(10):900-6.
88.

Musacchio A. The Molecular Biology of Spindle Assembly Checkpoint Signaling Dynamics. *Current biology : CB.* 2015;25(20):R1002-18.
89.

Lara-Gonzalez P, Westhorpe FG, Taylor SS. The spindle assembly checkpoint. *Current biology : CB.* 2012;22(22):R966-80.
90.

Foley EA, Kapoor TM. Microtubule attachment and spindle assembly checkpoint signalling at the kinetochore. *Nat Rev Mol Cell Biol.* 2013;14(1):25-37.
91.

Hauf S. The spindle assembly checkpoint: progress and persistent puzzles. *Biochem Soc Trans.* 2013;41(6):1755-60.
92.

Musacchio A, Salmon ED. The spindle-assembly checkpoint in space and time. *Nat Rev Mol Cell Biol.* 2007;8(5):379-93.
93.

Tanaka TU. Kinetochore-microtubule interactions: steps towards bi-orientation. *The EMBO journal.* 2010;29(24):4070-82.
94.

Tanaka TU, Clayton L, Natsume T. Three wise centromere functions: see no error, hear no break, speak no delay. *EMBO reports.* 2013;14(12):1073-83.
95.

Cimini D, Cameron LA, Salmon ED. Anaphase spindle mechanics prevent mis-segregation of merotelically oriented chromosomes. *Current biology : CB.* 2004;14(23):2149-55.
96.

Gregan J, Polakova S, Zhang L, Tolic-Norrelykke IM, Cimini D. Merotelic kinetochore attachment: causes and effects. *Trends in cell biology.* 2011;21(6):374-81.
97.

Tanaka TU, Stark MJ, Tanaka K. Kinetochore capture and bi-orientation on the mitotic spindle. *Nat Rev Mol Cell Biol.* 2005;6(12):929-42.
98.

Akiyoshi B, Sarangapani KK, Powers AF, Nelson CR, Reichow SL, Arellano-Santoyo H, et al. Tension directly stabilizes reconstituted kinetochore-microtubule attachments. *Nature.* 2010;468(7323):576-9.
99.

Zhou J, Yao J, Joshi HC. Attachment and tension in the spindle assembly checkpoint. *Journal of cell science*. 2002;115(Pt 18):3547-55.
100.

Rieder CL, Cole RW, Khodjakov A, Sluder G. The checkpoint delaying anaphase in response to chromosome monoorientation is mediated by an inhibitory signal produced by unattached kinetochores. *The Journal of cell biology*. 1995;130(4):941-8.
101.

Li X, Nicklas RB. Mitotic forces control a cell-cycle checkpoint. *Nature*. 1995;373(6515):630-2.
102.

King JM, Nicklas RB. Tension on chromosomes increases the number of kinetochore microtubules but only within limits. *Journal of cell science*. 2000;113 Pt 21:3815-23.
103.

Weaver BA, Bonday ZQ, Putkey FR, Kops GJ, Silk AD, Cleveland DW. Centromere-associated protein-E is essential for the mammalian mitotic checkpoint to prevent aneuploidy due to single chromosome loss. *The Journal of cell biology*. 2003;162(4):551-63.
104.

Collin P, Nashchekina O, Walker R, Pines J. The spindle assembly checkpoint works like a rheostat rather than a toggle switch. *Nat Cell Biol*. 2013;15(11):1378-85.
105.

Dick AE, Gerlich DW. Kinetic framework of spindle assembly checkpoint signalling. *Nat Cell Biol*. 2013;15(11):1370-7.
106.

Wild T, Larsen MS, Narita T, Schou J, Nilsson J, Choudhary C. The Spindle Assembly Checkpoint Is Not Essential for Viability of Human Cells with Genetically Lowered APC/C Activity. *Cell Rep*. 2016;14(8):1829-40.
107.

Li M, Zhang P. The function of APC/CCdh1 in cell cycle and beyond. *Cell Div*. 2009;4:2.
108.

Izawa D, Pines J. The mitotic checkpoint complex binds a second CDC20 to inhibit active APC/C. *Nature*. 2015;517(7536):631-4.
109.

Galli M, Morgan DO. Cell Size Determines the Strength of the Spindle Assembly Checkpoint during Embryonic Development. *Dev Cell*. 2016;36(3):344-52.
110.

Hoyt MA, Totis L, Roberts BT. *S. cerevisiae* genes required for cell cycle arrest in response to loss of microtubule function. *Cell*. 1991;66(3):507-17. 111.

Li R, Murray AW. Feedback control of mitosis in budding yeast. *Cell*. 1991;66(3):519-31. 112.

Weiss E, Winey M. The *Saccharomyces cerevisiae* spindle pole body duplication gene MPS1 is part of a mitotic checkpoint. *The Journal of cell biology*. 1996;132(1-2):111-23. 113.

Taylor SS, Ha E, McKeon F. The human homologue of Bub3 is required for kinetochore localization of Bub1 and a Mad3/Bub1-related protein kinase. *The Journal of cell biology*. 1998;142(1):1-11. 114.

Hardwick KG, Murray AW. Mad1p, a phosphoprotein component of the spindle assembly checkpoint in budding yeast. *The Journal of cell biology*. 1995;131(3):709-20. 115.

Baker DJ, Jin F, Jeganathan KB, van Deursen JM. Whole chromosome instability caused by Bub1 insufficiency drives tumorigenesis through tumor suppressor gene loss of heterozygosity. *Cancer Cell*. 2009;16(6):475-86. 116.

Barr FA, Sillje HH, Nigg EA. Polo-like kinases and the orchestration of cell division. *Nat Rev Mol Cell Biol*. 2004;5(6):429-40. 117.

Llamazares S, Moreira A, Tavares A, Girdham C, Spruce BA, Gonzalez C, et al. polo encodes a protein kinase homolog required for mitosis in *Drosophila*. *Genes Dev*. 1991;5(12A):2153-65. 118.

Chan GK, Jablonski SA, Starr DA, Goldberg ML, Yen TJ. Human Zw10 and ROD are mitotic checkpoint proteins that bind to kinetochores. *Nat Cell Biol*. 2000;2(12):944-7. 119.

Bischoff JR, Anderson L, Zhu Y, Mossie K, Ng L, Souza B, et al. A homologue of *Drosophila* aurora kinase is oncogenic and amplified in human colorectal cancers. *The EMBO journal*. 1998;17(11):3052-65. 120.

Yen TJ, Compton DA, Wise D, Zinkowski RP, Brinkley BR, Earnshaw WC, et al. CENP-E, a novel human centromere-associated protein required for progression from metaphase to anaphase. *The EMBO journal*. 1991;10(5):1245-54.

121.

Howell BJ, Moree B, Farrar EM, Stewart S, Fang G, Salmon ED. Spindle checkpoint protein dynamics at kinetochores in living cells. *Current biology* : CB. 2004;14(11):953-64.

122.

Sudakin V, Chan GK, Yen TJ. Checkpoint inhibition of the APC/C in HeLa cells is mediated by a complex of BUBR1, BUB3, CDC20, and MAD2. *The Journal of cell biology*. 2001;154(5):925-36.

123.

Kulukian A, Han JS, Cleveland DW. Unattached kinetochores catalyze production of an anaphase inhibitor that requires a Mad2 template to prime Cdc20 for BubR1 binding. *Dev Cell*. 2009;16(1):105-17.

124.

Chao WC, Kulkarni K, Zhang Z, Kong EH, Barford D. Structure of the mitotic checkpoint complex. *Nature*. 2012;484(7393):208-13.

125.

Fang G. Checkpoint protein BubR1 acts synergistically with Mad2 to inhibit anaphase-promoting complex. *Mol Biol Cell*. 2002;13(3):755-66.

126.

Peters JM. The anaphase-promoting complex: proteolysis in mitosis and beyond. *Molecular cell*. 2002;9(5):931-43.

127.

De Antoni A, Pearson CG, Cimini D, Canman JC, Sala V, Nezi L, et al. The Mad1/Mad2 complex as a template for Mad2 activation in the spindle assembly checkpoint. *Current biology* : CB. 2005;15(3):214-25.

128.

Luo X, Yu H. Protein metamorphosis: the two-state behavior of Mad2. *Structure*. 2008;16(11):1616-25.

129.

Jia L, Kim S, Yu H. Tracking spindle checkpoint signals from kinetochores to APC/C. *Trends Biochem Sci*. 2013;38(6):302-11.

130.

Luo X, Tang Z, Xia G, Wassmann K, Matsumoto T, Rizo J, et al. The Mad2 spindle checkpoint protein has two distinct natively folded states. *Nat Struct Mol Biol*. 2004;11(4):338-45.

131.

Yang M, Li B, Liu CJ, Tomchick DR, Machius M, Rizo J, et al. Insights into mad2 regulation in the spindle checkpoint revealed by the crystal structure of the symmetric mad2 dimer. *PLoS Biol*. 2008;6(3):e50.

132.

Luo X, Tang Z, Rizo J, Yu H. The Mad2 spindle checkpoint protein undergoes similar major conformational changes upon binding to either Mad1 or Cdc20. *Molecular cell*. 2002;9(1):59-71.

133.

Sironi L, Mapelli M, Knapp S, De Antoni A, Jeang KT, Musacchio A. Crystal structure of the tetrameric Mad1-Mad2 core complex: implications of a 'safety belt' binding mechanism for the spindle checkpoint. *The EMBO journal*. 2002;21(10):2496-506.

134.

Izawa D, Pines J. Mad2 and the APC/C compete for the same site on Cdc20 to ensure proper chromosome segregation. *The Journal of cell biology*. 2012;199(1):27-37.

135.

Hara M, Ozkan E, Sun H, Yu H, Luo X. Structure of an intermediate conformer of the spindle checkpoint protein Mad2. *Proc Natl Acad Sci U S A*. 2015;112(36):11252-7.

136.

Simonetta M, Manzoni R, Mosca R, Mapelli M, Massimiliano L, Vink M, et al. The influence of catalysis on mad2 activation dynamics. *PLoS Biol*. 2009;7(1):e10.

137.

Mapelli M, Filipp FV, Rancati G, Massimiliano L, Nezi L, Stier G, et al. Determinants of conformational dimerization of Mad2 and its inhibition by p31comet. *The EMBO journal*. 2006;25(6):1273-84.

138.

Tipton AR, Wang K, Link L, Bellizzi JJ, Huang H, Yen T, et al. BUBR1 and closed MAD2 (C-MAD2) interact directly to assemble a functional mitotic checkpoint complex. *J Biol Chem*. 2011;286(24):21173-9.

139.

Mariani L, Chiroli E, Nezi L, Muller H, Piatti S, Musacchio A, et al. Role of the Mad2 dimerization interface in the spindle assembly checkpoint independent of kinetochores. *Current biology : CB*. 2012;22(20):1900-8.

140.

Maciejowski J, George KA, Terret ME, Zhang C, Shokat KM, Jallepalli PV. Mps1 directs the assembly of Cdc20 inhibitory complexes during interphase and mitosis to control M phase timing and spindle checkpoint signaling. *The Journal of cell biology*. 2010;190(1):89-100.

141.

Hewitt L, Tighe A, Santaguida S, White AM, Jones CD, Musacchio A, et al. Sustained Mps1 activity is required in mitosis to recruit O-Mad2 to the Mad1-C-Mad2 core complex. *The Journal of cell biology*. 2010;190(1):25-34.

142.

Tipton AR, Ji W, Sturt-Gillespie B, Bekier ME, 2nd, Wang K, Taylor WR, et al. Monopolar spindle 1 (MPS1) kinase promotes production of closed MAD2 (C-MAD2) conformer and assembly of the mitotic checkpoint complex. *J Biol Chem*. 2013;288(49):35149-58.

143.

Santaguida S, Tighe A, D'Alise AM, Taylor SS, Musacchio A. Dissecting the role of MPS1 in chromosome biorientation and the spindle checkpoint through the small molecule inhibitor reversine. *The Journal of cell biology*. 2010;190(1):73-87.

144.

London N, Biggins S. Mad1 kinetochore recruitment by Mps1-mediated phosphorylation of Bub1 signals the spindle checkpoint. *Genes Dev*. 2014;28(2):140-52.

145.

Sharp-Baker H, Chen RH. Spindle checkpoint protein Bub1 is required for kinetochore localization of Mad1, Mad2, Bub3, and CENP-E, independently of its kinase activity. *The Journal of cell biology*. 2001;153(6):1239-50.

146.

Johnson VL, Scott MI, Holt SV, Hussein D, Taylor SS. Bub1 is required for kinetochore localization of BubR1, Cenp-E, Cenp-F and Mad2, and chromosome congression. *Journal of cell science*. 2004;117(Pt 8):1577-89.

147.

Chang L, Zhang Z, Yang J, McLaughlin SH, Barford D. Molecular architecture and mechanism of the anaphase-promoting complex. *Nature*. 2014;513(7518):388-93.

148.

Moyle MW, Kim T, Hattersley N, Espeut J, Cheerambathur DK, Oegema K, et al. A Bub1-Mad1 interaction targets the Mad1-Mad2 complex to unattached kinetochores to initiate the spindle checkpoint. *The Journal of cell biology*. 2014;204(5):647-57.

149.

Seeley TW, Wang L, Zhen JY. Phosphorylation of human MAD1 by the BUB1 kinase in vitro. *Biochem Biophys Res Commun*. 1999;257(2):589-95.

150.

Brady DM, Hardwick KG. Complex formation between Mad1p, Bub1p and Bub3p is crucial for spindle checkpoint function. *Current biology : CB*. 2000;10(11):675-8.

151.

Baron AP, von Schubert C, Cubizolles F, Siemeister G, Hitchcock M, Mengel A, et al. Probing the catalytic functions of Bub1 kinase using the small molecule inhibitors BAY-320 and BAY-524. *Elife*. 2016;5.

152.

- Yu H. Cdc20: a WD40 activator for a cell cycle degradation machine. *Molecular cell*. 2007;27(1):3-16.
153.
- Kallio MJ, Beardmore VA, Weinstein J, Gorbsky GJ. Rapid microtubule-independent dynamics of Cdc20 at kinetochores and centrosomes in mammalian cells. *The Journal of cell biology*. 2002;158(5):841-7.
154.
- Benanti JA, Toczyski DP. Cdc20, an activator at last. *Molecular cell*. 2008;32(4):460-1.
155.
- Reis A, Levasseur M, Chang HY, Elliott DJ, Jones KT. The CRY box: a second APC^{Cdh1}-dependent degron in mammalian cdc20. *EMBO reports*. 2006;7(10):1040-5.
156.
- Pfleger CM, Kirschner MW. The KEN box: an APC recognition signal distinct from the D box targeted by Cdh1. *Genes Dev*. 2000;14(6):655-65.
157.
- Ravid T, Hochstrasser M. Diversity of degradation signals in the ubiquitin-proteasome system. *Nat Rev Mol Cell Biol*. 2008;9(9):679-90.
158.
- Fang G, Yu H, Kirschner MW. The checkpoint protein MAD2 and the mitotic regulator CDC20 form a ternary complex with the anaphase-promoting complex to control anaphase initiation. *Genes Dev*. 1998;12(12):1871-83.
159.
- Peters JM. The anaphase promoting complex/cyclosome: a machine designed to destroy. *Nat Rev Mol Cell Biol*. 2006;7(9):644-56.
160.
- Lara-Gonzalez P, Scott MI, Diez M, Sen O, Taylor SS. BubR1 blocks substrate recruitment to the APC/C in a KEN-box-dependent manner. *Journal of cell science*. 2011;124(Pt 24):4332-45.
161.
- Diaz-Martinez LA, Tian W, Li B, Warrington R, Jia L, Brautigam CA, et al. The Cdc20-binding Phe box of the spindle checkpoint protein BubR1 maintains the mitotic checkpoint complex during mitosis. *J Biol Chem*. 2015;290(4):2431-43.
162.
- Kim SH, Lin DP, Matsumoto S, Kitazono A, Matsumoto T. Fission yeast Slp1: an effector of the Mad2-dependent spindle checkpoint. *Science*. 1998;279(5353):1045-7.
163.
- Zhang Y, Lees E. Identification of an overlapping binding domain on Cdc20

for Mad2 and anaphase-promoting complex: model for spindle checkpoint regulation. *Molecular and cellular biology*. 2001;21(15):5190-9.
164.

Luo X, Fang G, Coldiron M, Lin Y, Yu H, Kirschner MW, et al. Structure of the Mad2 spindle assembly checkpoint protein and its interaction with Cdc20. *Nat Struct Biol*. 2000;7(3):224-9.
165.

Tian W, Li B, Warrington R, Tomchick DR, Yu H, Luo X. Structural analysis of human Cdc20 supports multisite degron recognition by APC/C. *Proc Natl Acad Sci U S A*. 2012;109(45):18419-24.
166.

Davenport J, Harris LD, Goorha R. Spindle checkpoint function requires Mad2-dependent Cdc20 binding to the Mad3 homology domain of BubR1. *Exp Cell Res*. 2006;312(10):1831-42.
167.

Tipton AR, Tipton M, Yen T, Liu ST. Closed MAD2 (C-MAD2) is selectively incorporated into the mitotic checkpoint complex (MCC). *Cell cycle*. 2011;10(21):3740-50.
168.

Han JS, Holland AJ, Fachinetti D, Kulukian A, Cetin B, Cleveland DW. Catalytic assembly of the mitotic checkpoint inhibitor BubR1-Cdc20 by a Mad2-induced functional switch in Cdc20. *Molecular cell*. 2013;51(1):92-104.
169.

Caldas GV, Deluca JG. Mad2 "opens" Cdc20 for BubR1 binding. *Molecular cell*. 2013;51(1):3-4.
170.

Tang Z, Bharadwaj R, Li B, Yu H. Mad2-Independent inhibition of APCCdc20 by the mitotic checkpoint protein BubR1. *Dev Cell*. 2001;1(2):227-37.
171.

King EM, van der Sar SJ, Hardwick KG. Mad3 KEN boxes mediate both Cdc20 and Mad3 turnover, and are critical for the spindle checkpoint. *PLoS one*. 2007;2(4):e342.
172.

Sczaniecka M, Feoktistova A, May KM, Chen JS, Blyth J, Gould KL, et al. The spindle checkpoint functions of Mad3 and Mad2 depend on a Mad3 KEN box-mediated interaction with Cdc20-anaphase-promoting complex (APC/C). *J Biol Chem*. 2008;283(34):23039-47.
173.

Primorac I, Musacchio A. Panta rhei: the APC/C at steady state. *The Journal of cell biology*. 2013;201(2):177-89.
174.

Elowe S, Dulla K, Uldschmid A, Li X, Dou Z, Nigg EA. Uncoupling of the spindle-checkpoint and chromosome-congression functions of BubR1. *Journal of cell science*. 2010;123(Pt 1):84-94.
175.

Burton JL, Solomon MJ. Mad3p, a pseudosubstrate inhibitor of APCCdc20 in the spindle assembly checkpoint. *Genes Dev*. 2007;21(6):655-67.
176.

Lischetti T, Zhang G, Sedgwick GG, Bolanos-Garcia VM, Nilsson J. The internal Cdc20 binding site in BubR1 facilitates both spindle assembly checkpoint signalling and silencing. *Nat Commun*. 2014;5:5563.
177.

Di Fiore B, Davey NE, Hagting A, Izawa D, Mansfeld J, Gibson TJ, et al. The ABBA motif binds APC/C activators and is shared by APC/C substrates and regulators. *Dev Cell*. 2015;32(3):358-72.
178.

Tauchman EC, Boehm FJ, DeLuca JG. Stable kinetochore-microtubule attachment is sufficient to silence the spindle assembly checkpoint in human cells. *Nat Commun*. 2015;6:10036.
179.

Funabiki H, Wynne DJ. Making an effective switch at the kinetochore by phosphorylation and dephosphorylation. *Chromosoma*. 2013;122(3):135-58.
180.

Nijenhuis W, Vallardi G, Teixeira A, Kops GJ, Saurin AT. Negative feedback at kinetochores underlies a responsive spindle checkpoint signal. *Nat Cell Biol*. 2014;16(12):1257-64.
181.

Espert A, Uluocak P, Bastos RN, Mangat D, Graab P, Gruneberg U. PP2A-B56 opposes Mps1 phosphorylation of Knl1 and thereby promotes spindle assembly checkpoint silencing. *The Journal of cell biology*. 2014;206(7):833-42.
182.

Vanoosthuyse V, Hardwick KG. A novel protein phosphatase 1-dependent spindle checkpoint silencing mechanism. *Current biology : CB*. 2009;19(14):1176-81.
183.

Pinsky BA, Nelson CR, Biggins S. Protein phosphatase 1 regulates exit from the spindle checkpoint in budding yeast. *Current biology : CB*. 2009;19(14):1182-7.
184.

Liu D, Vleugel M, Backer CB, Hori T, Fukagawa T, Cheeseman IM, et al. Regulated targeting of protein phosphatase 1 to the outer kinetochore by

KNL1 opposes Aurora B kinase. *The Journal of cell biology*. 2010;188(6):809-20.
185.

Ghongane P, Kapanidou M, Asghar A, Elowe S, Bolanos-Garcia VM. The dynamic protein Knl1 - a kinetochore rendezvous. *Journal of cell science*. 2014;127(Pt 16):3415-23.
186.

Sivakumar S, Janczyk PL, Qu Q, Brautigam CA, Stukenberg PT, Yu H, et al. The human SKA complex drives the metaphase-anaphase cell cycle transition by recruiting protein phosphatase 1 to kinetochores. *Elife*. 2016;5.
187.

Bokros M, Gravenmier C, Jin F, Richmond D, Wang Y. Fin1-PP1 Helps Clear Spindle Assembly Checkpoint Protein Bub1 from Kinetochores in Anaphase. *Cell Rep*. 2016;14(5):1074-85.
188.

Suijkerbuijk SJ, Vleugel M, Teixeira A, Kops GJ. Integration of kinase and phosphatase activities by BUBR1 ensures formation of stable kinetochore-microtubule attachments. *Dev Cell*. 2012;23(4):745-55.
189.

Xu P, Raetz EA, Kitagawa M, Virshup DM, Lee SH. BUBR1 recruits PP2A via the B56 family of targeting subunits to promote chromosome congression. *Biol Open*. 2013;2(5):479-86.
190.

Kruse T, Zhang G, Larsen MS, Lischetti T, Streicher W, Kragh Nielsen T, et al. Direct binding between BubR1 and B56-PP2A phosphatase complexes regulate mitotic progression. *Journal of cell science*. 2013;126(Pt 5):1086-92.
191.

Shepherd LA, Meadows JC, Sochaj AM, Lancaster TC, Zou J, Buttrick GJ, et al. Phosphodependent recruitment of Bub1 and Bub3 to Spc7/KNL1 by Mph1 kinase maintains the spindle checkpoint. *Current biology : CB*. 2012;22(10):891-9.
192.

von Schubert C, Cubizolles F, Bracher JM, Sliedrecht T, Kops GJ, Nigg EA. Plk1 and Mps1 Cooperatively Regulate the Spindle Assembly Checkpoint in Human Cells. *Cell Rep*. 2015;12(1):66-78.
193.

Krenn V, Overlack K, Primorac I, van Gerwen S, Musacchio A. KI motifs of human Knl1 enhance assembly of comprehensive spindle checkpoint complexes around MELT repeats. *Current biology : CB*. 2014;24(1):29-39.
194.

Breit C, Bange T, Petrovic A, Weir JR, Muller F, Vogt D, et al. Role of Intrinsic

and Extrinsic Factors in the Regulation of the Mitotic Checkpoint Kinase Bub1. *PLoS one*. 2015;10(12):e0144673.
195.

Vallardi G, Saurin AT. Mitotic kinases and phosphatases cooperate to shape the right response. *Cell cycle*. 2015;14(6):795-6.
196.

Foley EA, Maldonado M, Kapoor TM. Formation of stable attachments between kinetochores and microtubules depends on the B56-PP2A phosphatase. *Nat Cell Biol*. 2011;13(10):1265-71.
197.

Chen RH, Waters JC, Salmon ED, Murray AW. Association of spindle assembly checkpoint component XMad2 with unattached kinetochores. *Science*. 1996;274(5285):242-6.
198.

Taylor SS, McKeon F. Kinetochores localization of murine Bub1 is required for normal mitotic timing and checkpoint response to spindle damage. *Cell*. 1997;89(5):727-35.
199.

Jablonski SA, Chan GK, Cooke CA, Earnshaw WC, Yen TJ. The hBUB1 and hBUBR1 kinases sequentially assemble onto kinetochores during prophase with hBUBR1 concentrating at the kinetochore plates in mitosis. *Chromosoma*. 1998;107(6-7):386-96.
200.

Chen RH, Shevchenko A, Mann M, Murray AW. Spindle checkpoint protein Xmad1 recruits Xmad2 to unattached kinetochores. *The Journal of cell biology*. 1998;143(2):283-95.
201.

Chan GK, Jablonski SA, Sudakin V, Hittle JC, Yen TJ. Human BUBR1 is a mitotic checkpoint kinase that monitors CENP-E functions at kinetochores and binds the cyclosome/APC. *The Journal of cell biology*. 1999;146(5):941-54.
202.

Silva PM, Reis RM, Bolanos-Garcia VM, Florindo C, Tavares AA, Bousbaa H. Dynein-dependent transport of spindle assembly checkpoint proteins off kinetochores toward spindle poles. *FEBS Lett*. 2014;588(17):3265-73.
203.

Wang Y, Jin F, Higgins R, McKnight K. The current view for the silencing of the spindle assembly checkpoint. *Cell cycle*. 2014;13(11):1694-701.
204.

Gill SR, Schroer TA, Szilak I, Steuer ER, Sheetz MP, Cleveland DW. Dynactin, a conserved, ubiquitously expressed component of an activator of vesicle motility mediated by cytoplasmic dynein. *The Journal of cell biology*. 1991;115(6):1639-50.

205.

Schroer TA, Sheetz MP. Two activators of microtubule-based vesicle transport. *The Journal of cell biology*. 1991;115(5):1309-18.

206.

Schroer TA. Dynactin. *Annu Rev Cell Dev Biol*. 2004;20:759-79.

207.

King SJ, Schroer TA. Dynactin increases the processivity of the cytoplasmic dynein motor. *Nat Cell Biol*. 2000;2(1):20-4.

208.

Karess R. Rod-Zw10-Zwilch: a key player in the spindle checkpoint. *Trends in cell biology*. 2005;15(7):386-92.

209.

Griffis ER, Stuurman N, Vale RD. Spindly, a novel protein essential for silencing the spindle assembly checkpoint, recruits dynein to the kinetochore. *The Journal of cell biology*. 2007;177(6):1005-15.

210.

Chan YW, Fava LL, Uldschmid A, Schmitz MH, Gerlich DW, Nigg EA, et al. Mitotic control of kinetochore-associated dynein and spindle orientation by human Spindly. *The Journal of cell biology*. 2009;185(5):859-74.

211.

Sivaram MV, Wadzinski TL, Redick SD, Manna T, Doxsey SJ. Dynein light intermediate chain 1 is required for progress through the spindle assembly checkpoint. *The EMBO journal*. 2009;28(7):902-14.

212.

Sacristan C, Kops GJ. Joined at the hip: kinetochores, microtubules, and spindle assembly checkpoint signaling. *Trends in cell biology*. 2015;25(1):21-8.

213.

Howell BJ, McEwen BF, Canman JC, Hoffman DB, Farrar EM, Rieder CL, et al. Cytoplasmic dynein/dynactin drives kinetochore protein transport to the spindle poles and has a role in mitotic spindle checkpoint inactivation. *The Journal of cell biology*. 2001;155(7):1159-72.

214.

Gassmann R, Holland AJ, Varma D, Wan X, Civril F, Cleveland DW, et al. Removal of Spindly from microtubule-attached kinetochores controls spindle checkpoint silencing in human cells. *Genes Dev*. 2010;24(9):957-71.

215.

Raaijmakers JA, Tanenbaum ME, Medema RH. Systematic dissection of dynein regulators in mitosis. *The Journal of cell biology*. 2013;201(2):201-15.

216.

Barisic M, Sohm B, Mikolcevic P, Wandke C, Rauch V, Ringer T, et al. Spindly/CCDC99 is required for efficient chromosome congression and mitotic checkpoint regulation. *Mol Biol Cell*. 2010;21(12):1968-81.

217.

Habu T, Kim SH, Weinstein J, Matsumoto T. Identification of a MAD2-binding protein, CMT2, and its role in mitosis. *The EMBO journal*. 2002;21(23):6419-28.

218.

Habu T, Matsumoto T. p31(comet) inactivates the chemically induced Mad2-dependent spindle assembly checkpoint and leads to resistance to anti-mitotic drugs. *Springerplus*. 2013;2:562.

219.

Yang M, Li B, Tomchick DR, Machius M, Rizo J, Yu H, et al. p31comet blocks Mad2 activation through structural mimicry. *Cell*. 2007;131(4):744-55.

220.

Mo M, Arnaoutov A, Dasso M. Phosphorylation of *Xenopus* p31(comet) potentiates mitotic checkpoint exit. *Cell cycle*. 2015;14(24):3978-85.

221.

Vink M, Simonetta M, Transidico P, Ferrari K, Mapelli M, De Antoni A, et al. In vitro FRAP identifies the minimal requirements for Mad2 kinetochore dynamics. *Current biology : CB*. 2006;16(8):755-66.

222.

Westhorpe FG, Tighe A, Lara-Gonzalez P, Taylor SS. p31comet-mediated extraction of Mad2 from the MCC promotes efficient mitotic exit. *Journal of cell science*. 2011;124(Pt 22):3905-16.

223.

Hagan RS, Manak MS, Buch HK, Meier MG, Meraldi P, Shah JV, et al. p31(comet) acts to ensure timely spindle checkpoint silencing subsequent to kinetochore attachment. *Mol Biol Cell*. 2011;22(22):4236-46.

224.

Teichner A, Eytan E, Sitry-Shevah D, Miniowitz-Shemtov S, Dumin E, Gromis J, et al. p31comet Promotes disassembly of the mitotic checkpoint complex in an ATP-dependent process. *Proc Natl Acad Sci U S A*. 2011;108(8):3187-92.

225.

Miniowitz-Shemtov S, Eytan E, Ganoth D, Sitry-Shevah D, Dumin E, Hershko A. Role of phosphorylation of Cdc20 in p31(comet)-stimulated disassembly of the mitotic checkpoint complex. *Proc Natl Acad Sci U S A*.

2012;109(21):8056-60.

226.

Eytan E, Wang K, Miniowitz-Shemtov S, Sitry-Shevah D, Kaisari S, Yen TJ, et

al. Disassembly of mitotic checkpoint complexes by the joint action of the AAA-ATPase TRIP13 and p31(comet). *Proc Natl Acad Sci U S A*. 2014;111(33):12019-24. 227.

Ricke RM, van Deursen JM. Aurora B hyperactivation by Bub1 overexpression promotes chromosome missegregation. *Cell cycle*. 2011;10(21):3645-51. 228.

Holland AJ, Cleveland DW. Boveri revisited: chromosomal instability, aneuploidy and tumorigenesis. *Nat Rev Mol Cell Biol*. 2009;10(7):478-87. 229.

Williams BR, Amon A. Aneuploidy: cancer's fatal flaw? *Cancer Res*. 2009;69(13):5289-91. 230.

Schuyler SC, Wu YF, Kuan VJ. The Mad1-Mad2 balancing act--a damaged spindle checkpoint in chromosome instability and cancer. *Journal of cell science*. 2012;125(Pt 18):4197-206. 231.

Chi YH, Jeang KT. Aneuploidy and cancer. *J Cell Biochem*. 2007;102(3):531-8. 232.

Schvartzman JM, Sotillo R, Benezra R. Mitotic chromosomal instability and cancer: mouse modelling of the human disease. *Nat Rev Cancer*. 2010;10(2):102-15. 233.

Michel L, Diaz-Rodriguez E, Narayan G, Hernando E, Murty VV, Benezra R. Complete loss of the tumor suppressor MAD2 causes premature cyclin B degradation and mitotic failure in human somatic cells. *Proc Natl Acad Sci U S A*. 2004;101(13):4459-64. 234.

Dobles M, Liberal V, Scott ML, Benezra R, Sorger PK. Chromosome missegregation and apoptosis in mice lacking the mitotic checkpoint protein Mad2. *Cell*. 2000;101(6):635-45. 235.

Basu J, Bousbaa H, Logarinho E, Li Z, Williams BC, Lopes C, et al. Mutations in the essential spindle checkpoint gene *bub1* cause chromosome missegregation and fail to block apoptosis in *Drosophila*. *The Journal of cell biology*. 1999;146(1):13-28. 236.

Cahill DP, Lengauer C, Yu J, Riggins GJ, Willson JK, Markowitz SD, et al. Mutations of mitotic checkpoint genes in human cancers. *Nature*. 1998;392(6673):300-3.

237.

Hanks S, Coleman K, Reid S, Plaja A, Firth H, Fitzpatrick D, et al. Constitutional aneuploidy and cancer predisposition caused by biallelic mutations in BUB1B. *Nat Genet.* 2004;36(11):1159-61.

238.

Li Y, Benezra R. Identification of a human mitotic checkpoint gene: hsMAD2. *Science.* 1996;274(5285):246-8.

239.

Grabsch H, Takeno S, Parsons WJ, Pomjanski N, Boecking A, Gabbert HE, et al. Overexpression of the mitotic checkpoint genes BUB1, BUBR1, and BUB3 in gastric cancer--association with tumour cell proliferation. *J Pathol.* 2003;200(1):16-22.

240.

240.

Sotillo R, Hernando E, Diaz-Rodriguez E, Teruya-Feldstein J, Cordon-Cardo C, Lowe SW, et al. Mad2 overexpression promotes aneuploidy and tumorigenesis in mice. *Cancer Cell.* 2007;11(1):9-23.

241.

Iwanaga Y, Jeang KT. Expression of mitotic spindle checkpoint protein hsMAD1 correlates with cellular proliferation and is activated by a gain-of-function p53 mutant. *Cancer Res.* 2002;62(9):2618-24.

242.

Chun AC, Jin DY. Transcriptional regulation of mitotic checkpoint gene MAD1 by p53. *J Biol Chem.* 2003;278(39):37439-50.

243.

Daniel J, Coulter J, Woo JH, Wilsbach K, Gabrielson E. High levels of the Mps1 checkpoint protein are protective of aneuploidy in breast cancer cells. *Proc Natl Acad Sci U S A.* 2011;108(13):5384-9.

244.

Salvatore G, Nappi TC, Salerno P, Jiang Y, Garbi C, Ugolini C, et al. A cell proliferation and chromosomal instability signature in anaplastic thyroid carcinoma. *Cancer Res.* 2007;67(21):10148-58.

245.

Tannous BA, Kerami M, Van der Stoop PM, Kwiatkowski N, Wang J, Zhou W, et al. Effects of the selective MPS1 inhibitor MPS1-IN-3 on glioblastoma sensitivity to antimetabolic drugs. *J Natl Cancer Inst.* 2013;105(17):1322-31.

246.

Lens SM, Voest EE, Medema RH. Shared and separate functions of polo-like kinases and aurora kinases in cancer. *Nat Rev Cancer.* 2010;10(12):825-41.

247.

Janssen A, Kops GJ, Medema RH. Elevating the frequency of chromosome

mis-segregation as a strategy to kill tumor cells. *Proc Natl Acad Sci U S A*. 2009;106(45):19108-13.
248.

Nyati S, Schinske-Sebolt K, Pitchiaya S, Chekhovskiy K, Chator A, Chaudhry N, et al. The kinase activity of the Ser/Thr kinase BUB1 promotes TGF-beta signaling. *Sci Signal*. 2015;8(358):ra1.
249.

Brunet S, Pahlavan G, Taylor S, Maro B. Functionality of the spindle checkpoint during the first meiotic division of mammalian oocytes. *Reproduction*. 2003;126(4):443-50.
250.

Hached K, Xie SZ, Buffin E, Cladiere D, Rachez C, Sacras M, et al. Mps1 at kinetochores is essential for female mouse meiosis I. *Development*. 2011;138(11):2261-71.
251.

Wassmann K, Niault T, Maro B. Metaphase I arrest upon activation of the Mad2-dependent spindle checkpoint in mouse oocytes. *Current biology : CB*. 2003;13(18):1596-608.
252.

McGuinness BE, Anger M, Kouznetsova A, Gil-Bernabe AM, Helmhart W, Kudo NR, et al. Regulation of APC/C activity in oocytes by a Bub1-dependent spindle assembly checkpoint. *Current biology : CB*. 2009;19(5):369-80.
253.

Niault T, Hached K, Sotillo R, Sorger PK, Maro B, Benezra R, et al. Changing Mad2 levels affects chromosome segregation and spindle assembly checkpoint control in female mouse meiosis I. *PloS one*. 2007;2(11):e1165.
254.

Bernard P, Maure JF, Javerzat JP. Fission yeast Bub1 is essential in setting up the meiotic pattern of chromosome segregation. *Nat Cell Biol*. 2001;3(5):522-6.
255.

Leland S, Nagarajan P, Polyzos A, Thomas S, Samaan G, Donnell R, et al. Heterozygosity for a Bub1 mutation causes female-specific germ cell aneuploidy in mice. *Proc Natl Acad Sci U S A*. 2009;106(31):12776-81.
256.

Battaglia DE, Goodwin P, Klein NA, Soules MR. Influence of maternal age on meiotic spindle assembly in oocytes from naturally cycling women. *Hum Reprod*. 1996;11(10):2217-22.
257.

Steuerwald N, Cohen J, Herrera RJ, Sandalinas M, Brenner CA. Association between spindle assembly checkpoint expression and maternal age in human oocytes. *Mol Hum Reprod*. 2001;7(1):49-55.

258.

LeMaire-Adkins R, Radke K, Hunt PA. Lack of checkpoint control at the metaphase/anaphase transition: a mechanism of meiotic nondisjunction in mammalian females. *The Journal of cell biology*. 1997;139(7):1611-9.
259.

Wang X, Dai W. Shugoshin, a guardian for sister chromatid segregation. *Exp Cell Res*. 2005;310(1):1-9.
260.

Watanabe Y, Kitajima TS. Shugoshin protects cohesin complexes at centromeres. *Philos Trans R Soc Lond B Biol Sci*. 2005;360(1455):515-21, discussion 21.
261.

Kerrebrock AW, Miyazaki WY, Birnby D, Orr-Weaver TL. The *Drosophila* mei-S332 gene promotes sister-chromatid cohesion in meiosis following kinetochore differentiation. *Genetics*. 1992;130(4):827-41.
262.

Katis VL, Galova M, Rabitsch KP, Gregan J, Nasmyth K. Maintenance of cohesin at centromeres after meiosis I in budding yeast requires a kinetochore-associated protein related to MEI-S332. *Current biology : CB*. 2004;14(7):560-72.
263.

Marston AL, Tham WH, Shah H, Amon A. A genome-wide screen identifies genes required for centromeric cohesion. *Science*. 2004;303(5662):1367-70.
264.

Kitajima TS, Kawashima SA, Watanabe Y. The conserved kinetochore protein shugoshin protects centromeric cohesion during meiosis. *Nature*. 2004;427(6974):510-7.
265.

Gutierrez-Caballero C, Cebollero LR, Pendas AM. Shugoshins: from protectors of cohesion to versatile adaptors at the centromere. *Trends Genet*. 2012;28(7):351-60.
266.

Rabitsch KP, Gregan J, Schleiffer A, Javerzat JP, Eisenhaber F, Nasmyth K. Two fission yeast homologs of *Drosophila* Mei-S332 are required for chromosome segregation during meiosis I and II. *Current biology : CB*. 2004;14(4):287-301.
267.

Marston AL. Shugoshins: Tension-Sensitive Pericentromeric Adaptors Safeguarding Chromosome Segregation. *Molecular and cellular biology*. 2015;35(4):634-48.
268.

- McGuinness BE, Hirota T, Kudo NR, Peters JM, Nasmyth K. Shugoshin prevents dissociation of cohesin from centromeres during mitosis in vertebrate cells. *PLoS Biol.* 2005;3(3):e86.
269.
- Kitajima TS, Hauf S, Ohsugi M, Yamamoto T, Watanabe Y. Human Bub1 defines the persistent cohesion site along the mitotic chromosome by affecting Shugoshin localization. *Current biology : CB.* 2005;15(4):353-9.
270.
- Tang Z, Shu H, Qi W, Mahmood NA, Mumby MC, Yu H. PP2A is required for centromeric localization of Sgo1 and proper chromosome segregation. *Dev Cell.* 2006;10(5):575-85.
271.
- Tang Z, Sun Y, Harley SE, Zou H, Yu H. Human Bub1 protects centromeric sister-chromatid cohesion through Shugoshin during mitosis. *Proc Natl Acad Sci U S A.* 2004;101(52):18012-7.
272.
- Xu Z, Cetin B, Anger M, Cho US, Helmhart W, Nasmyth K, et al. Structure and function of the PP2A-shugoshin interaction. *Molecular cell.* 2009;35(4):426-41.
273.
- Liu H, Rankin S, Yu H. Phosphorylation-enabled binding of SGO1-PP2A to cohesin protects sororin and centromeric cohesion during mitosis. *Nat Cell Biol.* 2013;15(1):40-9.
274.
- Kawashima SA, Yamagishi Y, Honda T, Ishiguro K, Watanabe Y. Phosphorylation of H2A by Bub1 prevents chromosomal instability through localizing shugoshin. *Science.* 2010;327(5962):172-7.
275.
- Liu H, Jia L, Yu H. Phospho-H2A and cohesin specify distinct tension-regulated Sgo1 pools at kinetochores and inner centromeres. *Current biology : CB.* 2013;23(19):1927-33.
276.
- Karamysheva Z, Diaz-Martinez LA, Crow SE, Li B, Yu H. Multiple anaphase-promoting complex/cyclosome degrons mediate the degradation of human Sgo1. *J Biol Chem.* 2009;284(3):1772-80.
277.
- Fu G, Hua S, Ward T, Ding X, Yang Y, Guo Z, et al. D-box is required for the degradation of human Shugoshin and chromosome alignment. *Biochem Biophys Res Commun.* 2007;357(3):672-8.
278.
- Nasmyth K, Peters JM, Uhlmann F. Splitting the chromosome: cutting the ties that bind sister chromatids. *Science.* 2000;288(5470):1379-85.

279.

Gerton J. Chromosome cohesion: a cycle of holding together and falling apart. *PLoS Biol.* 2005;3(3):e94.

280.

Nasmyth K, Haering CH. Cohesin: its roles and mechanisms. *Annu Rev Genet.* 2009;43:525-58.

281.

Haering CH, Nasmyth K. Building and breaking bridges between sister chromatids. *Bioessays.* 2003;25(12):1178-91.

282.

Hauf S, Watanabe Y. Kinetochore orientation in mitosis and meiosis. *Cell.* 2004;119(3):317-27.

283.

Panizza S, Tanaka T, Hochwagen A, Eisenhaber F, Nasmyth K. Pds5 cooperates with cohesin in maintaining sister chromatid cohesion. *Current biology : CB.* 2000;10(24):1557-64.

284.

Rankin S, Ayad NG, Kirschner MW. Sororin, a substrate of the anaphase-promoting complex, is required for sister chromatid cohesion in vertebrates. *Molecular cell.* 2005;18(2):185-200.

285.

Nishiyama T, Ladurner R, Schmitz J, Kreidl E, Schleiffer A, Bhaskara V, et al. Sororin mediates sister chromatid cohesion by antagonizing Wapl. *Cell.* 2010;143(5):737-49.

286.

Zhang N, Pati D. Sororin is a master regulator of sister chromatid cohesion and separation. *Cell cycle.* 2012;11(11):2073-83.

287.

Shintomi K, Hirano T. Releasing cohesin from chromosome arms in early mitosis: opposing actions of Wapl-Pds5 and Sgo1. *Genes Dev.* 2009;23(18):2224-36.

288.

Nasmyth K. Cohesin: a catenase with separate entry and exit gates? *Nat Cell Biol.* 2011;13(10):1170-7.

289.

Gandhi R, Gillespie PJ, Hirano T. Human Wapl is a cohesin-binding protein that promotes sister-chromatid resolution in mitotic prophase. *Current biology : CB.* 2006;16(24):2406-17.

290.

Ouyang Z, Zheng G, Tomchick DR, Luo X, Yu H. Structural Basis and IP6

- Requirement for Pds5-Dependent Cohesin Dynamics. *Molecular cell*. 2016;62(2):248-59. 291.
- Ladurner R, Kreidl E, Ivanov MP, Ekker H, Idarraga-Amado MH, Busslinger GA, et al. Sororin actively maintains sister chromatid cohesion. *The EMBO journal*. 2016;35(6):635-53. 292.
- Kitajima TS, Sakuno T, Ishiguro K, Iemura S, Natsume T, Kawashima SA, et al. Shugoshin collaborates with protein phosphatase 2A to protect cohesin. *Nature*. 2006;441(7089):46-52. 293.
- Sumara I, Vorlaufer E, Gieffers C, Peters BH, Peters JM. Characterization of vertebrate cohesin complexes and their regulation in prophase. *The Journal of cell biology*. 2000;151(4):749-62. 294.
- Losada A, Hirano M, Hirano T. Cohesin release is required for sister chromatid resolution, but not for condensin-mediated compaction, at the onset of mitosis. *Genes Dev*. 2002;16(23):3004-16. 295.
- Hauf S, Waizenegger IC, Peters JM. Cohesin cleavage by separase required for anaphase and cytokinesis in human cells. *Science*. 2001;293(5533):1320-3. 296.
- Sumara I, Vorlaufer E, Stukenberg PT, Kelm O, Redemann N, Nigg EA, et al. The dissociation of cohesin from chromosomes in prophase is regulated by Polo-like kinase. *Molecular cell*. 2002;9(3):515-25. 297.
- Gimenez-Abian JF, Sumara I, Hirota T, Hauf S, Gerlich D, de la Torre C, et al. Regulation of sister chromatid cohesion between chromosome arms. *Current biology : CB*. 2004;14(13):1187-93. 298.
- Nishiyama T, Sykora MM, Huis in 't Veld PJ, Mechtler K, Peters JM. Aurora B and Cdk1 mediate Wapl activation and release of acetylated cohesin from chromosomes by phosphorylating Sororin. *Proc Natl Acad Sci U S A*. 2013;110(33):13404-9. 299.
- Hara K, Zheng G, Qu Q, Liu H, Ouyang Z, Chen Z, et al. Structure of cohesin subcomplex pinpoints direct shugoshin-Wapl antagonism in centromeric cohesion. *Nat Struct Mol Biol*. 2014;21(10):864-70. 300.
- Barbero JL. Cohesins: chromatin architects in chromosome segregation,

control of gene expression and much more. *Cell Mol Life Sci.* 2009;66(13):2025-35.
301.

Stern BM, Murray AW. Lack of tension at kinetochores activates the spindle checkpoint in budding yeast. *Current biology : CB.* 2001;11(18):1462-7.
302.

Kawashima SA, Tsukahara T, Langegger M, Hauf S, Kitajima TS, Watanabe Y. Shugoshin enables tension-generating attachment of kinetochores by loading Aurora to centromeres. *Genes Dev.* 2007;21(4):420-35.
303.

Vanoosthuysse V, Prykhozhiy S, Hardwick KG. Shugoshin 2 regulates localization of the chromosomal passenger proteins in fission yeast mitosis. *Mol Biol Cell.* 2007;18(5):1657-69.
304.

Huang H, Feng J, Famulski J, Rattner JB, Liu ST, Kao GD, et al. Tripin/hSgo2 recruits MCAK to the inner centromere to correct defective kinetochore attachments. *The Journal of cell biology.* 2007;177(3):413-24.
305.

Kiburz BM, Amon A, Marston AL. Shugoshin promotes sister kinetochore biorientation in *Saccharomyces cerevisiae*. *Mol Biol Cell.* 2008;19(3):1199-209.
306.

Storchova Z, Becker JS, Talarek N, Kogelsberger S, Pellman D. Bub1, Sgo1, and Mps1 mediate a distinct pathway for chromosome biorientation in budding yeast. *Mol Biol Cell.* 2011;22(9):1473-85.
307.

Indjeian VB, Stern BM, Murray AW. The centromeric protein Sgo1 is required to sense lack of tension on mitotic chromosomes. *Science.* 2005;307(5706):130-3.
308.

Nerusheva OO, Galander S, Fernius J, Kelly D, Marston AL. Tension-dependent removal of pericentromeric shugoshin is an indicator of sister chromosome biorientation. *Genes Dev.* 2014;28(12):1291-309.
309.

Eshleman HD, Morgan DO. Sgo1 recruits PP2A to chromosomes to ensure sister chromatid bi-orientation during mitosis. *Journal of cell science.* 2014;127(Pt 22):4974-83.
310.

Peplowska K, Wallek AU, Storchova Z. Sgo1 regulates both condensin and Ipl1/Aurora B to promote chromosome biorientation. *PLoS genetics.* 2014;10(6):e1004411.

311.

Yu HG, Koshland D. The Aurora kinase Ipl1 maintains the centromeric localization of PP2A to protect cohesin during meiosis. *The Journal of cell biology*. 2007;176(7):911-8.

312.

Verzijlbergen KF, Nerusheva OO, Kelly D, Kerr A, Clift D, de Lima Alves F, et al. Shugoshin biases chromosomes for biorientation through condensin recruitment to the pericentromere. *Elife*. 2014;3:e01374.

313.

Meppelink A, Kabeche L, Vromans MJ, Compton DA, Lens SM. Shugoshin-1 balances Aurora B kinase activity via PP2A to promote chromosome bi-orientation. *Cell Rep*. 2015;11(4):508-15.

314.

Carmena M, Wheelock M, Funabiki H, Earnshaw WC. The chromosomal passenger complex (CPC): from easy rider to the godfather of mitosis. *Nat Rev Mol Cell Biol*. 2012;13(12):789-803.

315.

Kelly AE, Funabiki H. Correcting aberrant kinetochore microtubule attachments: an Aurora B-centric view. *Curr Opin Cell Biol*. 2009;21(1):51-8.

316.

van der Horst A, Lens SM. Cell division: control of the chromosomal passenger complex in time and space. *Chromosoma*. 2014;123(1-2):25-42.

317.

Tsukahara T, Tanno Y, Watanabe Y. Phosphorylation of the CPC by Cdk1 promotes chromosome bi-orientation. *Nature*. 2010;467(7316):719-23.

318.

Yamagishi Y, Honda T, Tanno Y, Watanabe Y. Two histone marks establish the inner centromere and chromosome bi-orientation. *Science*.

2010;330(6001):239-43.

319.

Gassmann R, Carvalho A, Henzing AJ, Ruchaud S, Hudson DF, Honda R, et al. Borealin: a novel chromosomal passenger required for stability of the bipolar mitotic spindle. *The Journal of cell biology*. 2004;166(2):179-91.

320.

Sampath SC, Ohi R, Leismann O, Salic A, Pozniakovski A, Funabiki H. The chromosomal passenger complex is required for chromatin-induced microtubule stabilization and spindle assembly. *Cell*. 2004;118(2):187-202.

321.

Cheeseman IM, Anderson S, Jwa M, Green EM, Kang J, Yates JR, 3rd, et al. Phospho-regulation of kinetochore-microtubule attachments by the Aurora kinase Ipl1p. *Cell*. 2002;111(2):163-72.

322.

DeLuca JG, Gall WE, Ciferri C, Cimini D, Musacchio A, Salmon ED. Kinetochore microtubule dynamics and attachment stability are regulated by Hec1. *Cell*. 2006;127(5):969-82.

323.

Andrews PD, Ovechkina Y, Morrice N, Wagenbach M, Duncan K, Wordeman L, et al. Aurora B regulates MCAK at the mitotic centromere. *Dev Cell*. 2004;6(2):253-68.

324.

Cheng HC, Qi RZ, Paudel H, Zhu HJ. Regulation and function of protein kinases and phosphatases. *Enzyme Res*. 2011;2011:794089.

325.

Hunter T. Why nature chose phosphate to modify proteins. *Philos Trans R Soc Lond B Biol Sci*. 2012;367(1602):2513-6.

326.

Lahiry P, Torkamani A, Schork NJ, Hegele RA. Kinase mutations in human disease: interpreting genotype-phenotype relationships. *Nat Rev Genet*. 2010;11(1):60-74.

327.

Shchemelinin I, Sefc L, Necas E. Protein kinases, their function and implication in cancer and other diseases. *Folia Biol (Praha)*. 2006;52(3):81-100.

328.

Shi Y. Serine/threonine phosphatases: mechanism through structure. *Cell*. 2009;139(3):468-84.

329.

Tonks NK. Protein tyrosine phosphatases: from genes, to function, to disease. *Nat Rev Mol Cell Biol*. 2006;7(11):833-46.

330.

Ruediger R, Van Wart Hood JE, Mumby M, Walter G. Constant expression and activity of protein phosphatase 2A in synchronized cells. *Molecular and cellular biology*. 1991;11(8):4282-5.

331.

Xu Y, Chen Y, Zhang P, Jeffrey PD, Shi Y. Structure of a protein phosphatase 2A holoenzyme: insights into B55-mediated Tau dephosphorylation. *Molecular cell*. 2008;31(6):873-85.

332.

Seshacharyulu P, Pandey P, Datta K, Batra SK. Phosphatase: PP2A structural importance, regulation and its aberrant expression in cancer. *Cancer Lett*. 2013;335(1):9-18.

333.

Healy AM, Zolnierowicz S, Stapleton AE, Goebel M, DePaoli-Roach AA, Pringle JR. CDC55, a *Saccharomyces cerevisiae* gene involved in cellular morphogenesis: identification, characterization, and homology to the B subunit of mammalian type 2A protein phosphatase. *Molecular and cellular biology*. 1991;11(11):5767-80.

334.

Zolnierowicz S, Csontos C, Bondor J, Verin A, Mumby MC, DePaoli-Roach AA. Diversity in the regulatory B-subunits of protein phosphatase 2A: identification of a novel isoform highly expressed in brain. *Biochemistry*. 1994;33(39):11858-67.

335.

Strack S, Chang D, Zaucha JA, Colbran RJ, Wadzinski BE. Cloning and characterization of B delta, a novel regulatory subunit of protein phosphatase 2A. *FEBS Lett*. 1999;460(3):462-6.

336.

Janssens V, Goris J. Protein phosphatase 2A: a highly regulated family of serine/threonine phosphatases implicated in cell growth and signalling. *Biochem J*. 2001;353(Pt 3):417-39.

337.

Hendrix P, Mayer-Jackel RE, Cron P, Goris J, Hofsteenge J, Merlevede W, et al. Structure and expression of a 72-kDa regulatory subunit of protein phosphatase 2A. Evidence for different size forms produced by alternative splicing. *J Biol Chem*. 1993;268(20):15267-76.

338.

Moreno CS, Park S, Nelson K, Ashby D, Hubalek F, Lane WS, et al. WD40 repeat proteins striatin and S/G(2) nuclear autoantigen are members of a novel family of calmodulin-binding proteins that associate with protein phosphatase 2A. *J Biol Chem*. 2000;275(8):5257-63.

339.

Baharians Z, Schonthal AH. Autoregulation of protein phosphatase type 2A expression. *J Biol Chem*. 1998;273(30):19019-24.

340.

Stone SR, Hofsteenge J, Hemmings BA. Molecular cloning of cDNAs encoding two isoforms of the catalytic subunit of protein phosphatase 2A. *Biochemistry*. 1987;26(23):7215-20.

341.

Khew-Goodall Y, Hemmings BA. Tissue-specific expression of mRNAs encoding alpha- and beta-catalytic subunits of protein phosphatase 2A. *FEBS Lett*. 1988;238(2):265-8.

342.

Ruediger R, Hentz M, Fait J, Mumby M, Walter G. Molecular model of the A

subunit of protein phosphatase 2A: interaction with other subunits and tumor antigens. *Journal of virology*. 1994;68(1):123-9.
343.

Hemmings BA, Adams-Pearson C, Maurer F, Muller P, Goris J, Merlevede W, et al. alpha- and beta-forms of the 65-kDa subunit of protein phosphatase 2A have a similar 39 amino acid repeating structure. *Biochemistry*. 1990;29(13):3166-73.
344.

Archambault V, Lepine G, Kachaner D. Understanding the Polo Kinase machine. *Oncogene*. 2015;34(37):4799-807.
345.

Sunkel CE, Glover DM. polo, a mitotic mutant of *Drosophila* displaying abnormal spindle poles. *Journal of cell science*. 1988;89 (Pt 1):25-38.
346.

de Carcer G, Manning G, Malumbres M. From Plk1 to Plk5: functional evolution of polo-like kinases. *Cell cycle*. 2011;10(14):2255-62.
347.

Zitouni S, Nabais C, Jana SC, Guerrero A, Bettencourt-Dias M. Polo-like kinases: structural variations lead to multiple functions. *Nat Rev Mol Cell Biol*. 2014;15(7):433-52.
348.

de Carcer G, Escobar B, Higuero AM, Garcia L, Anson A, Perez G, et al. Plk5, a polo box domain-only protein with specific roles in neuron differentiation and glioblastoma suppression. *Molecular and cellular biology*. 2011;31(6):1225-39.
349.

Andrysik Z, Bernstein WZ, Deng L, Myer DL, Li YQ, Tischfield JA, et al. The novel mouse Polo-like kinase 5 responds to DNA damage and localizes in the nucleolus. *Nucleic Acids Res*. 2010;38(9):2931-43.
350.

Xie S, Wu H, Wang Q, Cogswell JP, Husain I, Conn C, et al. Plk3 functionally links DNA damage to cell cycle arrest and apoptosis at least in part via the p53 pathway. *J Biol Chem*. 2001;276(46):43305-12.
351.

Warnke S, Kemmler S, Hames RS, Tsai HL, Hoffmann-Rohrer U, Fry AM, et al. Polo-like kinase-2 is required for centriole duplication in mammalian cells. *Current biology : CB*. 2004;14(13):1200-7.
352.

Bettencourt-Dias M, Rodrigues-Martins A, Carpenter L, Riparbelli M, Lehmann L, Gatt MK, et al. SAK/PLK4 is required for centriole duplication and flagella development. *Current biology : CB*. 2005;15(24):2199-207.

353.

Matthew EM, Yen TJ, Dicker DT, Dorsey JF, Yang W, Navaraj A, et al. Replication stress, defective S-phase checkpoint and increased death in Plk2-deficient human cancer cells. *Cell cycle*. 2007;6(20):2571-8.

354.

Park JE, Soung NK, Johmura Y, Kang YH, Liao C, Lee KH, et al. Polo-box domain: a versatile mediator of polo-like kinase function. *Cell Mol Life Sci*. 2010;67(12):1957-70.

355.

Bruinsma W, Raaijmakers JA, Medema RH. Switching Polo-like kinase-1 on and off in time and space. *Trends Biochem Sci*. 2012;37(12):534-42.

356.

Elia AE, Cantley LC, Yaffe MB. Proteomic screen finds pSer/pThr-binding domain localizing Plk1 to mitotic substrates. *Science*. 2003;299(5610):1228-31.

357.

Lowery DM, Lim D, Yaffe MB. Structure and function of Polo-like kinases. *Oncogene*. 2005;24(2):248-59.

358.

Neef R, Preisinger C, Sutcliffe J, Kopajtich R, Nigg EA, Mayer TU, et al. Phosphorylation of mitotic kinesin-like protein 2 by polo-like kinase 1 is required for cytokinesis. *The Journal of cell biology*. 2003;162(5):863-75.

359.

Bruinsma W, Macurek L, Freire R, Lindqvist A, Medema RH. Bora and Aurora-A continue to activate Plk1 in mitosis. *Journal of cell science*. 2014;127(Pt 4):801-11.

360.

Lane HA, Nigg EA. Antibody microinjection reveals an essential role for human polo-like kinase 1 (Plk1) in the functional maturation of mitotic centrosomes. *The Journal of cell biology*. 1996;135(6 Pt 2):1701-13.

361.

Lee K, Rhee K. PLK1 phosphorylation of pericentrin initiates centrosome maturation at the onset of mitosis. *The Journal of cell biology*.

2011;195(7):1093-101.

362.

Li H, Liu XS, Yang X, Song B, Wang Y, Liu X. Polo-like kinase 1 phosphorylation of p150Glued facilitates nuclear envelope breakdown during prophase. *Proc Natl Acad Sci U S A*. 2010;107(33):14633-8.

363.

Smits VA, Klompaker R, Arnaud L, Rijksen G, Nigg EA, Medema RH. Polo-

- like kinase-1 is a target of the DNA damage checkpoint. *Nat Cell Biol.* 2000;2(9):672-6.
364.
- Hyun SY, Hwang HI, Jang YJ. Polo-like kinase-1 in DNA damage response. *BMB Rep.* 2014;47(5):249-55.
365.
- Tsvetkov L, Stern DF. Phosphorylation of Plk1 at S137 and T210 is inhibited in response to DNA damage. *Cell cycle.* 2005;4(1):166-71.
366.
- Seki A, Coppinger JA, Jang CY, Yates JR, Fang G. Bora and the kinase Aurora a cooperatively activate the kinase Plk1 and control mitotic entry. *Science.* 2008;320(5883):1655-8.
367.
- Qin B, Gao B, Yu J, Yuan J, Lou Z. Ataxia telangiectasia-mutated- and Rad3-related protein regulates the DNA damage-induced G2/M checkpoint through the Aurora A cofactor Bora protein. *J Biol Chem.* 2013;288(22):16139-44.
368.
- Degenhardt Y, Lampkin T. Targeting Polo-like kinase in cancer therapy. *Clin Cancer Res.* 2010;16(2):384-9.
369.
- Elowe S, Hummer S, Uldschmid A, Li X, Nigg EA. Tension-sensitive Plk1 phosphorylation on BubR1 regulates the stability of kinetochore microtubule interactions. *Genes Dev.* 2007;21(17):2205-19.
370.
- Huang H, Hittle J, Zappacosta F, Annan RS, Hershko A, Yen TJ. Phosphorylation sites in BubR1 that regulate kinetochore attachment, tension, and mitotic exit. *The Journal of cell biology.* 2008;183(4):667-80.
371.
- Liu XS, Song B, Tang J, Liu W, Kuang S, Liu X. Plk1 phosphorylates Sgt1 at the kinetochores to promote timely kinetochore-microtubule attachment. *Molecular and cellular biology.* 2012;32(19):4053-67.
372.
- Hauf S, Roitinger E, Koch B, Dittrich CM, Mechtler K, Peters JM. Dissociation of cohesin from chromosome arms and loss of arm cohesion during early mitosis depends on phosphorylation of SA2. *PLoS Biol.* 2005;3(3):e69.
373.
- Zhang N, Panigrahi AK, Mao Q, Pati D. Interaction of Sororin protein with polo-like kinase 1 mediates resolution of chromosomal arm cohesion. *J Biol Chem.* 2011;286(48):41826-37.
374.
- O'Connor A, Maffini S, Rainey MD, Kaczmarczyk A, Gaboriau D, Musacchio A,

et al. Requirement for PLK1 kinase activity in the maintenance of a robust spindle assembly checkpoint. *Biol Open*. 2015;5(1):11-9. 375.

Jia L, Li B, Yu H. The Bub1-Plk1 kinase complex promotes spindle checkpoint signalling through Cdc20 phosphorylation. *Nat Commun*. 2016;7:10818. 376.

Liu X, Winey M. The MPS1 family of protein kinases. *Annu Rev Biochem*. 2012;81:561-85. 377.

Tyler RK, Chu ML, Johnson H, McKenzie EA, Gaskell SJ, Evers PA. Phosphoregulation of human Mps1 kinase. *Biochem J*. 2009;417(1):173-81. 378.

Espeut J, Lara-Gonzalez P, Sassine M, Shiao AK, Desai A, Abrieu A. Natural Loss of Mps1 Kinase in Nematodes Uncovers a Role for Polo-like Kinase 1 in Spindle Checkpoint Initiation. *Cell Rep*. 2015;12(1):58-65. 379.

Winey M, Goetsch L, Baum P, Byers B. MPS1 and MPS2: novel yeast genes defining distinct steps of spindle pole body duplication. *The Journal of cell biology*. 1991;114(4):745-54. 380.

Kang J, Chen Y, Zhao Y, Yu H. Autophosphorylation-dependent activation of human Mps1 is required for the spindle checkpoint. *Proc Natl Acad Sci U S A*. 2007;104(51):20232-7. 381.

Liu ST, Chan GK, Hittle JC, Fujii G, Lees E, Yen TJ. Human MPS1 kinase is required for mitotic arrest induced by the loss of CENP-E from kinetochores. *Mol Biol Cell*. 2003;14(4):1638-51. 382.

Sliedrecht T, Zhang C, Shokat KM, Kops GJ. Chemical genetic inhibition of Mps1 in stable human cell lines reveals novel aspects of Mps1 function in mitosis. *PloS one*. 2010;5(4):e10251. 383.

Kwiatkowski N, Jelluma N, Filippakopoulos P, Soundararajan M, Manak MS, Kwon M, et al. Small-molecule kinase inhibitors provide insight into Mps1 cell cycle function. *Nat Chem Biol*. 2010;6(5):359-68. 384.

Castillo AR, Meehl JB, Morgan G, Schutz-Geschwender A, Winey M. The yeast protein kinase Mps1p is required for assembly of the integral spindle pole body component Spc42p. *The Journal of cell biology*. 2002;156(3):453-65. 385.

He X, Jones MH, Winey M, Sazer S. Mph1, a member of the Mps1-like family

of dual specificity protein kinases, is required for the spindle checkpoint in *S. pombe*. *Journal of cell science*. 1998;111 (Pt 12):1635-47.
386.

Fischer MG, Heeger S, Hacker U, Lehner CF. The mitotic arrest in response to hypoxia and of polar bodies during early embryogenesis requires *Drosophila* Mps1. *Current biology : CB*. 2004;14(22):2019-24.
387.

Cabral G, Sans SS, Cowan CR, Dammermann A. Multiple mechanisms contribute to centriole separation in *C. elegans*. *Current biology : CB*. 2013;23(14):1380-7.
388.

Pike AN, Fisk HA. Centriole assembly and the role of Mps1: defensible or dispensable? *Cell Div*. 2011;6:9.
389.

Yang CH, Kasbek C, Majumder S, Yusof AM, Fisk HA. Mps1 phosphorylation sites regulate the function of centrin 2 in centriole assembly. *Mol Biol Cell*. 2010;21(24):4361-72.
390.

Kasbek C, Yang CH, Yusof AM, Chapman HM, Winey M, Fisk HA. Preventing the degradation of mps1 at centrosomes is sufficient to cause centrosome reduplication in human cells. *Mol Biol Cell*. 2007;18(11):4457-69.
391.

Stucke VM, Sillje HH, Arnaud L, Nigg EA. Human Mps1 kinase is required for the spindle assembly checkpoint but not for centrosome duplication. *The EMBO journal*. 2002;21(7):1723-32.
392.

Schliekelman M, Cowley DO, O'Quinn R, Oliver TG, Lu L, Salmon ED, et al. Impaired Bub1 function in vivo compromises tension-dependent checkpoint function leading to aneuploidy and tumorigenesis. *Cancer Res*. 2009;69(1):45-54.
393.

Bolanos-Garcia VM, Blundell TL. BUB1 and BUBR1: multifaceted kinases of the cell cycle. *Trends Biochem Sci*. 2011;36(3):141-50.
394.

Elowe S. Bub1 and BubR1: at the interface between chromosome attachment and the spindle checkpoint. *Molecular and cellular biology*. 2011;31(15):3085-93.
395.

Roberts BT, Farr KA, Hoyt MA. The *Saccharomyces cerevisiae* checkpoint gene BUB1 encodes a novel protein kinase. *Molecular and cellular biology*. 1994;14(12):8282-91.

396.

Overlack K, Primorac I, Vleugel M, Krenn V, Maffini S, Hoffmann I, et al. A molecular basis for the differential roles of Bub1 and BubR1 in the spindle assembly checkpoint. *Elife*. 2015;4:e05269.

397.

Klebig C, Korinth D, Meraldi P. Bub1 regulates chromosome segregation in a kinetochore-independent manner. *The Journal of cell biology*. 2009;185(5):841-58.

398.

Zhang G, Lischetti T, Hayward DG, Nilsson J. Distinct domains in Bub1 localize RZZ and BubR1 to kinetochores to regulate the checkpoint. *Nat Commun*. 2015;6:7162.

399.

Vleugel M, Hoek TA, Tromer E, Sliedrecht T, Groenewold V, Omerzu M, et al. Dissecting the roles of human BUB1 in the spindle assembly checkpoint. *Journal of cell science*. 2015;128(16):2975-82.

400.

Kang J, Yang M, Li B, Qi W, Zhang C, Shokat KM, et al. Structure and substrate recruitment of the human spindle checkpoint kinase Bub1. *Molecular cell*. 2008;32(3):394-405.

401.

Lin Z, Jia L, Tomchick DR, Luo X, Yu H. Substrate-specific activation of the mitotic kinase Bub1 through intramolecular autophosphorylation and kinetochore targeting. *Structure*. 2014;22(11):1616-27.

402.

Bernard P, Hardwick K, Javerzat JP. Fission yeast bub1 is a mitotic centromere protein essential for the spindle checkpoint and the preservation of correct ploidy through mitosis. *The Journal of cell biology*.

1998;143(7):1775-87.

403.

Warren CD, Brady DM, Johnston RC, Hanna JS, Hardwick KG, Spencer FA. Distinct chromosome segregation roles for spindle checkpoint proteins. *Mol Biol Cell*. 2002;13(9):3029-41.

404.

Basu J, Logarinho E, Herrmann S, Bousbaa H, Li Z, Chan GK, et al. Localization of the Drosophila checkpoint control protein Bub3 to the kinetochore requires Bub1 but not Zw10 or Rod. *Chromosoma*. 1998;107(6-7):376-85.

405.

Wang X, Liu M, Li W, Suh CD, Zhu Z, Jin Y, et al. The function of a spindle checkpoint gene bub-1 in *C. elegans* development. *PloS one*.

2009;4(6):e5912.

406.

Gillett ES, Espelin CW, Sorger PK. Spindle checkpoint proteins and chromosome-microtubule attachment in budding yeast. *The Journal of cell biology*. 2004;164(4):535-46.

407.

Shah JV, Botvinick E, Bonday Z, Furnari F, Berns M, Cleveland DW. Dynamics of centromere and kinetochore proteins; implications for checkpoint signaling and silencing. *Current biology : CB*. 2004;14(11):942-52.

408.

Rischitor PE, May KM, Hardwick KG. Bub1 is a fission yeast kinetochore scaffold protein, and is sufficient to recruit other spindle checkpoint proteins to ectopic sites on chromosomes. *PLoS one*. 2007;2(12):e1342.

409.

Bolanos-Garcia VM, Kiyomitsu T, D'Arcy S, Chirgadze DY, Grossmann JG, Matak-Vinkovic D, et al. The crystal structure of the N-terminal region of BUB1 provides insight into the mechanism of BUB1 recruitment to kinetochores. *Structure*. 2009;17(1):105-16.

410.

Krenn V, Wehenkel A, Li X, Santaguida S, Musacchio A. Structural analysis reveals features of the spindle checkpoint kinase Bub1-kinetochore subunit Knl1 interaction. *The Journal of cell biology*. 2012;196(4):451-67.

411.

Qi W, Tang Z, Yu H. Phosphorylation- and polo-box-dependent binding of Plk1 to Bub1 is required for the kinetochore localization of Plk1. *Mol Biol Cell*. 2006;17(8):3705-16.

412.

Asghar A, Lajeunesse A, Dulla K, Combes G, Thebault P, Nigg EA, et al. Bub1 autophosphorylation feeds back to regulate kinetochore docking and promote localized substrate phosphorylation. *Nat Commun*. 2015;6:8364.

413.

Ricke RM, Jeganathan KB, Malureanu L, Harrison AM, van Deursen JM. Bub1 kinase activity drives error correction and mitotic checkpoint control but not tumor suppression. *The Journal of cell biology*. 2012;199(6):931-49.

414.

Nolen B, Taylor S, Ghosh G. Regulation of protein kinases; controlling activity through activation segment conformation. *Molecular cell*. 2004;15(5):661-75.

415.

Bayliss R, Fry A, Haq T, Yeoh S. On the molecular mechanisms of mitotic kinase activation. *Open Biol*. 2012;2(11):120136.

416.

Taylor SS, Hussein D, Wang Y, Elderkin S, Morrow CJ. Kinetochore

localisation and phosphorylation of the mitotic checkpoint components Bub1 and BubR1 are differentially regulated by spindle events in human cells. *Journal of cell science*. 2001;114(Pt 24):4385-95. 417.

Qi W, Yu H. KEN-box-dependent degradation of the Bub1 spindle checkpoint kinase by the anaphase-promoting complex/cyclosome. *J Biol Chem*. 2007;282(6):3672-9. 418.

Goto GH, Mishra A, Abdulle R, Slaughter CA, Kitagawa K. Bub1-mediated adaptation of the spindle checkpoint. *PLoS genetics*. 2011;7(1):e1001282. 419.

Pangilinan F, Spencer F. Abnormal kinetochore structure activates the spindle assembly checkpoint in budding yeast. *Mol Biol Cell*. 1996;7(8):1195-208. 420.

Yamaguchi S, Decottignies A, Nurse P. Function of Cdc2p-dependent Bub1p phosphorylation and Bub1p kinase activity in the mitotic and meiotic spindle checkpoint. *The EMBO journal*. 2003;22(5):1075-87. 421.

Vanoosthuysen V, Valsdottir R, Javerzat JP, Hardwick KG. Kinetochore targeting of fission yeast Mad and Bub proteins is essential for spindle checkpoint function but not for all chromosome segregation roles of Bub1p. *Molecular and cellular biology*. 2004;24(22):9786-801. 422.

Tournier S, Gachet Y, Buck V, Hyams JS, Millar JB. Disruption of astral microtubule contact with the cell cortex activates a Bub1, Bub3, and Mad3-dependent checkpoint in fission yeast. *Mol Biol Cell*. 2004;15(7):3345-56. 423.

Perera D, Tilston V, Hopwood JA, Barchi M, Boot-Handford RP, Taylor SS. Bub1 maintains centromeric cohesion by activation of the spindle checkpoint. *Dev Cell*. 2007;13(4):566-79. 424.

Encalada SE, Willis J, Lyczak R, Bowerman B. A spindle checkpoint functions during mitosis in the early *Caenorhabditis elegans* embryo. *Mol Biol Cell*. 2005;16(3):1056-70. 425.

Essex A, Dammermann A, Lewellyn L, Oegema K, Desai A. Systematic analysis in *Caenorhabditis elegans* reveals that the spindle checkpoint is composed of two largely independent branches. *Mol Biol Cell*. 2009;20(4):1252-67. 426.

Morrow CJ, Tighe A, Johnson VL, Scott MI, Ditchfield C, Taylor SS. Bub1 and

aurora B cooperate to maintain BubR1-mediated inhibition of APC/CCdc20. *Journal of cell science*. 2005;118(Pt 16):3639-52.
427.

Tang Z, Shu H, Oncel D, Chen S, Yu H. Phosphorylation of Cdc20 by Bub1 provides a catalytic mechanism for APC/C inhibition by the spindle checkpoint. *Molecular cell*. 2004;16(3):387-97.
428.

Meraldi P, Sorger PK. A dual role for Bub1 in the spindle checkpoint and chromosome congression. *The EMBO journal*. 2005;24(8):1621-33.
429.

Fernius J, Hardwick KG. Bub1 kinase targets Sgo1 to ensure efficient chromosome biorientation in budding yeast mitosis. *PLoS genetics*. 2007;3(11):e213.
430.

Perera D, Taylor SS. Sgo1 establishes the centromeric cohesion protection mechanism in G2 before subsequent Bub1-dependent recruitment in mitosis. *Journal of cell science*. 2010;123(Pt 5):653-9.
431.

Chen RH. BubR1 is essential for kinetochore localization of other spindle checkpoint proteins and its phosphorylation requires Mad1. *The Journal of cell biology*. 2002;158(3):487-96.
432.

Jeganathan K, Malureanu L, Baker DJ, Abraham SC, van Deursen JM. Bub1 mediates cell death in response to chromosome missegregation and acts to suppress spontaneous tumorigenesis. *The Journal of cell biology*. 2007;179(2):255-67.
433.

Heinrich S, Windecker H, Hustedt N, Hauf S. Mph1 kinetochore localization is crucial and upstream in the hierarchy of spindle assembly checkpoint protein recruitment to kinetochores. *Journal of cell science*. 2012;125(Pt 20):4720-7.
434.

Kim S, Sun H, Tomchick DR, Yu H, Luo X. Structure of human Mad1 C-terminal domain reveals its involvement in kinetochore targeting. *Proc Natl Acad Sci U S A*. 2012;109(17):6549-54.
435.

Li D, Morley G, Whitaker M, Huang JY. Recruitment of Cdc20 to the kinetochore requires BubR1 but not Mad2 in *Drosophila melanogaster*. *Molecular and cellular biology*. 2010;30(13):3384-95.
436.

Boyarchuk Y, Salic A, Dasso M, Arnaoutov A. Bub1 is essential for assembly of the functional inner centromere. *The Journal of cell biology*. 2007;176(7):919-28.

437.

Vigneron S, Prieto S, Bernis C, Labbe JC, Castro A, Lorca T. Kinetochores localization of spindle checkpoint proteins: who controls whom? *Mol Biol Cell*. 2004;15(10):4584-96.

438.

Riedel CG, Katis VL, Katou Y, Mori S, Itoh T, Helmhart W, et al. Protein phosphatase 2A protects centromeric sister chromatid cohesion during meiosis I. *Nature*. 2006;441(7089):53-61.

439.

Vaur S, Cubizolles F, Plane G, Genier S, Rabitsch PK, Gregan J, et al. Control of Shugoshin function during fission-yeast meiosis. *Current biology : CB*. 2005;15(24):2263-70.

440.

Foley EA, Kapoor TM. Chromosome congression: on the bi-orient express. *Nat Cell Biol*. 2009;11(7):787-9.

441.

Logarinho E, Resende T, Torres C, Bousbaa H. The human spindle assembly checkpoint protein Bub3 is required for the establishment of efficient kinetochore-microtubule attachments. *Mol Biol Cell*. 2008;19(4):1798-813.

442.

Shichiri M, Yoshinaga K, Hisatomi H, Sugihara K, Hirata Y. Genetic and epigenetic inactivation of mitotic checkpoint genes hBUB1 and hBUBR1 and their relationship to survival. *Cancer Res*. 2002;62(1):13-7.

443.

Giam M, Rancati G. Aneuploidy and chromosomal instability in cancer: a jackpot to chaos. *Cell Div*. 2015;10:3.

444.

Potapova TA, Zhu J, Li R. Aneuploidy and chromosomal instability: a vicious cycle driving cellular evolution and cancer genome chaos. *Cancer Metastasis Rev*. 2013;32(3-4):377-89.

445.

Zhang C, Min L, Zhang L, Ma Y, Yang Y, Shou C. Combined analysis identifies six genes correlated with augmented malignancy from non-small cell to small cell lung cancer. *Tumour Biol*. 2015.

446.

Wang Z, Katsaros D, Shen Y, Fu Y, Canuto EM, Benedetto C, et al. Biological and Clinical Significance of MAD2L1 and BUB1, Genes Frequently Appearing in Expression Signatures for Breast Cancer Prognosis. *PloS one*. 2015;10(8):e0136246.